HEINRICH HEINE
UNIVERSITÄT DÜSSELDORF

Evaluation of the therapeutic potential of nanoencapsulated curcumin towards inflammatory bowel disease

In vitro and *in vivo* approaches

Inaugural-Dissertation

zur Erlangung des Doktorgrades
der Mathematisch-Naturwissenschaftlichen Fakultät
der Heinrich-Heine-Universität Düsseldorf

vorgelegt von

Julia Kolling

aus Neunkirchen/Saar

Düsseldorf, Januar 2014

aus dem Leibniz-Institut für Umweltmedizinische Forschung (IUF) gGmbH
(Wissenschaftlicher Direktor: Prof. Dr. med. Jean Krutmann)

Gedruckt mit der Genehmigung der
Mathematisch-Naturwissenschaftlichen Fakultät der
Heinrich-Heine-Universität Düsseldorf

Referent: PD Dr. Klaus Unfried
Korreferent: Prof. Dr. Johannes Hegemann

Tag der mündlichen Prüfung: 02.06.2014

„Ernst zu nehmende Forschung erkennt man daran, dass plötzlich zwei Probleme existieren, wo es vorher nur eines gegeben hat.“

Thorstein Bunde Veblen

(amerikanischer Soziologe und Ökonom)

Für meine Eltern

Abbreviations

°C	Degrees Celcius
µl	Microliter
µg	Microgram
8-oxo-dG	8-hydroxydeoxyguanosine
APE/Ref-1	Apurinic endonuclease/redox-factor-1
ARE	Antioxidant responsive elements
ATF-6	Activating transcription factor 6
BCA	Bicinchonic acid
BSA	Bovine serum albumin
BSO	Buthionine sulfoximine
cDNA	Complementary deoxyribonucleic acid
CD	Crohn's diseases
CGD	Chronic granulomatous disease
CRC	Colorectal cancer
Ctr	Control
Curc	Curcumin
DC	Dendritic cells
DMSO	Dimethyl sulfoxide
DNA	Desoxyribonucleic acid
DNBS	Dinitrobenzene sulfonic acid
DLS	Dynamic light scattering
DSS	Dextran sulphate sodium
(I)EC	(intestinal) Epithelial cells
EDTA	Ethylenediaminetetraacetic acid
e.g.	Exempli gratia
eIF2α	Elongation initiation factor 2α
ER	Endoplasmic reticulum
ERAD	ER-associated degradation

ERQC	ER quality control mechanisms
EtOH	Ethanol
FCS	Foetal Calf Serum
Fpg	Formamidopyrimidine glycosylase
g	Gram
GALT	Gut-associated lymphoid tissue
γ-GCS	γ-glutamylcysteine synthetase
G-CSF	Granulocyte-colony stimulating factor
GM-CSF	Granulocyte-monocyte-colony stimulating factor
GSH	Glutathione
GSSG	Glutathione disulfide
HBSS	Hank's balanced salt solution
HEPES	4-(2-hydroxyethyl)-1piperazineethanesulfonic acid
HO-1	Heme oxygenase-1
IBD	Inflammatory bowel diseases
i.e.	Id est
IFN-γ	Interferon-γ
IgA	Immunoglobulin A
IL	Interleukin
iNOS	Inducible nitric oxide synthase
IRE-1	Inositol-requiring enzyme-1
KC	Keratinocyte chemoattractant
kg	Kilogram
l	Liter
LPS	Lipopolysaccharide
mA	Miliampere
mRNA	Messenger ribonucleic acid
MAPK	Mitogen-activated protein kinase
MCP-1	Monocyte chemoattractant protein-1

MEM	Minimal essential medium
mg	Miligram
ml	Mililiter
MIP-1	Macrophage inflammatory protein-1
MPO	Myeloperoxidase
MPS	Mononuclear phagocytic system
Muc2	Mucin 2
MWCO	Molecular Weight Cut-Off
NADPH	Nicotinamide adenine dinucleotide phosphate
NC	Nanocurcumin
NET	Neutrophil extracellular traps
NF-κB	Nuclear factor kappa B
nm	Nanometers
NOD	Nucleotide-binding oligomerization domain
NP	Nanoparticles
Nrf-2	Nuclear-factor-E2-related factor
OD	Optical density
OGG1	8-oxoguanine DNA glycosylase-1
PAMP	Pathogen-associated molecular pattern
PAS	Periodic Acid-Schiff
PBS	Phosphate buffered saline
PCR	Polymerase chain reaction
PDI	Polydispersity index
PEG	Poly ethylene glycol
PERK	Protein kinase related-like ER kinase
PLGA	Poly D,L-lactide co-glycolide
PMA	Phorbol myristate acetate
PMN	Polymorphonuclear neutrophils
PRR	Pathogen recognition receptors
PVA	Poly vinyl aldehyde

RANTES	Regulated on activation, normal T cell expressed and secreted
RNS	Reactive nitrogen species
Ro19-8022	[R]-1-[(10-chloro-4-oxo-3-phenyl-4H-benzo[*a*]quinolizin-1-yl)-carbonyl]-2-pyrrolidine-methanol
ROS	Reactive oxygen species
SDS	Sodium dodecyl sulphate
SNP	Single nucleotide polymorphism
SOD	Superoxide dismutase
SSA	Specific surface area
TEM	Transmission electron microscope
TLR	Toll-like receptors
TNBS	Trinitrobenzene sulfonic acid
TNF-α	Tumor necrosis factor-α
UC	Ulcerative colitis
UPR	Unfolded protein response
W	Watt
WST-1	Water-soluble tetrazolium salt
XBP1	X-box binding protein 1
ZP	Zeta potential

Table of contents

1. Introduction

1.1 The intestine

The intestine is part of the gastrointestinal tract and serves for the optimal uptake of nutrients and water from the ingested food. In humans, this tubular system is about 8.5 m long and divided into small and large intestine. The small intestine is split into three different sections: The duodenum contains most of the digestive enzymes and the bile, and in the jejunum and the ileum products of digestion, like sugars, amino acids and fatty acids are absorbed into the bloodstream. The large intestine, also known as colon, is named so due to its larger diameter, and is mostly used to store faeces or waste which consists of bacteria, undigested cellulose of plant cell walls, minerals and water. The cecum (with the appendix) receives faecal material from the ileum and is connected to the ascending colon (proximal colon) which is passed into transverse colon (mid colon), descending colon (distal colon) and sigmoid colon (see Figure 1.1).

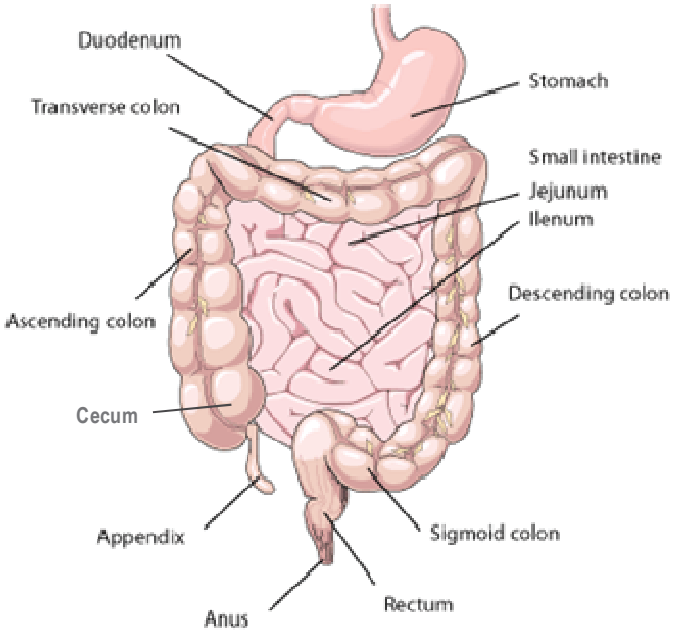

Figure 1.1: The digestive tract (source: www.GastroPatientEducation.com)

In the colon the electrolytes and water are reabsorbed, before the undigested food and waste are eliminated through the rectum and finally the anus. For an effective digestion and nutrient absorption, the surface area is largely increased in the small intestine by crypts, also known as Lieberkühn crypts, villi and microvilli. In the colon the surface is smooth and its area is merely enhanced because of the presents of crypts (DeSesso and Jacobson, 2001). All together the intestine possesses an immense surface area of approximately 300 m^3 (Wells et al., 1995).

The epithelium lines the intestinal surface as a single cell layer and plays therefore an essential role in the selective absorption, but it is also responsible for protection, cellular transport and secretion of e.g. mucins which form the protective mucus layer above the epithelial cells (Chichlowski and Hale, 2008). According to their functions, three different types of epithelial cell are present in the colon. The enterocytes are responsible for nutrient absorption and secretion of hydrolases, the goblet cells secret the mucus, and the enteroendocrine cells secret several hormones such as secretin and serotonin (Krause et al., 1985; Snoeck et al., 2005). In the small intestine additionally the Paneth cells are located. Usually, the life span of epithelial cells is limited around five days, before they undergo apoptosis, followed by shedding from the surface of the epithelium (Ramachandran et al., 2000). Therefore, it is necessary that a high rate of epithelial renewal exists. This is afforded by highly proliferative stem cells that reside at, or close to the crypt bottom. By migration along the crypt-villus axis the newly produced cells proliferate several times, before they finally differentiate into the appropriate types of epithelial cells (Crosnier et al., 2006; Ramachandran et al., 2000).

Due to the fact that the intestine is an open tubular system harmful substances and pathogens easily reach the lumen. As such, the mucosal layer is in direct contact with the external environment and vulnerable to invasion of viruses, bacteria, fungi and parasites. However, in addition to the pathogens also beneficial microorganisms reside in the intestine. These commensal bacteria are necessary to facilitate the digestion and absorption of nutrients but they also play a key role in the development of the intestinal immune system, detoxification and protection against pathogens (Backhed et al., 2005; Wu and Wu, 2012). Whereas the density of beneficial bacteria is relatively low in the proximal small intestine, the distal part and colon is populated by 10^9 to 10^{12} microorganisms, representing members of eukarya, archae and bacteria composed of 500-1000 species (Artis, 2008; Ley et al., 2006; Wells et al., 2010). This high density of microbes is a big challenge for the intestine and causes a continuous interaction with the host intestinal immune system, which has to differentiate between friend and foe.

1.1.1 The intestinal immune system

The intestine is continuously exposed to potential pathogens and commensal microbes as mentioned before, and it is thus no surprise that the immune system in the intestine is the largest of the body. The key feature of the intestinal immune system is to maintain the balance between the defence against harmful substances and pathogens on the one side and immune tolerance to resident intestinal microorganisms on the other side (Abraham and Medzhitov, 2011; Hill and Artis, 2010). To prohibit the excessive entry of luminal microbes in

the underlying lamina propria which contains the gut-associated lymphoid tissue (GALT), the intestinal epithelium layer serves as physical barrier. In the epithelium different types of intestinal epithelial cells (IEC) are present with specialised functions, also depending on their location within the intestinal tube. The goblet cells are glandular epithelial cells present throughout the whole intestine. They secrete glycosylated mucins in the intestinal lumen, so a viscous and relatively impermeable mucus layer is formed onto the apical surface of the epithelium to reinforce the physical barrier function (McAuley et al., 2007; Sansonetti, 2004). Furthermore, the IEC affect the initiation and regulation of antimicrobial immune responses. In the small intestine, so-called M (Microfold) cells are contained in follicle-associated epithelium that overlies Peyer's patches and isolated lymph follicles (Schulz and Pabst, 2013). These M cells are specialised to sample antigens and microbes and transport them by transcytosis to the subepithelial dome which contains antigen-presenting cells (Mabbott et al., 2013; Neutra, 1999). Followed by the antigen presentation via dendritic cells (DC) and macrophages, the adaptive T cell and B cell immune responses are activated. Upon encountering the antigen, the T cells, B cells and memory cells in the interfollicular T cell and B cell areas within the Peyer's Patches are stimulated. Via lymphatic vessels, these cells pass to mesenteric lymph nodes, and subsequently amplify the immune response (Artis, 2008; Nagler-Anderson, 2001; Richaud-Patin et al., 2005).

The initial recognition of microorganisms by IEC but also by DC, macrophages and Paneth cells occurs via pathogen recognition receptors (PRR) including Toll-like receptors (TLR) and intracellular nucleotide-binding oligomerization domain (NOD)-like receptors which identify pathogen-associated molecular pattern (PAMP) such as lipopolysaccharide (LPS) (Medzhitov, 2007; Wells et al., 2010). These specific interactions can result in secretion of antimicrobial proteins such as defensins and lectins, in activation of cytokine and chemokine signalling pathways, in unfolded protein responses and in the initiation of the adaptive immune responses (Abraham and Medzhitov, 2011). The release of pro-inflammatory cytokines such as tumor necrosis factor-α (TNF-α) and interleukin-1β (IL-1β) activates and recruits polymorphonuclear neutrophils (PMN) to the site of injury (Adams and Lloyd, 1997). Commonly, the migration of neutrophils through the blood vessels into the inflammatory tissue is one of the first steps in the host immune response. Neutrophils are phagocytes with antimicrobial function, not only by ingestion of microbes but also by destroying the pathogens via oxidative burst (Babior, 2000b). Furthermore, they are able to produce themselves pro-inflammatory cytokines and so they trigger the recruitment of further immune cells (Nathan, 2006) . This mechanism is described in more in detail in chapter 1.1.3 of this thesis.

To maintain the immune homeostasis, not only the defence against pathogens is important, but also the intestinal immune tolerance. Therefore, the strategy of the intestinal immune system is to minimise pathogen exposure e.g. by enhancement of the physical

barrier with mucins or by secretion of intestinal immunoglobulin A (IgA) in the mucus layer for antigen neutralisation and to down-regulate immune responses (Abraham and Medzhitov, 2011). However, presently it is still incompletely understood how the intestinal immune system is able to differentiate between friend and foe. Molecular mechanisms must exist to facilitate the recognition of commensal bacteria and to prevent the immune responses to these microorganisms (Artis, 2008). Different studies have shown that the intestinal innate immune cells, particularly DC and macrophages are a unique population with large differences compared to their peripheral counterparts. For example, activated DC and macrophages in the lamina propria produce anti-inflammatory interleukin-10 (IL-10) during intestinal inflammation to maintain the optimal activity of regulatory T cells (T_{regs}) (Coombes and Powrie, 2008; Denning et al., 2007; Murai et al., 2009).

1.1.2 Inflammatory bowel diseases

Inflammatory bowel diseases (IBD) like ulcerative colitis (UC) and Crohn's diseases (CD) are chronic inflammatory disorders in the gastro-intestinal tract and affect approximately 1-2 of every 1000 people in developed countries (Blumberg et al., 2011). Hereby, environmental, genetic and immunological factors are considered to be the key players for the recurrent inflammation observed in these patients (Molodecky and Kaplan, 2010; Sartor, 2006; Wirtz and Neurath, 2007). In UC just the colon is affected, in which the diffuse mucosal inflammation usually starts from the rectum and extends in the proximally part of the large intestine. In contrast, CD can involve the whole gastro-intestinal tract, even if the terminal ileum is the most common part (Xavier and Podolsky, 2007). UC and CD patients suffer from weight loss, fever, abdominal pain and severe diarrhoea, often combined with rectal bleeding. In both diseases the symptoms are usually frequently manifested in early adulthood as well as up to 50 to 70 years of age. Although some similar characteristics exist between UC and CD, both diseases markedly differ in genetic alterations, the profile of immunological responses, clinical pathogenesis and treatment strategies (Fatahzadeh, 2009; Hendrickson et al., 2002).

In Europe, UC has a higher incidence rate, from 1.5 to 20.3 cases per 100 000 person-years, than CD with 0.7 to 9.8 cases per 100 000 person-years (Loftus, 2004). Characteristic histopathological features of UC are crypt abscesses, a significant increase in neutrophil infiltration and an epithelial barrier dysfunction. In addition, UC may lead to loss of goblet cells and a depleted mucus layer, induced by a reduced Muc2 mucin synthesis (Hendrickson et al., 2002; Van Klinken et al., 1999). In addition, patients with UC possess an increased risk for colorectal cancer (Ullman and Itzkowitz, 2011). The disturbance of the intestinal immune homeostasis in regards to immune system defence and immune tolerance

to intestinal antigens and microbes is thought to contribute to the pathogenesis of IBD (Abraham and Medzhitov, 2011). UC is driven by the recruitment and migration of activated lymphocytes, granulocytes and macrophages into the mucosa connected with the increased production of cytokines and chemokines such as IL-1 β, TNF-α and IL-8. In experimentally induced colitis, using the chemical dextran sulphate sodium (DSS), numerous inflammatory mediators could be located with an increased expression profile including IL-1α, IL-1β, IL-6, IL-17, granulocyte-colony stimulating factor (G-CSF), granulocyte-monocyte-colony stimulating factor (GM-CSF), monocyte chemoattractant protein-1 (MCP-1), keratinocyte chemoattractant (KC), macrophage inflammatory protein (MIP-1α), MIP-1β and regulated on activation, normal T cell expressed and secreted (RANTES) (Coburn et al., 2012).

The main T cell response in UC exhibits a T_H2-like profile associated with an increased IL-13 and IL-5 release. In contrast, CD shows a T_H1 dominated T-cell response related with an increased production of IL-12 and interferon-γ (IFN-γ) (Fuss et al., 2004; Strober and Fuss, 2011). However, an additional T_H17 cell response is identified which is involved in both diseases and indicates a more complex and overlapping mechanism in development of UC and CD (Abraham and Cho, 2009). The differentiation of the CD4 T cell lineage T_H17 is promoted by IL-23 and leads to an overexpression of IL-17 in inflamed gut mucosa (Kastelein et al., 2007; Weaver et al., 2007). Several studies have demonstrated that the IL-23/IL-17 axis is linked to IBD (Sarra et al., 2010). However, neutrophils have also a crucial part in formation of UC. In colitic tissue of patients, the degree of local inflammation correlates with the number of neutrophils (Mitsuyama et al., 1994). Moreover, mice which lack the key neutrophil chemokine receptor CXCR2, display an inhibited neutrophil infiltration possess and an associated reduction of clinical colitis symptoms upon DSS treatment, in comparison to the wild type mice (Buanne et al., 2007).

1.1.3 The role of neutrophils in the intestinal immune system

The role of neutrophils, also named polymorphonuclear granulocytes (PMN) in the immune response against extracellular pathogens was already discovered more than 100 years ago by Elie Metchnikoff. Since then it is proposed that neutrophils are “wandering” cells in the blood which migrate to the site of infection and eliminate the pathogens (Babior, 2000b). The PMN are the first line of host defence against acute infection. Around 1-2 x 10^{11} PMN are produced daily in the human body, and they account for 60 to 70% of all white blood cells (Wessels et al., 2010). This abundance is important due to the fact that they are the most active phagocytes in human, while they exhibit only a short life time of 8 to 12 hours during circulation in the bloodstream (Hampton et al., 1998; Panda et al., 2009; Simon and Kim, 2010).

In the presence of inflammation, the life span and mobility of neutrophils becomes affected by the release of pro-inflammatory cytokines and chemokines such as IL-1β, IL-6, G-CSF, GM-CSF, IFN-γ and TNF (Gomez et al., 2008; Schroder and Rink, 2003; Wessels et al., 2010). This network of chemoattractants, and in particular IL-8, causes the recruitment of neutrophils to the site of injury. From the blood, the PMN adhere to the vascular endothelium mediated by interaction of specific adhesion molecules onto the surface of PMN and EC including β2-integrin and ICAM-1. Followed by extravasation and migration across the endothelium, the PMN achieve the inflamed tissue (Drost and MacNee, 2002; Evangelista et al., 1996; Naito et al., 2007). In addition, the PMN effector function can also be activated by sensing of pathogens through pathogen recognition receptors (PRR) (Mantovani et al., 2011). Once activated, the neutrophils ingest the invading pathogens into their phagosomes and destroy them via different defence strategies. One strategy is the release of antimicrobial molecules in the phagosome by fusing with cytosolic granules (Kumar and Sharma, 2010). Neutrophils contain peroxidase-positive granules, also named primary or azurophilic granules. These granules are filled with myeloperoxidase (MPO) and various serine proteases including cathepsin G, neutrophil elastases and proteinase 3 (Bainton and Farquhar, 1968). Furthermore, PMN possess peroxidase negative granules, known as secondary granules and tertiary granules which are characterised by a high content of lactoferrin and gelatinase, respectively. The secretory vesicles are more material to integral membrane proteins such as integrins and components of the nicotinamide adenine dinucleotide phosphate (NADPH) oxidase enzyme complex (Borregaard et al., 1993). Neutrophils build also neutrophil extracellular traps (NET), composed of chromatin material and some granule proteins to control the inflammation. NETs act as mesh to capture the pathogens, followed by the release of antimicrobial agents i.e. serin proteases to kill microorganisms extracellularly (Remijsen et al., 2011). The most important strategy of neutrophils to eliminate bacteria, however, is the production of reactive oxygen species (ROS) and reactive nitrogen species (RNS). This oxidative burst is initiated by NADPH oxidase, a membrane-bound enzyme complex which is composed of many subunits (Babior, 2000a). The process is based on the increased consumption of molecular oxygen from the cells and leads to the NADPH oxidase driven formation of superoxide anion radicals ($O_2^{\cdot-}$), and subsequent formation of further oxidants including hydrogen peroxide (H_2O_2) and hypochlorous acid (HOCl) (Freitas et al., 2009). The fundamental role of the oxidative burst is noticeable in patients suffering from chronic granulomatous disease (CGD), which have a genetic defect in the NADPH oxidase resulting in an impaired oxidative burst and an increased predisposition to bacterial infections (Holland, 2010; Rosenzweig, 2008).

As already mentioned, activated neutrophils are also involved in the further activation and regulation of the innate and adaptive immune system. PMN are able to produce a variety

of pro-inflammatory cytokines themselves such as IL-1β, IL-6, IL-23, MIP-1α, MIP-1β and TNF-α. Accordingly, they can initiate a complex bidirectional crosstalk with macrophages, dendritic cells, natural killer cells and lymphocytes (Mantovani et al., 2011; Wessels et al., 2010). Amongst others, neutrophils contribute to the maturation of DC and recruitment and activation of macrophages, which in turn are able to prolong their life span and induce the proliferation and activation capacity of PMN (Costantini et al., 2010; Jaillon et al., 2013; Kumar and Sharma, 2010).

1.1.4 Oxidative stress in IBD

Inflammatory bowel diseases and oxidative stress are closely connected. Oxidative stress is defined as imbalance between the amount of ROS in the cell and the ability of the biological system to detoxify these reactive intermediates with antioxidants (Sies, 1997). The most important and essential source of intracellular oxidants in IBD, as mentioned before, is the oxidative burst of activated neutrophils in response to pathogens. In this process, four different enzymes are involved, namely NADPH-oxidase, superoxide dismutase (SOD), MPO and inducible nitric oxide synthase (iNOS) (Babior, 2000b; Knaapen et al., 2006). The NADPH-oxidase is a membrane-bound enzyme complex which initiates the oxygen radical generation and can be stimulated by various agents including the experimentally often applied chemical phorbol myristate acetate (PMA) (Suzuki and Lehrer, 1980). The core component is composed of the catalytic subunit NOX2 (gp91phox) and the regulatory subunit p22phox formed together the flavocytochrome b_{558} (Nauseef, 2007). This complex is localised in the plasma membrane and within the membrane of the granules in which NOX2 is thought to serve as H^+-channel for charge compensation across the membrane (Maturana et al., 2002). Upon its activation, the cytosolic subunits, namely p40phox, p47phox, p67phox and the guanosine triphosphate hydrolase (GTPase) Rac1/2 migrate to the membrane-bound subunits and form the active oxidase. The enzyme then catalyzes the production of $O_2^{\cdot -}$ which is released into the phagosomes or the extracellular microenvironment. This highly reactive anion radical is rapidly dismutated into hydrogen peroxide (H_2O_2). This process occurs spontaneously, but is markedly enhanced in the presence of the SOD. The relatively stable H_2O_2 is capable to cross cellular membranes and to diffuse between cells. This also explains why the impact of the neutrophilic oxidative burst is not only localised at the site of activation. During neutrophilic inflammation, the majority of H_2O_2 is rapidly used by the highly abundant MPO enzyme to form the highly bactericidal HOCl. Apart from Cl^- ions, also Br^-, I^-, and SNC^- can be used to form the corresponding acids (Freitas et al., 2009). Finally, neutrophils can also generate RNS, catalysed by the enzyme iNOS. In this process, nitric oxide ($NO^{\cdot}$) is produced from L-arginine, oxygen and NADPH. However, compared to

macrophages, the expression of iNOS is rather low in neutrophils, and hence RNS are not considered to play an essential role in neutrophil defence (Knaapen et al., 2006; Weinberg et al., 1995).

Cells are equipped with elaborate antioxidant defence mechanisms to prevent oxidative stress. Several antioxidant enzymes such as SOD, catalase and glutathione protect against oxidative damage to cellular components such as DNA, proteins and lipids (Speit et al., 2000). The tripeptide glutathione (GSH; L-γ-glutamyl-L-cysteinyl-glycine) exhibits a central role in maintaining the cell redox state. Due to its thiol groups, GSH acts as reducing agent and can serve as electron donor for free radicals and other oxidants. Upon the reaction with the oxidants such as H_2O_2, the GSH is converted to glutathione disulfide (GSSG). This oxidized form can be reduced back by the enzyme glutathione reductase using NADPH as electron donor (Sies, 1997, 1999). The ratio of reduced glutathione to oxidized glutathione can be used as a marker of oxidative stress in cells and tissues (Pastore et al., 2003). Severe oxidative stress will lead to a depletion of the total cellular glutathione pool (Ichiseki et al., 2006). The enzyme gamma-glutamylcysteine synthetase (γ-GCS) is the rate limiting factor for the *de novo* synthesis of GSH (Drew & Miners 1984). Its mRNA expression has therefore been proposed as a sensitive marker of oxidative stress (Gerloff et al., 2012a; van Berlo et al., 2010). The chemical buthionine sulfoximine (BSO) has been used in many studies to investigate the role of GSH in cellular redox status maintenance and defence against exogenous oxidants. Treatment of cells with this compound causes depletion of the intracellular GSH level by the inhibition of γ-GCS, and BSO is therefore often used to study the importance of the glutathione pool in oxidant induced toxicity. A further oxidative stress marker is the heme oxygenase-1 (HO-1), which plays also an important role to maintain the cellular homeostasis. In presence of oxidative stress, HO-1 is activated and causes the degradation of the pro-oxidant heme, followed by the accumulation of the antioxidant bilirubin (Speit et al., 2000). Hence, the expression of HO-1 on mRNA as well as protein level has been proposed as a marker of oxidative stress in experimental settings (Gerloff et al., 2012a; van Berlo et al., 2010). The transcription of γ-GCS, HO-1 and many further antioxidant genes including SOD and catalase is highly regulated by the nuclear-factor-E2-related factor (Nrf)-2 signal pathway. Oxidants including hydrogen peroxide are well-known activators of this pathway, which results in the enhanced binding of the Nrf2 protein to antioxidant responsive elements (ARE) of such antioxidant genes (Kang et al., 2005; Yanaka et al., 2005).

The counteractions of the aforementioned cellular antioxidant defence systems are considered to operate adequate during situations of mild and transient oxidative stress. However, in situations of severe and more persistent inflammation, as can occur e.g. in IBD, the generation of ROS becomes exaggerated and additionally the antioxidant defence mechanisms become decreased and impaired leading to considerable oxidative stress in the

chronically inflamed colon mucosa (Buffinton and Doe, 1995; Grisham, 1994; Lih-Brody et al., 1996; Roessner et al., 2008).

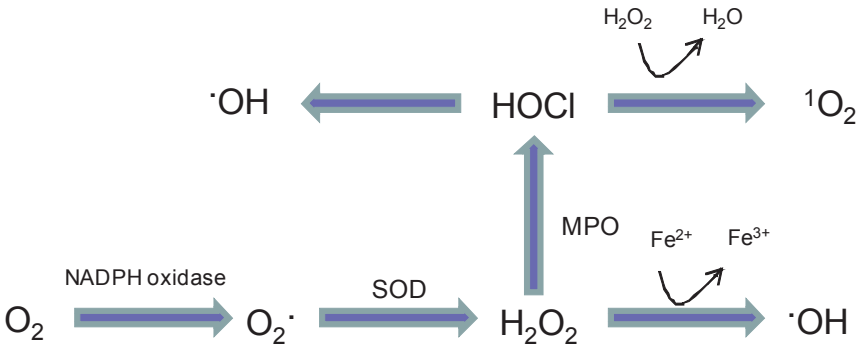

Figure 1.2: Schematic overview of the generation of reactive oxygen species produced by neutrophils (modified from Knaapen et al., 2006). Activated neutrophils are potent generators of superoxide anion radicals via their nicotinamide adenine dinucleotide phosphate (NADPH) oxidase activity. Superoxide can be converted to hydrogen peroxide by the enzyme superoxide dismutase (SOD). In the presence of iron (or other transition metals), the highly reactive hydroxyl radicals are formed via the Fenton reaction. Neutrophils also contain large amounts of myeloperoxidase (MPO), which lead to the generation of hypochlorous acid (HOCl). HOCl can also react with superoxide to form hydroxyl-radicals, or with hydrogen peroxide to form singlet oxygen ($^1O_2$).

1.1.5 Genomic instability and carcinogenesis in IBD

The risk of colorectal cancer (CRC) is significantly increased in patients with IBD (Jess et al., 2006; Ullman and Itzkowitz, 2011). This extended risk correlates with the ongoing inflammation and the increased oxidative stress. Phagocyte-derived ROS are associated in a wide range of processes that could contribute to DNA damage, lipid peroxidation and modulation of enzyme activities including those of antioxidant and DNA repair enzymes. ROS induced DNA damage can occur by oxidation, nitration, depurination, methylation and deamination (Knaapen et al., 2006). The best investigated and highly abundant oxidative DNA lesion is 8-hydroxydeoxyguanosine (8-oxo-dG), generated by oxidation at the C-8 position of the guanine base. This DNA modification may lead to a G:T transversion mutation due to the preferred incorporation of dAMP instead of dCMP opposite 8-oxo-dG (Shibutani et al., 1991). Many studies have established that 8-oxo-dG is premutagenic and that it has an increased occurrence in cancer (Roessner et al., 2008). In colorectal biopsies of UC patients, 8-oxo-dG levels are found to be significantly increased (D'Inca et al., 2004). Therefore, it has been proposed to use 8-oxo-dG as marker for oxidative stress in carcinogenesis (Kasai, 1997). The steady state level of oxidative DNA bases in the cells also depends on the activity

of DNA repair enzymes. For repair of 8-oxo-dG, the most important repair enzyme is the 8-oxoguanine DNA glycosylase 1 (OGG1), which initiates the base excision repair pathway by removing the modified bases via cleavage of N-glycosylic bonds (Krokan et al., 2000). To detect and quantify oxidative DNA modifications in laboratory experiments, the OGG1 bacterial homologue formamidopyrimidine glycosylase (Fpg) is often used (Bjoras et al., 1997). A second important base excision repair enzyme is the apurinic (apyrimidic) endonuclease/redox-factor 1 (APE/Ref1) which cleaves the phosphodiester backbone at the created apurinic/apyrimidic (AP) sites resulting in DNA single-stand breaks (Fritz, 2000). It could be observed that both enzymes are enhanced in CRC patients (Obtulowicz et al., 2010). Animal experiments have demonstrated that a deficiency of OGG1 is associated with a significant increase in 8-oxo-dG levels and a significantly higher number of carcinomas in a DSS-induced ulcerative colitis models (Liao et al., 2008).

1.1.6 ER stress with resulting unfolded protein response in IBD

The protein synthesis and the post-translational modifications of transmembrane, secretory and cell surface proteins are affected to the endoplasmic reticulum (ER). The ER is responsible for their proper folding, assembly and sorting before proteins are transported to the Golgi apparatus for further modifications (Pfeffer and Rothman, 1987). Due to the highly oxidative environment in the ER lumen, disulphide bonds are formed which are essential for the correct conformation and stability of the proteins. Nevertheless, protein misfolding is a common event due to the high amount of synthesised proteins and the complexity of the assembly and folding process. Especially proteins with a high molecular mass and a complex structure with crucial modifications for their function are a challenge for the ER. Therefore, the ER contains ER quality control mechanisms (ERQC) (Araki and Nagata, 2012). On the one side, the productive folding mechanism is regulated by a number of chaperones and folding enzymes, located within the ER. On the other side is the ER-associated degradation (ERAD) of terminally unfolded or misfolded proteins (Hirsch et al., 2009). These proteins are transported from ER to cytosol for proteasom mediated degradation.

Generally, protein misfolding can disturb the ER homeostasis and results in ER stress with adverse effects. In presence of ER stress, the ER protein folding capacity is increased by induction of the unfolded protein response (UPR) (Schroder and Kaufman, 2005). In this network of signal transduction pathways, the HSP70 chaperon GRP78/BiP is an important regulator which senses the misfolded proteins and causes the activation of the three key ER transmembrane proteins IRE1 (inositol-requiring enzyme 1), PERK (protein kinase related-like ER kinase) and ATF6 (activating transcription factor 6) (Kaser et al., 2013). Under non-stressed conditions these three membrane proteins are inactivate by binding of GRP78, but

in ER stress, the chaperon GRP78 releases them and binds the misfolded proteins to prevent the protein transport to Golgi (Rao and Bredesen, 2004). The most conserved UPR-involved protein is IRE1 which occurs in two isoforms. While IRE1-α is present in all cells of the body, IRE1-β is only expressed in gut epithelium (Tirasophon et al., 2000; Wang and Kaufman, 2012). The endoribonuclease IRE1 is activated by auto-phosphorylation and induces the splicing of XBP1 (X-box binding protein 1) mRNA. Here, 26 nucleotides are removed resulting in a frame shift. Only the spliced XBP1 (sXBP1) is transcriptionally active and encodes a transcription factor for UPR target genes including chaperons and ERAD component. In contrast, the unspliced XBP1 (usXBP1) encodes a transcription factor which represses UPR target genes. Consequently, the ratio of spliced to unspliced XBP1 mRNA represents the level of UPR activation (Lee et al., 2002; Wang and Kaufman, 2012). Upon UPR induction, also the transmembrane kinase PERK is activated and inhibits eIF2α (elongation initiation factor 2α) by phosphorylation. This causes the attenuation of general protein translation to discharge the ER by reduced protein synthesis. In addition, PERK-eIF2α activates the transcription factor ATF4 which regulates the expression of genes which are involved in amino acid import, glutathione biosynthesis and resistance to oxidative stress (Fels and Koumenis, 2006; Harding et al., 2000). The complex network of UPR pathways is supposed to contribute to the recovery of the ER homeostasis. However, prolonged and very severe ER stress can cause inflammation and apoptosis, which is also due to activation of the transcription factor nuclear factor kappa B (NF-κB) which regulates the gene expression of pro-inflammatory cytokines and chemokines (Hotamisligil, 2010). Therefore, ER stress and the activation of UPR are considered to play an important role in inflammatory bowel diseases. In patients with UC and CD, ER stress has been established in intestinal epithelial cells from both inflamed and non-inflamed tissue of small and large intestine (Kaser et al., 2013). Furthermore, from genetic analyses it has been discovered that genetic loci from UPR factors such as XBP1 are associated with the risk for IBD. Thus, XBP1 deficiency in intestinal epithelium is associated with the development of spontaneous inflammation, similar to the inflammation in IBD with crypt abscesses and infiltration of inflammatory cells. Importantly in this regard, it could be demonstrated that XBP1$^{-/-}$ (IEC) mice are more sensitive to DSS induced colitis compared to wild type (Kaser et al., 2008).

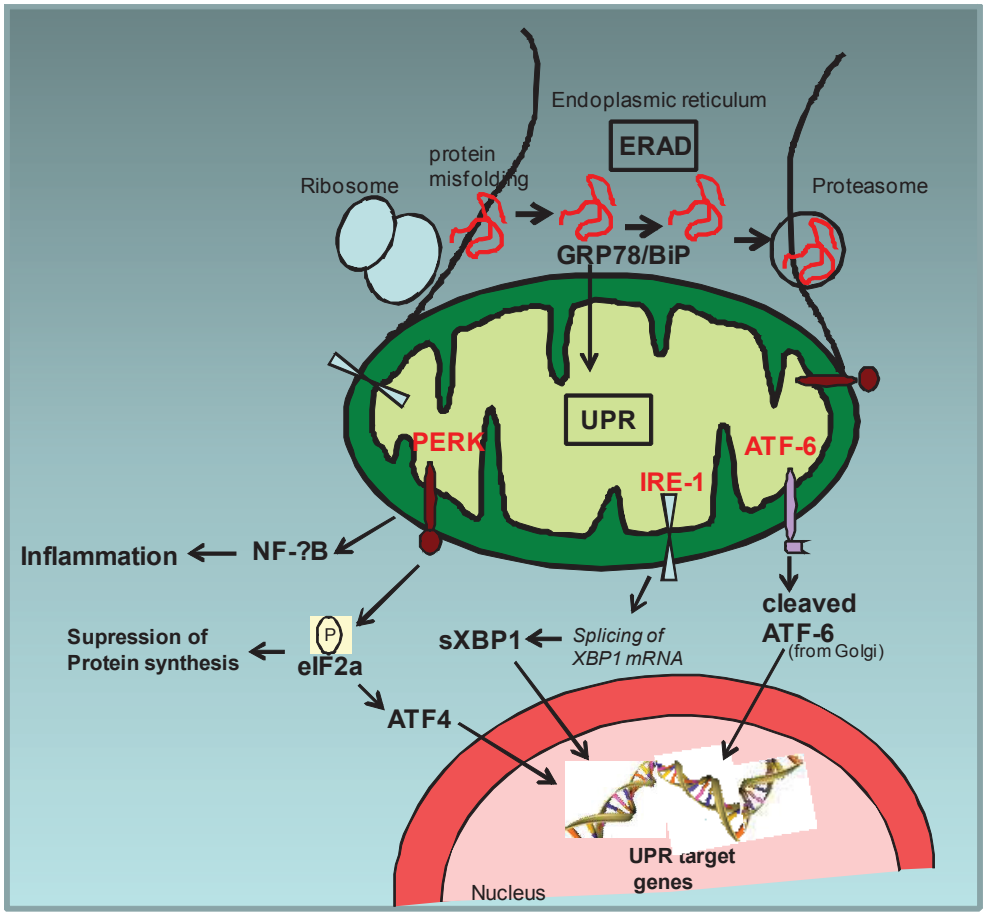

Figure 1.3: Endoplasmic reticulum (ER) stress induced by protein misfolding is associated with the activation of unfolded protein response (UPR) signalling pathways. Under non-stressed conditions the three membrane proteins IRE1 (inositol-requiring enzyme 1), PERK (protein kinase related-like ER kinase) and ATF6 (activating transcription factor 6) are inactivate due to their binding of heat shock protein HSP70 chaperon GRP78/BiP. Under conditions of ER stress, GRP78/BiP releases the three membrane proteins and binds the misfolded proteins to prevent the protein transport to Golgi. IRE1 induces the splicing of XBP1 (X-box binding protein 1) mRNA which encodes a transcription factor that represses UPR target genes. PERK inhibits eIF2α (elongation initiation factor 2α) by phosphorylation and causes thus suppression of protein synthesis as well as the activation of ATF4, a transcription factor for UPR target genes. Furthermore PERK activates NF-κB and thereby induces inflammation. After the detection of misfolded proteins, ATF6 is processed within the Golgi apparatus and the released cytoplasmic domain acts as transcription factor for UPR target genes. However, terminally unfolded/misfolded proteins activate the ER-associated degradation (ERAD). Based on (Boltin et al., 2013) and (Kaser et al., 2013).

1.1.7 Disrupted mucus barrier and aberrant mucins in IBD

In the gastrointestinal tract a mucus layer covers the epithelial cells to protect the epithelial surface against adhesion and invasion of microorganisms, bacterial toxins and antigens (Corazziari, 2009). This first line of defence in the gut is important for a competent epithelial

barrier function. The major components of the extracellular mucus are the secreted and cell surface mucins. The mucins are large complex O-glycosylated proteins categorised into two groups, the secreted and the cell surface mucins. The cell surface mucins such as Muc1 are important for cell signalling, adhesion and regulation of intestinal immune responses (McAuley et al., 2007; Van Klinken et al., 1995). In the gastrointestinal tract, nine different cell surface mucins (see Figure 1.4 A.) exist which are mainly expressed in enterocytes and occur on the apical membrane with large extracellular domains (Sheng et al., 2012).

A defect in the large glycoproteins can lead to disruption of the mucus barrier and may cause damage of the underlying epithelial cells by penetration of pathogens and infiltration of inflammatory cells, resulting in immune response and inflammation. Next to its barrier function, the mucus is also a major substrate and adhesion component for bacteria that live within the microenvironment of this layer. So, on the one side, the formation of microbial population can be influenced by altered mucin compositions, but on the other side, also a change of microbes and immunological factors in presence of inflammation can affect the mucin production (McGuckin et al., 2009; Sheng et al., 2012). The mucus consists of two layers, a thinner inner layer of around 100 µm and thicker outer layer of 700 µm. The inner firmly adherent layer is sterile, micro-aerobic and rich in anti-microbial peptides, which is critical for the gut homeostasis. The more loosely adherent outer layer is composed of degenerating mucins and contains diluted anti-microbials and some transiting bacteria (McGuckin et al., 2009) (see Figure 1.4 C.).

The major component of the intestinal mucus is the Muc2 mucin which is one of the six secreted mucins in the gastrointestinal tract (see Figure 1.4 A.). The Muc2 mucin is composed of a large protein backbone containing two central tandem repeat units (VNTR) with proline, threonine and serine repeated sequences, also called PTS domains (See Figure 1.4 B.). A large number of complex O-linked oligosaccharide chains are bound on the PTS domains which are sialylated and sulphated (Hansson, 2012; Thornton et al., 2008). This modifications lead to a highly negative surface charge and make the mucin resistant to protease action which is critical for their protective features. Additionally, Muc2 contains cysteine rich D domains, three within the N- terminal region and one within the C-terminal region. These domains can homo-oligomerise by building of inter-molecular disulphide bonds which give the viscous feature to the mucus (Linden et al., 2008; McGuckin et al., 2011; Sheng et al., 2012). The biosynthesis of Muc2 starts in the ER and after the N-glycosylation and dimerisation on their C-terminal domains follows the O-glycosylation and N-terminal oligomerisation in the Golgi (Heazlewood et al., 2008; Sheng et al., 2012). In a last step, the Muc2 is packed and stored in secretory granules. The most abundant Muc2 producing intestinal epithelial cells are the goblet cells. They store Muc2 in the so called theca from where the Muc2 is secreted constitutively and in a bigger amount after stimulation. Due to

the complex structure of the highly secreted protein, Muc2 is a favoured candidate for ER stress induction due to protein misfolding. It is proven that patients with UC possess a reduced mucus layer which correlates with a reduced number of goblet cells as well as a decreased Muc2 production and the accumulation of Muc2 precursor with immature glycosylation (Heazlewood et al., 2008; Van Klinken et al., 1999).

A.

Cell Surface Mucins	Secreted Mucins
Muc1, Muc3A, Muc3B, Muc4, Muc12, Muc13, Muc15, Muc16, Muc17	Muc2, Muc5AC, Muc5B, Muc6, Muc7, Muc19

B.

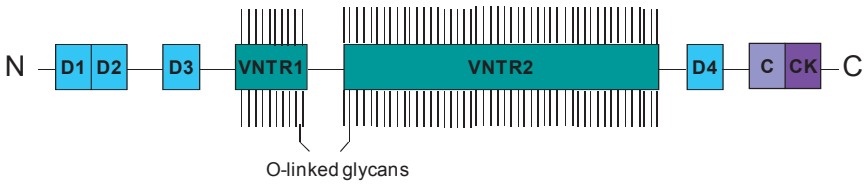

C.

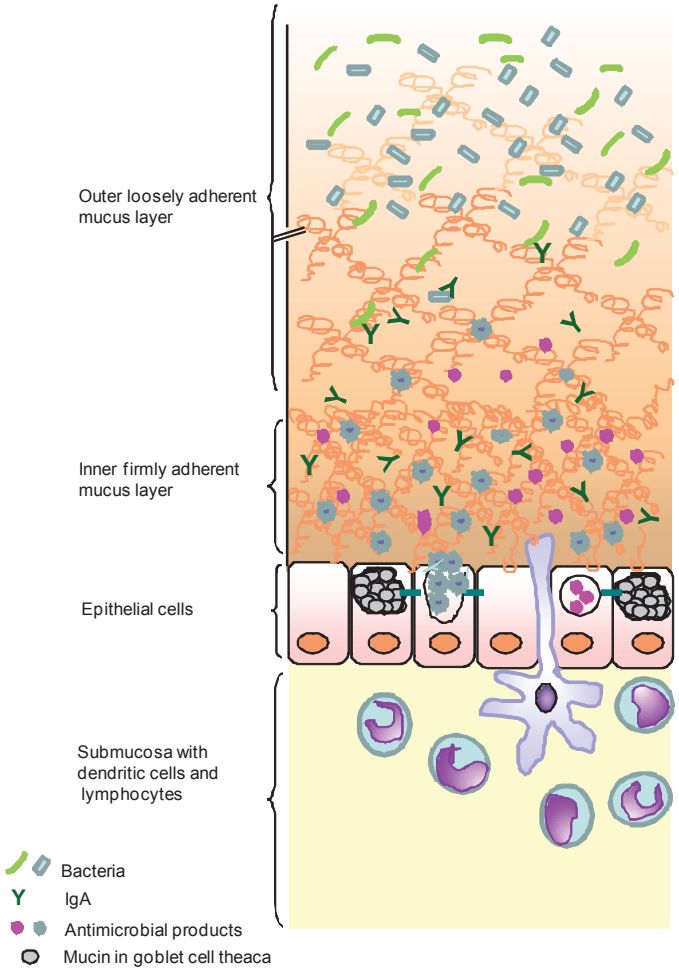

Figure 1.4: Mucins and the intestinal mucus barrier. Nine different types of cell surface mucins and six different types of secreted mucins are expressed in the digestive tract (panel A.). The major component of the intestinal mucus is the secreted Muc2 mucin. The Muc2 protein domain is composed of two central tandem repeat units (VNTR domains) which are heavily O-glycosylated. The four D-domains (D1 to D4) are involved in homo-oligomerisation and the cystine knot (CK) domain is involved in initial Muc2 dimerisation (see panel B.; modified after Sheng *et al.*, 2011); In Panel C. a schematic overview of the intestinal mucus barrier is shown. The outer loosely adherent barrier (composed of secreted mucins, i.e. Muc2) contains microbes, whereas the inner firmly adherent mucus layer (consists of cell surface mucins), rich in anti-microbials (secreted from epithelial cells) is sterile. In the healthy intestine, the epithelial cells are covered by the two mucus barriers. Modified after (Kim and Ho, 2010)

1.1.8 Mouse models of intestinal inflammation

The most commonly applied experimental approach to investigate colitis is the chemically induced model through DSS feeding of mice. This is being applied in conventional mouse strains, but also at increasing rate in transgenic and immunodeficient mice. The non-genotoxic sulphated polysaccharide is usually administered via the drinking water for 5 to 7 constitutive days and as such induces an acute colitis with blood diarrhoea, weight loss and the induction of ulcerations (Okayasu et al., 1990; Westbrook et al., 2010). The DSS is directly toxic to the intestinal epithelial cells and causes the disturbance of the intestinal crypts and the epithelial barrier, which results in infiltration of granulocytes into the mucosa. This mouse model is eligible to study the innate immune mechanisms of colitis as well as the epithelial repair mechanisms, whereas the adaptive immune system does not play an important role (Wirtz and Neurath, 2007). Moreover, using cyclic administration of DSS, chronic colitis is developed. Besides the DSS model, further chemically induced colitis models are hapten-induced colitis models using trinitrobenzene sulfonic acid (TNBS), dinitrobenzene sulfonic acid (DNBS) or oxazolone dissolved in ethanol (Morris et al., 1989; Wirtz et al., 2007). The use of chemicals is a very simple method to induce colitis-like symptoms in mice. Genetic models have the advantage that they likely reflect more physiologically relevant defects involved in IBD, along with the systemic reaction of the whole body. This is not only a benefit for pharmacological studies in regards to development of potential therapeutics for colitis treatment. The genetically induced colitis models can be grouped into models of impaired epithelial barrier function and bacterial sensing, impaired innate immune cells and impaired T and B cell regulation (Wirtz and Neurath, 2007). Commonly used genetically induced colitis models are listed in Table 1.

A recently introduced genetic model is the *Winnie* model. This is murine model of spontaneous colitis triggered by a missense mutation in the Muc2 mucin gene that causes ER stress. The generation of the *Winnie* mice occurred by N-ethyl-N-nitrosourea (ENU) treatment of wild type C57BL/6 mice which resulted in a single nucleotide polymorphism (SNP) in the D3 domain of Muc2 (see Figure 1.6). This mutation causes the replacement of cysteine with tyrosine in the N-terminal oligomerisation domain, resulting in a hyper-oligomerisation of Muc2. The aberrant assembled Muc2 protein accumulates in the ER, which results in distinctive ER vacuolization and induction of ER stress. Thus, the characteristic phenotype of *Winnie* mice arises with the depletion of the secreted mucus layer, which is linked to decreased goblet cell numbers, smaller goblet cell thecae, reduced secretion of mature Muc2, and an increased epithelial cell proliferation and apoptosis, similar to UC. Furthermore, the *Winnie* mice exhibit increased intestinal permeability and induction of spontaneous inflammation via the NF-κB pathway with increased production of T_H1, T_H2

and T_H17 cytokines such as IL1-β, IL-13, TNF-α and IFN-γ (Heazlewood et al., 2008; Sheng et al., 2012).

Table 1: Mouse models of genetically induced IBD

Animal model	Characteristic	Reference
1. Defects in epithelial barrier		
Mdr1α$^{-/-}$	Spontaneous bowel inflammation similar to UC caused by deficient transport protein p-glycoprotein resulting in dysfunction of epithelial cells	*(Panwala et al., 1998)* *(Schwab et al., 2003)*
Ikk-γ (NEMO)	NEMO $^{IEC-/-}$ mice demonstrate a primary epithelial defect resulting in impairment of integrity and antimicrobial defense of the gut epithelium and development of IBD-like disease	*(Nenci et al., 2007)*
DN N-cadherin	Expression of mutant adhesion molecule N-cadherin in IEC along crypt villus axis disturb proliferation, migration and death program, leading to CD like chronic inflammation and intestinal neoplasia	*(Hermiston and Gordon, 1995)*
2. Defects in innate immune system		
STAT3	STAT3 deficiency in myeloid cells offer enhanced Th1 activity and develops chronic intestinal inflammation	*(Takeda et al., 1999)*
A20	A20 deficiency causes spontaneous inflammation; also in mice lacking T and B cells; A20 inhibits TNF-induced NF-κB activity	*(Lee et al., 2000)*
3. Defects in adaptive immune system		
IL-2	IL-2 deficient mice develop spontaneous colitis due to altered immune system with enhanced number of activated T- and B cells, elevated Ig secretion and aberrant expression of class II MHC molecules	*(Sadlack et al., 1993)*
IL-10	IL-10-/- mice develop chronic enterocolitis with massive infiltration of lymphocytes, macrophages and neutrophils; IL-10 is suppressor of Th1 cells and macrophages	*(Kuhn et al., 1993)*
4. Stress response		
Agr2	Agr2-/- mice develop ER stress with increased XBP1 splicing causing spontaneous granulomatous ileocolitis and alterations in Paneth and goblet cells	(Zhao et al., 2010) (Zheng et al., 2006)

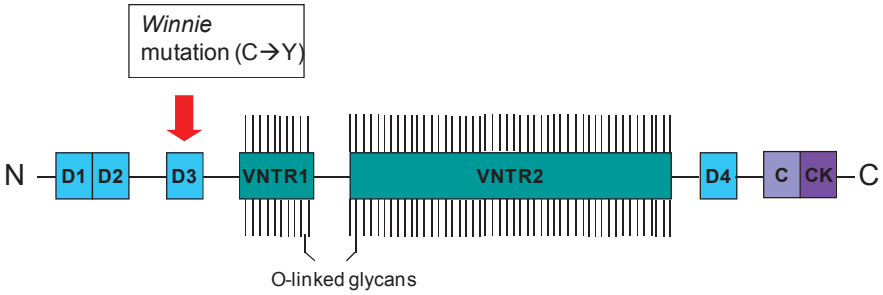

Figure 1.5: Single nucleotide polymorphism (SNP) in the D3 domain of Muc2.

With increasing age, clinical symptoms are developed in the model, which above all includes diarrhoea and rectal bleeding. These processes are very severe in 1 year old *Winnie* mice. The *Winnie* model confirms previous studies indicating that ER stress and the associated pathways are related to UC; this includes studies which established that the knockout of UPR involved proteins, such as IRE1β and XBP1, leads to intestinal inflammation and increased sensitivity to DSS-induced colitis (Bertolotti et al., 2001; Kaser et al., 2008).

1.1.9 Caco-2 cells

The Caco-2 cell line is widely used in laboratories as *in vitro* model of human intestine. The cells were originally isolated from the primary colon tumour of a 72-year-old Caucasian man. Cultured under normal conditions, the colon carcinoma cells are hyperproliferative epithelial cells with the gene expression pattern characteristic of human colon cancer cells. Due to their hyperproliferative nature they might represent an inflamed intestinal epithelium as it occurs in ulcerative colitis (Huang et al., 1997). However, the Caco-2 cells exhibit a further unique feature. Upon increased cell-cell contact they undergo a cell cycle arrest and accumulate in G_0/G_1 phase. After reaching confluence, therefore, Caco-2 cells lose their colonic phenotype and differentiate spontaneously to enterocyte-like cells with the expression profile of small intestine cells markers such as villin and various brush-border associated hydrolases like sucrose, lactase and alkaline phosphatase (Pinto 1983). Caco-2 cells are therefore also often used as an in vitro intestinal epithelial barrier model (Artursson, 1990; Hidalgo et al., 1989; Sambuy et al., 2005).

1.2 IBD therapeutics

Inflammatory bowel diseases are characterised by a dysregulation of immune responses, associate with the infiltration of inflammatory cells in the mucosa and the occurrence of epithelial barrier defects in the gut. Current therapeutic strategies aim to induce and maintain remission of chronic intestinal inflammation as well as mucosal healing and reduction of the inflammation-associated cancer development (Rutgeerts et al., 2007). Major therapeutic targets include inflammatory pathways such as NF-κB, which is an essential transcription factor of proinflammatory cytokines, as well as the mitogen-activated protein kinase p38, which is linked to TNF-α signalling and controls cellular responses to cytokines and cellular stress (Jobin and Sartor, 2000; Waetzig et al., 2002). A further common therapeutic target is the inflammatory cytokine TNF-α itself, which is mainly produced by macrophages and activates the NF-κB and mitogen-activated protein kinase (MAPK) pathways (Bosani et al., 2009). In recent years there has also been renewed interest in targeting IL-1β signalling (Hamilton et al., 2012).

For the treatment of IBD, the most commonly used conventional therapeutics are aminosalicylates, antibiotics, corticosteroids (CS), immunomodulators (e.g. thiopurines such as azathioprine (AZA) and 6-mercaptopurine (6-MP) and methotrexate). Additionally biological therapies such as anti-TNF-α agents (e.g. infliximab, adalimumab and certolizumab pegol) are applied as well as humanized monoclonal antibodies against the cellular adhesion molecule α_4 integrin (Afif and Loftus, 2010; Ali et al., 2012). However, many studies illustrate that the clinical efficacy of the conventional drugs is limited with a low rate of sustained remission. In addition, the use of CS, thiopurines and anti-TNF-α agents, and particularly the combination therapy of AZA and infliximab increase the risk of opportunistic infections dramatically (Toruner et al., 2008). Above all, certain therapeutics, including agents from the TNF-α based therapy cause malignancies (Bongartz et al., 2006). Due to these limitations and side-effects of the conventional medicine, the so called “complementary and alternative medicine” (CAM) approach gains more and more interest as therapeutic approach and is already commonly used in IBD treatment (Hilsden et al., 2011). One promising candidate that has been discussed herein is the ingredient of turmeric, curcumin.

1.2.1 Curcumin

Curcumin (diferuloylmethane) is derived from the rhizome of the herb *curcuma longa*, a member of the ginger family. The brightly yellow component of turmeric is a popular Indian spice and the most essential ingredient in curry powder. The hydrophobic polyphenol is used worldwide as cooking spice, flavouring agent and food colorant, listed under the internationally approved food additive list as E100. As such, amongst others, it is used to

colour mustard, mayonnaise, marmalade and for instance also present in the popular fruit gum candy “Gummy bears”. Chemically, curcumin is a bis-α, β-unsaturated β-diketone, exhibiting keto-enol tautomerism with a predominant enol form in acidic and neutral solutions, and a stable enol form in alkaline environment (see Figure 1.7). Depending on the substitution of the aryl rings by hydroxy or methoxy groups, different curcumin analogues can be formed. Naturally, the curcuminoids contain 77% diferuloylmethane, 17% demethoxycurcumin and 3% bis-demethoxycurcumin (Anand et al., 2008; Epstein et al., 2010b).

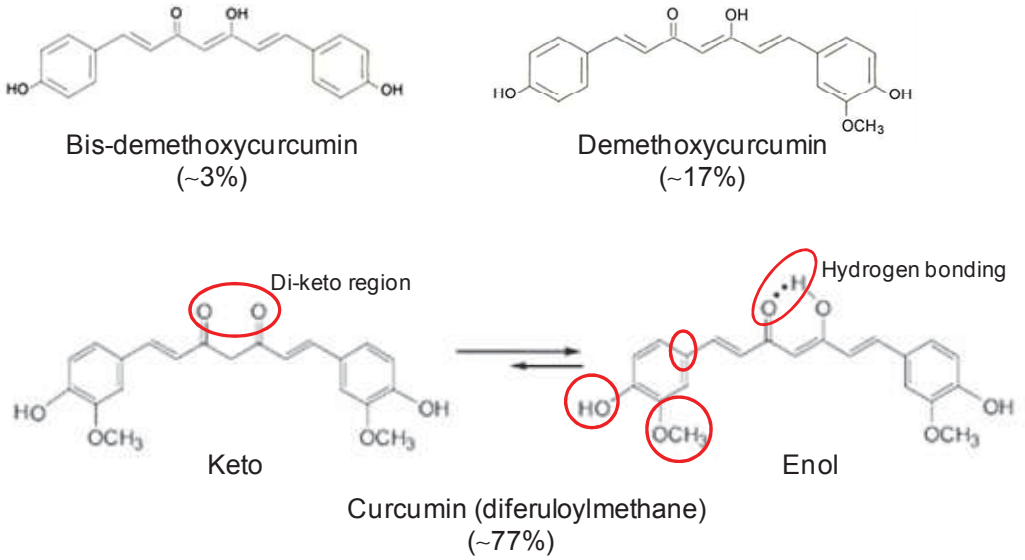

Figure 1.7: Chemical structure of curcumin (diferuloylmethane) and its natural analogues. Curcumin exists as keto-enol tautomer, with a more stable enol form. The apparent sites responsible for its antioxidative biological activities (by radical trapping) are highlighted.

Curcumin has already been used for at least 4000 years in the Indian Ayurvedic medicine and the Chinese medicine. Also in Western medicine curcumin gains more and more interest due to the established beneficial pharmacological effects, which include antioxidant, anti-inflammatory, antiproliferative, antiangiogenic and anticarcinogenic activities (Goel et al., 2008; Ramsewak et al., 2000; Ruby et al., 1995). Currently, the therapeutic potential of curcumin is analysed for many different diseases such as inflammatory diseases, neurodegenerative diseases, cardiovascular diseases, respiratory diseases and cancer. A particular focus for the use of curcumin is on the gut, also in view of the traditional oral uptake route by food. Many studies have provided clues for beneficial effects of curcumin in inflammatory bowel diseases such as ulcerative colitis. In different types of colitis models, the potential improvement of the colonic morphology and survival could be established, related to the downregulation of proinflammatory pathways (Ali et al., 2012; Billerey-Larmonier et al.,

2008; Camacho-Barquero et al., 2007; Deguchi et al., 2007; Sugimoto et al., 2002). By reducing cytokine and chemokine production, curcumin is considered to modulate proliferation and activation of many inflammatory cells including macrophages, T-cells and B-cells (Jagetia and Aggarwal, 2007). Also mucosal neutrophil infiltration was shown to be affected by an inhibition of the expression of chemoattractant molecules such as IL-1β. A prominent molecular target of curcumin is the NF-κB pathway (Larmonier et al., 2011). As underlying mechanism, it is suggested that curcumin inhibits the activation of IκB kinase (IKK) causing a reduced phosphorylation and degradation of the cytosolic NF-κB inhibitor IκB-α. These actions lead to cell cycle arrest, apoptosis and suppressed proliferation as well as the regulation of pro-inflammatory enzymes like cyclo-oxygenase 2 (COX2), 5-lipoxygenase and nitric oxide synthase. Also the activity of the MAP kinase p38 is inhibited by curcumin and thereby considered to contribute to the clinical benefits in gut inflammation, as well as cancer development (Shishodia et al., 2005a; Singh and Aggarwal, 1995).

In view of to the pre-clinical evidence of beneficial curcumin applications in inflammation, curcumin may be a novel promising therapeutic agent in several inflammatory diseases. Currently, in human trials, the clinical effect of curcumin is investigated in a variety of diseases, including IBD (reviewed in Epstein et al., 2010). However, until now only two human studies have been performed in response to encouraging results with curcumin and IBD. In a pilot study, Holt *et al.* observed improved clinical outcomes in patients with ulcerative proctosigmoiditis and CD, following repeated application of curcumin in a range of 360 mg and 550 mg up to 4 times daily for several months (Holt et al., 2005). In a randomized, double-blind, multicenter trial, Hanai *et al.* evaluated the treatment of 89 patients with quiescent UC for 6 months. One group with 45 patients received 1 g curcumin two times per day in combination with the conventional IBD therapeutic agent sulfasalazine or mesalamine. In the placebo group 44 patients received placebos plus sulfasalazine or mesalamine. In the curcumin group 2 of the 45 patients violated the protocol, but only 2 of the other 43 patients relapsed during the 6 month of the therapy (4.65%) in contrast to 8 of 39 patients (20.51%) relapsed in the placebo group. In addition to the significant difference in relapse rate, curcumin improved the clinical activity index and the endoscopic index which are associated with the morbidity of UC (Hanai et al., 2006). Based on these two studies curcumin application may be a promising and safe medication in IBD. Data from India indicate that the lifelong curcumin ingestion up to 100 mg per day is safe. In further human trials, it could be shown that even oral doses up to 12 g per day are safe, tolerable and non-toxic (Lao et al., 2006). After short-term, high dose administrations of curcumin only minor side effects such as diarrhoea have been observed. However, curcumin has a poor oral bioavailability in rodents and humans, this is due to a combination of an efficient first pass metabolism, poor gastrointestinal absorption, rapid elimination and a poor aqueous solubility

(Epstein et al., 2010b). Curcumin elimination is mostly driven by hepatic glucuronidation but also by sulphation (Pan et al., 1999). This indicates problems in efficiency of drug delivery. Moreover, some studies point out that curcumin has pro-oxidant potentials, and cytotoxic and DNA damaging effects have been shown *in vitro* (Li et al., 2008; Sandur et al., 2007). Therefore, new strategies have to be designed based on the drug formulation to improve the bioavailability and to reduce potential side effects. In this regard, strategies that use drug loaded nanoparticles play an increasing role.

1.3 Nanotechnology and the development of nanoparticles

The development and production of nanoparticles is gaining more and more interest in different economic fields such as food and cosmetic industry, automotive and microelectronic industry, but also in the medicine and pharmacology. Nanoparticles (NP) are defined as small particles with one or more external dimensions between 1 and 100 nm (Stone et al., 2009). In addition to the spherical particles, also nano-objects such as nanotubes, nanofibers, nanowires and nanorings are implicated in this definition (Oberdörster et al., 2005). Due to their small size, NP offer some new and specific physico-chemical properties compared to lager-sized microparticles of the same chemical composition (Oberdörster et al., 2005). As a consequence of the decreased particle size, the specific surface area (SSA) of smaller particles becomes exponentially increased, resulting in increased surface reactivity and thus enhanced biological activity (Oberdörster et al., 2005). As such, NP can possess various interesting and useful features that differ from larger sized particles e.g. in terms of solubility, biokinetic behaviour, light absorption and scattering properties etc. (Tiede et al., 2008).

The food industry already uses inorganic microparticles for a long time as approved food additives in conventional as well as functional foods. A daily ingestion of 10^{12}-10^{14} particles has been estimated, assumed with increasing tendency (Lomer et al., 2001; Lomer et al., 2004). Indeed, the food sector has shown increasing interests in the development and use of engineered NP because of various attractive features. For example, while microsize titanium dioxide (TiO_2) has been used for many decades as food whitener, nanosize TiO_2 which has lost its white colour, can be used as a transparent film to prevent confectionary products from melting or to improve food shelf life (Chaudhry et al., 2008; Gerloff et al., 2012a). Furthermore, TiO_2 NP also can operate as an oxygen barrier or UV absorber in food packaging products. Another known UV-absorber in plastics is silicon dioxide (SiO_2). Amorphous SiO_2 NP, which are also contained in cosmetics (e.g. in sunscreen and pharmaceutical products), are widely used as food additives e.g. in milk powders and instant soups (Chaudhry et al., 2008; Schmid and Riediker, 2008). Further metal oxide NP

established in food packaging include zinc oxide (ZnO) and magnesium oxide (MgO), due to their antimicrobial potential. Additionally, NP serve also as promising tool in medical diagnostics and in therapeutic approaches. Due to their characteristic biokinetics, they are very convenient amongst others for targeted drug delivery (Moghimi et al., 2005; Oberdörster et al., 2005). Various types of nanoparticles used in the nanomedical field as well as their specific application as promising diagnostic and therapeutic tool is discussed in detail in paragraph 1.3.3.

1.3.1 Nanosafety concerns

While nanotechnology represents a tremendously growing field, amongst others in the food sector and in medical applications, safety aspects of NP are also increasingly debated. In the early stages of nanotoxicology research, most studies were focused on the evaluation of potential adverse health effects of inhaled NP (Borm, 2002). Parallels were drawn between the potential health effects of inhaled NP and larger sized particles, like crystalline silica, diesel engine particles, coal mine dusts and asbestos, for which toxicity and pathogenicity is nowadays evident from classic toxicology and epidemiological research (Borm et al., 2004). Pioneering nanotoxicology studies with specific types of materials including nanosize carbon black and TiO_2, demonstrated that the inflammatory and pro-oxidative potential of NP is related to the greater surface area per unit mass, and hence they may represent an emerging risk (Brown et al., 2001; Oberdörster et al., 2005). However, it is very difficult to predict the hazards and risks of NP because several of their physico-chemical properties such as size, chemical composition and solubility all may have an impact on their mechanism of action. Importantly, the size and SSA of NP also influence their interactions with the microenvironment in biological systems, the rate and mechanism of uptake and subsequent subcellular translocation within cells (Unfried et al., 2007). Inhalation studies have shown that NP are less well recognised by alveolar macrophages, which resulting in increased contact with epithelial cells and interstitionalization, i.e. penetration into deeper regions of the lung (Donaldson et al., 2005; Ferin and Oberdorster, 1992; Unfried et al., 2007).

1.3.2 Potential mechanisms of nanoparticle toxicity

As discussed before, the adverse side effects of NP are depending very much on the feature of the specific particle type. Due to the high biological activity, specific NP interact more likely, and in a different manner with cells, and may have direct access to sub-cellular structures and molecules such as mitochondria, proteins and DNA. The cellular uptake of NP is triggered by different active or passive mechanism including phagocytosis,

macropinocytosis, clathrin-mediated- and non-clathrin-mediated endocytosis, caveolae-mediated endocytosis as well as diffusion, depending on the physicochemical properties of the NP and the exposed cell type (Unfried et al., 2007). As main mechanism contributing to NP toxicity, the generation of ROS is considered (Donaldson et al., 2005; Oberdörster et al., 2005). The NP-induced ROS formation can occur direct on the surface of metal containing particles via Fenton–like reactions, but also indirect upon singlet electron transfer which may be catalysed by NADPH oxidase or may arise as side reaction of electron transport along the mitochondrial respiratory chain (Klotz, 2002; Unfried et al., 2007). In both cases, molecular oxygen is reduced to $O2^{\cdot-}$, resulting in the formation of H_2O_2 (as already described in paragraphs 1.1.3 and 1.1.4). In addition, specific NP can offer photochemical reactivity by building of singlet oxygen ($^1O_2$), followed by conversion in $O2^{\cdot-}$ radicals. However, this mechanisms of NP-induced ROS generation is more relevant for skin exposure e.g. with NP-containing cosmetics. The NP-mediated ROS generation and associated oxidative stress induction can cause various adverse effects in cells. Depending on the concentration and persistence, these range can vary from activation pro-inflammatory and proliferative signal cascades to the induction of apoptosis and oxidative damage to cellular proteins, lipids and DNA (Clift and Rothen-Rutishauser, 2013; Unfried et al., 2007; Xia et al., 2006). Persistent, high levels of ROS are implicated in the induction of oxidative DNA lesions, mutagenesis and/or apoptosis (Schins and Knaapen, 2007). At less high concentrations which not induce harmful oxidative damage, ROS can also modulate cellular signalling cascades that control cellular proliferation and inflammatory processes (Barthel and Klotz, 2005; Unfried et al., 2007). Indeed, various types of NP have been demonstrated, respectively, to induce cell proliferation and the production of inflammatory mediators including cytokines and chemokines. Finally, even lower levels of ROS are associated with the induction of antioxidant defence responses, predominantly driven by the transcriptional factor Nrf2, serving to prevent or counteract the potentially adverse oxidative effects of NP (Nel et al., 2006).

A further mechanism by which NP may cause adverse health effects involves the action of inflammatory cells and mediators. As already mentioned specifically for IBD (see paragraphs 1.1.3 and 1.1.4), inflammatory cytokines and chemokines lead to the recruitment and activation of ROS and RNS-producing cells. Depending on the severity and persistence of these NP-driven inflammatory processes, the cellular antioxidant and DNA damage repair capacities are insufficient and may lead to cell and tissue remodelling and induction of DNA damage and mutagenesis (Schins and Knaapen, 2007). These mechanisms are well described and investigated for the effects of inhaled NP to the lung (Oberdörster et al., 2005), in marked contrast to the possible toxicity in the gastrointestinal tract for NP after oral uptake. In our group, Gerloff *et al.*, 2009 investigated the cytotoxic and DNA damaging

potential of various types of NP in the human intestinal Caco-2 cell line (Gerloff et al., 2009). Among others, amorphous SiO_2 and ZnO showed toxic potential in this experiment, and in a follow-up study, the additional impact of particle digestion was therefore evaluated with establishment of a NP pre-treatment protocol digestion-mimicking fluids prior to cell treatment (Gerloff et al., 2012b). Moreover, in this study, we compared the effects of the digested NP in both undifferentiated and differentiated Caco-2 cells. The latter, which after differentiation preserve characteristics of small intestine enterocytes, were found to be less sensitive with regard to the cytotoxic and pro-inflammatory properties of the NP (Gerloff et al., 2012b). In a further study, we evaluated the cytotoxic analysis of a panel of TiO_2 particles in the Caco-2 cell model, and figured out that both the SSA and the specific crystalline structure contribute to the toxicity of these types of NP: Whereas anatase-rutile mixture TiO_2 NP induced significant membrane damage and DNA strand breakage in proportion to the administered surface area, pure rutile TiO_2 samples showed no strong deleterious effects. Moreover, no role could be established for ROS formation, since effects were not associated with a panel of oxidative stress markers (Gerloff et al., 2012a). Taken together, these findings support the hypothesis that the intestine may be a relevant target for the potential adverse health effects of NP, and that these effects not solely depend on their small size but also on their chemical composition. In view of the steadily increasing interest in the use of NP in the food sector as well as in various applications in medicine and pharmacology, further research on nanosafety aspects is warranted.

1.3.3 Nanomedicine

The application of nanobiotechnology to medicine is defined as nanomedicine and based on the use of nanoscale materials in therapeutics, diagnostics and imaging (Parveen et al., 2012). This includes nanoscale robots and devices in nanosurgery, as well as different types of nanoparticulate systems, used as imaging agents for efficient diagnostic or as therapeutic agents for efficient drug delivery (Jain, 2010). A main focus in nanomedicine is the formulation of therapeutic agents in biocompatible carriers. Many conventional drugs are limited in their effects and efficacy due to poor solubility, aggregation, nonspecific delivery, high toxicity and short circulating half-lifes (Parveen et al., 2012). To improve the therapeutic value of drugs, NP can be used as drug-delivery systems, whereby the drugs can be loaded on NP by encapsulation, surface attachment or entrapment. The typical size range of the colloidal NP used in nanomedicine is about 10 to 1000 nm, unlike the classical nanoparticle definition, which ranges from 1 to 100 nm. This is explainable with the need to load a sufficient amount of drug onto the particles (De Jong and Borm, 2008; Sahoo and Labhasetwar, 2003). Different drug delivery systems are distinguishable, such as polymeric

NP, solid-lipid NP, ceramic NP, magnetic NP or metal based NP. Additionally, some microsized carriers exist such as polymeric micelles and dendrimers. These various carrier systems facilitate the release of bioactive agents at specific rate and at specific site, and is referred to a targeted drug delivery (Parveen et al., 2012). Due to their small size and often also because of further surface modifications, the designed NP are able to penetrate across biological barriers including the intestinal barrier, the blood-brain barrier and the alveolar-capillary barrier in the lung, to achieve improved accumulation of the drug at target site. As such, the therapeutic efficiency is improved and the toxic side-effects are limited (Yih and Al-Fandi, 2006). Further NP induced advantages are the protection from drug degradation and the increased solubility of drugs in aqueous solutions. The targeted drug delivery can take place by passive targeting based on the longevity of the carriers or by active targeting e.g. by conjugating carriers with cell or tissue-specific ligands or antibodies (Parveen et al., 2012). The therapeutic application of NP can vary from cancer therapeutics, vaccine or gene delivery and the specific targeting of current drugs. One of the best approved drugs in the nanoparticle scale is the albumin-bound paclitaxel, named Abraxane. This chemotherapeutic agent is already successfully used in phase III trials for breast cancer therapy (Gradishar et al., 2005).

Also polymeric NP play an essential role in targeted drug delivery due to their beneficial properties such as high biodegradability, biocompatibility and the good pharmacokinetic control, caused by simple surface modification and functionalization with different ligands. Depending on the preparation method of the polymeric NP, nanospheres or nanocapsules arise. Caused by their matrix-like structure, in nanospheres the therapeutic compounds are strongly absorbed at their surface, entrapped or even dissolved within the matrix. Nanocapsules are composed of a polymeric shell and an inner core, whereby the active substance is normally dissolved in the core, but can also be absorbed at the surface (Panyam and Labhasetwar, 2003; Pinto Reis et al., 2006; Sahoo and Labhasetwar, 2003). A prominent polymer to form drug loaded particles is the poly D,L-lactide co-glycolide (PLGA), which is synthesised by co-polymerisation of its two monomers, polylactide (PLA) and polyglycolide (PGA) (Jain, 2000) (Figure 1.8).

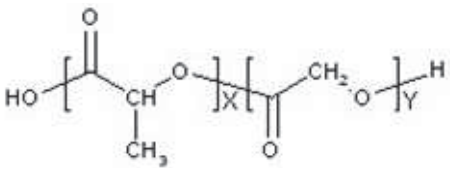

PLGA

X : number of units of lactic acid (PLA)
Y: number of units of glycolic acid (PGA)

Figure 1.8: Chemical structure of poly D,L-lactide co-glycolide (PLGA)

PLGA has a minimal systemic toxicity and a sustained drug delivery. A study in HeLa cells has established that paclitaxel-loaded PLGA NP exhibit a greater sustained antiproliferative activity, and thus are considered to have a promising future in clinical application (Yang et al., 2009). However, even though the use of nanobiotechnology approaches in medicine is very promising and the benefits seem to be large, there is still a strong research need to minimize potential risks.

1.3.4 Nanocurcumin

Currently, curcumin is tested in many in *in vitro* and *in vivo* studies in terms of its therapeutic potential in various diseases such as IBD, various types of cancer, cardio-vascular diseases and Alzheimer disease (Goel et al., 2008). As already described in paragraph 1.2.1, a wide variety of molecular targets of curcumin (NF-κB, glutathione, caspases and MAP kinases) could be identified, thus ascribing many beneficial cellular properties of this compound including anti-inflammatory, antioxidant, pro-apoptotic, anti-cancer and anti-bacterial properties (Anand et al., 2007; Biswas et al., 2005; Epstein et al., 2010a). However, the therapeutic potential of curcumin cannot by fully exploited due to its relative low solubility in water, its low bioavailability and poor pharmacokinetic behaviour. This limited efficacy is an essential handicap of curcumin and a main reason why its successful progress from the laboratory to the clinic is prohibited. Therefore, currently several different approaches of curcumin administration are being investigated including the development of synthetic analogues and complexation strategies with phospholipids and cyclodextrins, as well as its introduction into nanoparticle-based drug delivery (Bhawana et al., 2011; Maiti et al., 2007; Yallapu et al., 2010b). The design of nanoparticle drug delivery systems is a promising tool to improve the clinical efficacy of curcumin, because of the unique feature of the nanocarriers. Amongst others, nanocarriers can protect the drug from degradation, can prevent its interaction with the biological environment and also lead to an enhanced cellular uptake at the target tissue. Various nanoforms of curcumin are already developed and currently analysed as a potential therapeutic approach using *in vitro* as well as *in vivo* studies. In this context, used curcumin nanoforms include lipid-based NP, solid-lipid-NP, polymeric micelles, liposomes and dendrimers (Rachmawati, 2013). Most commonly used at present are polymeric NP such as PLGA encapsulated curcumin NP. PLGA polymers have a high biodegradability, biocompatibility and versatile degradation kinetic. In addition, PLGA is approved by the U.S. Food and Drug Administration for pharmaceutical applications.
Shaikh *et al.* demonstrated that curcumin loaded PLGA NP improved the oral bioavailability of curcumin at least 9-fold compared to curcumin administered with piperine as absorption

enhancer (Shaikh et al., 2009). Anand *et al*. established as well an improved bioavailability and a longer half-life of curcumin-PLGA NP *in vivo*. They also showed enhanced cellular uptake and inhibition of cancer cell growth due to the increased bioactivity *in vitro* (Anand et al., 2007; Anand et al., 2010). Investigations by Yallapu *et al.* exhibited an increased therapeutic effect of PLGA encapsulated curcumin in metastatic cancer cells (Yallapu et al., 2010a).

Summarizing, a number of previous studies demonstrate promising capacities of nanocurcumin particles (NC). However, to date most studies of NC focus on the preparation technique with different materials and the potential therapeutic application in cancer treatment. So far, not much is known about the usefulness of nanocurcumin in inflammatory diseases including IBD. More studies are needed to investigate the generally pharmacological features of nanocurcumin, as well as its safety, in inflammatory diseases, in particular also its efficiency and efficacy in the treatment or prevention of inflammatory bowel diseases.

2. Aim of the thesis

Inflammatory bowel diseases (IBD) have a high incidence in industrialized countries with a dramatically increase in the 20th century. As declared per European Crohn's and Colitis Organisation, more than 3 million people are affected in Europe. IBD is characterised by periodic exacerbation and remission of symptoms such as abdominal pain, bloody diarrhoea and altered bowel habits, often also resulting in cancer development. A high morbidity and mortality is associated with this disease (Hendrickson et al., 2002). Even the pathophysiology is still not completely understood, it is noted that environmental, immunological and genetic factors can influence the development of IBD. It is assumed that a disturbed immune homeostasis in the intestine may contribute to the chronic inflammation with enhanced innate and adaptive immune responses. Many studies highlight the essential role of NF-κB which represents a master regulator of the expression of many pro-inflammatory cytokines and chemokines (Wullaert, 2010). Furthermore, alterations in mucin expression are often established in IBD, causing defect mucosal barrier integrity with an increased infiltration of immune cells in the epithelium (Eri et al., 2010). In the first line of host defence, neutrophils play an important role and it could be shown that the number of neutrophils which accumulates within the intestinal mucosa correlates with the clinical diseases activity (Naito et al., 2007). Amongst others, neutrophil- induced ROS production and oxidative stress leads to increased epithelial injury. Finally, ER stress and the failing of unfolded protein response are also linked to IBD (Niederreiter and Kaser, 2011).

So far, however, the clinical efficacy of the currently used therapeutics is limited, due to a low sustained remission and an enhanced infection risk as well as malignancies (Ali et al., 2012). The use of herbal medications in IBD, such as curcumin, gains strong interest, also due to promising effects from *in vitro* and *in vivo* studies. Curcumin possesses many beneficial pharmacological effects such as anti-inflammatory and antioxidative bioactivities. However, due to its poor water solubility, low bioavailability and rapid metabolism in the human body, the efficiency of curcumin is also limited. To increase the cellular uptake and to prevent rapid drug degradation, the formation of nanosized curcumin drug delivery systems seems to be a promising tool. Herein, the polymeric nanocarrier PLGA represents an interesting approach, due to its high biodegradability, biocompatibility and versatile degradation kinetic (Anand et al., 2010).

The aim of the present thesis was to generate and characterise PLGA encapsulated curcumin NP and to analyse their potential therapeutic efficacy using *in vitro* and *in vivo* models of IBD, in particular of UC.

In the first stage of the project, nanocurcumin was prepared, and characterised for its particle size, polydispersity index, zeta potential and the release kinetics of the curcumin. In the second, i.e. *in vitro* part, the potential antioxidant properties of nanocurcumin versus non-encapsulated, free curcumin, as well as their respective cytotoxicity were tested in the human Caco-2 epithelial cell line. To explore the bioactivity and therapeutic properties of nanosized versus bulky curcumin, the antioxidative capacity and preventive properties against oxidant induced DNA damage were evaluated. In the third, i.e. *in vivo* part, two different murine models of colitis, the DSS-induced colitis model and the *Winnie* model, were used to investigate and compare the therapeutic efficacies of nanocurcumin and curcumin. In the DSS model, colitis-like symptoms were chemically induced in C57BL/6 mice, whereas the *Winnie* mice represent a spontaneous genetically-induced colitis model featuring altered mucin expression and assembly due to a missense mutation in the Muc2 mucin gene (Heazlewood et al., 2008; Wirtz et al., 2007). In both colitis models the effects of nanocurcumin and curcumin were monitored by analysing body weight, colon length, colon weight, colitis score, histopathology and mucin expression. Additionally the mRNA expression was evaluated of pro-inflammatory genes, ER stress marker genes and oxidative DNA damage repair genes as well as the protein expression of a panel of inflammatory cytokines.

3. Materials and Methods

3.1 Materials

3.1.1 Chemicals

Name	Company, Head Office
Alcain blue	Merck Millipore, Darmstadt, Germany
Acetic acid	Sigma-Aldrich, St.Louis, USA
Ammonium chloride	Merck Millipore, Darmstadt, Germany
Bicinchoninic acid solution	Sigma-Aldrich, St.Louis, USA
Bio-Plex murine cytokine 11-plex panel	BioRad, Hercules, USA
Bovine serum albumin	Sigma-Aldrich, St.Louis, USA
L-Buthionine-sulfoximine	Sigma-Aldrich, St.Louis, USA
Calcium chloride	Merck Millipore, Darmstadt
Cell proliferation reagent WST-1	Roche, Basel, Switzerland
Chloroform	Sigma-Aldrich, St.Louis, USA
Complete Protease Inhibitor	Roche, Basel, Switzerland
Copper(II)sulfate solution	Sigma-Aldrich, St. Louis, USA
Curcumin (> 94 %)	Sigma-Aldrich, St.Louis, USA
DEPEX mounting medium	Serva, Heidelberg, Germany
Dulbecco's Ca^{2+}/Mg^{2+}-free phosphate buffered saline (PBS)	Sigma-Aldrich, St.Louis, USA
EDTA	Roche, Basel, Switzerland
Ethanol (> 99.8 %)	Carl Roth, Karlsruhe, Germany
Ethylenediaminetetraacetic acid disodium salt dehydrate (EDTA)	Carl Roth, Karlsruhe, Germany
Fetal calf serum (FCS)	Sigma-Aldrich, St.Louis, USA

Glucose	Sigma-Aldrich, St.Louis, USA
Glycine	Carl Roth, Karlsruhe, Germany
Haematoxylin	Merck Millipore, Darmstadt, Germany
Hanks balanced salt solution	Invitrogen, Carlsbad, USA
High Pure RNA Isolation Kit	Roche, Basel, Switzerland
Hydrogen peroxide	Carl Roth, Karlsruhe, Germany
iQ SYBER Green Supermix	BioRad, Hercules, USA
iScript™ reverse transcriptase	BioRad, Hercules, USA
Isopropanol	Sigma-Aldrich, St.Louis, USA
L-glutamine	Sigma-Aldrich, St.Louis, USA
Glutathione	Sigma-Aldrich, St.Louis, USA
Glutathione reductase	Sigma-Aldrich, St.Louis, USA
Low melting point agarose	Sigma-Aldrich, St.Louis, USA
LymphoPrep	Axis Shield, Heidelberg, Germany
Magnesium chloride	Merck Millipore, Darmstadt, Germany
Minimum essential Medium (MEM) with Earle's salts	Invitrogen, Carlsbad, USA
NP-40 (Igepal)	USB, Cleavland, USA
Nuclease-free water	Quiagen, Hilden, Germany
Penicillin-Streptomycin	Sigma-Aldrich, St.Louis, USA
Periodic acid	Sigma-Aldrich, St.Louis, USA
Phorbol myristate acetate	Sigma-Aldrich, St.Louis, USA
Potassium bicarbonate	Sigma-Aldrich, St.Louis, USA
Potassium chloride	Merck Millipore, Darmstadt, Germany
Potassium phosphate (KH2PO4)	Merck Millipore, Darmstadt, Germany
Di-Potassium hydrogen phosphate	Merck Millipore, Darmstadt, Germany
ProLong® Gold antifade reagent	Invitrogen, Carlsbad, USA
Ro19-8022	Roche, Basel, Switzerland
Schiff's reagent	Merck Millipore, Darmstadt, Germany

Sodium chloride	Carl Roth, Karlsruhe, Germany
Sodium deoxycholate	Merck Millipore, Darmstadt, Germany
Sodium dodecyl sulphate	Sigma-Aldrich, St.Louis, USA
Sodium hydroxide	Sigma-Aldrich, St.Louis, USA
5-Sulfosalicylic acid dihydrate	Sigma-Aldrich, St.Louis, USA
Tris	Carl Roth, Karlsruhe, Germany
Trypsin	Sigma-Aldrich, St.Louis, USA
Triton X-100	Sigma-Aldrich, St.Louis, USA
Trizol	Invitrogen, Carlsbad, USA
TWEEN80	Serva, Heidelberg, Germany

- Formamidopyrimidine glycosylase enzyme (Fpg) was kindly provided by Prof. Andrew Collins (University of Oslo)
- Ro19-8022 compound was a kind gift from Hoffmann-LaRoche (Basel, Switzerland)

3.1.2 Laboratory equipment/ consumables

Name	Company, Head Office
Falcon tubes	BD Bioscience, Canaan, USA
Microliter pipets research (0.5 – 1000µl)	Eppendorf, Hamburg, Germany
Pipettips	Greiner bio-one, Freckenhausen
Reaction tubes (0.5 - 2.0 ml)	Eppendorf, Hamburg, Germany
Pipetus	Hirschmann Laborgeräte, Eberstadt, Germany
Tissue culture flasks with filter (75 cm^2)	Greiner bio-one, Freckenhausen, Germany

Tissue culture plates (6-wells, 96-wells)	Greiner bio-one, Frickenhausen, Germany
Realtime-PCR 96 well Plate	Peqlab, Erlangen
UV-cuvette	Brand, Wertheim

3.1.3 Technical equipment

Name	Company, Head Office
BX60 microscope	Olympus, Japan
Camera AxioCam MRc	Carl Zeiss, Jena, Germany
Centrifuge 5417R	Eppendorf, Hamburg, Germany
Dialysis membrane Viva Flow 50	Sartorius Stedim Biotech, Göttingen
Hera Cell 240 incubator	Thermo Fischer Scientific,USA
High speed homogenizer Ultra Turrax	IKA Werke, Staufen, Germany
Microscope Axiophot	Carl Zeiss, Jena, Germany
Multiscan Ascent plate reader	Labsystems Oy Helsinki, Finland
NanoSight	NanoSight, Amersbury, UK
Photometer Bio	Eppendorf, Hamburg, Germany
Power supply PS1006	Aplexe, France
Realtime-PCR System iQ5	BioRad, Hercules, USA
Sonorex TK52 water-bath	Bandelin, Berlin, Germany
Thermocycler professional	Biometra, Göttingen, Germany
Transmission electron microscope CM200	Philips, Netherland
Zetasizer Nano	Malvern Instruments, Herrenberg, Germany

3.1.4 Primer Sequences

Murine Primer:

IL-1β Forward	5'-CAACCAACAAGTGATATTCTCCATG-3'
IL-1β Reverse	5'-GATCCACACTCTCCAGCTGCA-3'
Muc2 Forward	5'-CCATTGAGTTTGGGAACATGC-3'
Muc2 Reverse	5'-TTCGGCTCGGTGTTCAGAG-3'
IL-23 Forward	5'-TCCCTACTAGGACTCAGCCAAC-3'
IL-23 Reverse	5'-GCTGCCACTGCTGACTAGAA-3'
Unspliced XBP-1 Forward	5'- CAGCACTCAGACTATGTGCACCTC - 3'
Unspliced XBP-1 Reverse	5'- AAAGGATATCAGACTCAGAATCTGAAGA-3'
Spliced XBP1 Forward	5'-GAGTCCGCAGCAGGTGC-3'
Spliced XBP1 Reverse	5'-CAAAAGGATATCAGACTCAGAATCTGAA-3'
β-actin Forward	5'-GAAATCGTGCGTGACATCAAA-3'
β-actin Reverse	5'-CACAGGATTCCATACCCAAG-3'
TNFα Forward	5'-AGGCTGCCCCGACTACGT-3'
TNFα Reverse	5'-ACTTTCTCCTGGTATGAGATAGCAAAT-3'
Ogg1 Forward	5'-CCAAGGTGTGAGACTGCTGAGA-3'
Ogg1 Reverse	5'-AGCAATGTTGTTGTTGGAGGAA-3'
APE/Ref-1 Forward	5'-TCAAGAAGGCCGGGTGATT-3'
APE/Ref-1 Reverse	5'-TTGGGAACATAGGCTGTTACCA-3'

Human Primer:

HO-1 Forward	5'-AACTTTCAGAAGGGCCAGGT-3'
HO-1 Reverse	5'-CCT CCAGGGCCACATAGAT-3'
γ-GCS Forward	5'- GACAAAACACAGTTGGAACAGC-3'
γ-GCS Reverse	5'-CAGTCAAATCTGGTGGCATC-3'
β-actin Forward	5'-CCCCAGGCACCAGGGCGTGAT-3'
β-actin Reverse	5'-GGT CAT CTT CTC GCG GTT GGC CTT GGG GT-3'

3.2 Methods

3.2.1 Preparation of PLGA-encapsulated curcumin

The PLGA-encapsulated curcumin nanoparticles and the PLGA vehicles, i.e. “blank nanoparticles” were prepared by an emulsion-diffusion method (emulsification solvent evaporation method) as illustrated in Figure 3.1. Therefore, 20 mg curcumin (Sigma) and 100 mg poly(lactic-co-glycolic acid) (PLGA) in ratio 1:1 respectively only PLGA were dissolved in 5 ml ethyl acetate (AcOEt) while stirring for 1 hour at room temperature. This organic phase was added dropwise via a peristaltic pump to the equal amount of aqueous solution containing polyvinyl alcohol as surfactant stabilizer (PVA 2% w/v, pH 7.3). To form an emulsion, the biphasic solution was emulsified in a high speed homogenizer (Ultra Turrax, IKA Werke GmbH & Co.) at 20,000 x g for 10 minutes. The addition of water to the emulsion under gentle stirring forces the complete diffusion of organic solvent to the aqueous phase. By this diffusions step the dispersed droplets were converted into nanocapsules. Afterwards the solvent was evaporated by continuous stirring over night. Finally, the particles were filtered by using a dialysis membrane (Viva Flow 50, 10 000 MWCO PES, from Sartorius Stedim). The particles were then washed in water and freeze dried. Three different batches of nanocurcumin (NC) and two batches of PLGA vehicles were prepared and used for the studies described in the *in vitro* experimental part of this thesis. In addition, nanocurcumin particles with sorbitol (NC-S) were produced for application in the *in vivo* investigations. For this purpose, the same procedure with emulsion- diffusion method was used as described before. However, the emulsification was performed by homogenization at 13 000 rpm for 20 minutes and the purified suspension was freeze dried using D-sorbitol as cryoprotectant at a ratio of 1:1 calculated relatively to the amount of PLGA. In total three batches of NC-S and one batch of PLGA-S was produced for these experiments. All particles were stored at 4°C and protected from light.

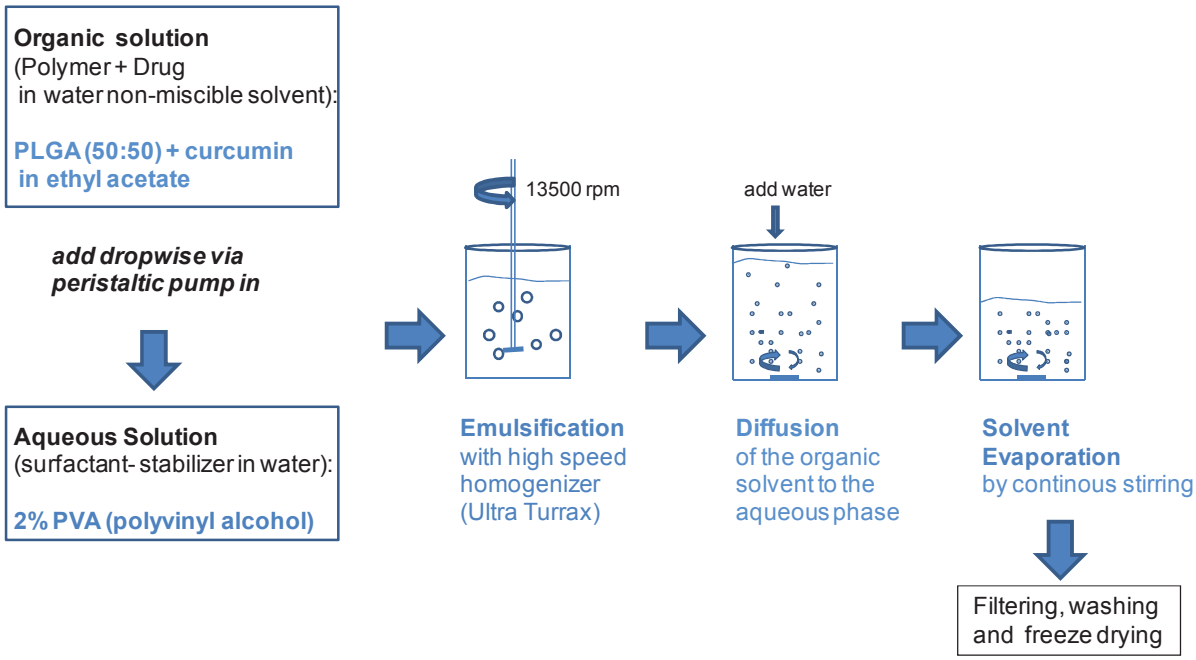

Figure 3.1: Emulsion-Diffusion method

3.2.2 Physical characterisation of nanocurcumin and PLGA vehicle particles

3.2.2.1 Particle characterisation by Zetasizer Nano ZS

The prepared NC and the PLGA vehicles were analysed in particle size, zeta potential and polydispersity index. Therefore, the Zetasizer Nano ZS from Malvern was used. This system is based on the principle of dynamic light scattering as explained in further detail in the following paragraphs. All measurements were performed in triplicate. For the experiments performed in the framework of this thesis, three different batches of nanocurcumin particles, four different batches of nanocurcumin particles with sorbitol, two different batches of PLGA vehicles and three different batches of PLGA vehicles with sorbitol were used, respectively. The mean average of particle size was calculated from all batches.

3.2.2.1.1 Size determination of particles

The thermal movement of particles suspended in a liquid (Brownian motion) is related to the size of particles which is observed and measured by illuminating the particles with a laser and analysing the rate of intensity fluctuations in the scattered light. Small particles move quickly and large particles move more slowly under these conditions. This relationship between the particle size and the speed of Brownian motion is defined in the Stokes-Einstein equation. The Zetasizer Nano measures the fluctuation in scattering intensity via a digital correlator which basically measures the degree of similarity between two signals over a

period of time. Due to the fact that small particles move quickly, the signal of the scattered light will change quickly and consequently the scattering intensity will fluctuate quickly. Large particles move slowly, therefore the scattering intensity fluctuation is also slow. This implies that large particles scatter more light than small particles.

3.2.2.1.2 Zeta potential principle

Since the particles are charged, when suspended, the opposite charged ions in the surrounding liquid become attracted to the surface of the particles. An electrical double layer is built up around each particle. In the inner layer, the so called Stern layer, ions are strongly bound to the particle, whereas in the outer layer, ions are less tightly attached (see also Figure 3.2). Within the diffuse layer a fictive boundary exists, referred to as slipping plane. Here, the ions and particles build a stabile unit and these ions will move with the particle in the liquid. Any ions outside of this boundary do not migrate with the particle. The electrostatic potential (charge) at this slipping plane is called the zeta potential and can be analysed by determination of the electrophoretic mobility. Accordingly, the movement of the charged particle in an applied electric field is measured by the Zetasizer apparatus. Suspended particles with a large negative or positive zeta potential have no tendency to flocculate due to the rejection of the same charge. A high zeta potential value prohibits that the particles agglomerate together, and thus, particles with a zeta potential more positive than +30 mV or more negative than – 30 mV are considered stable.

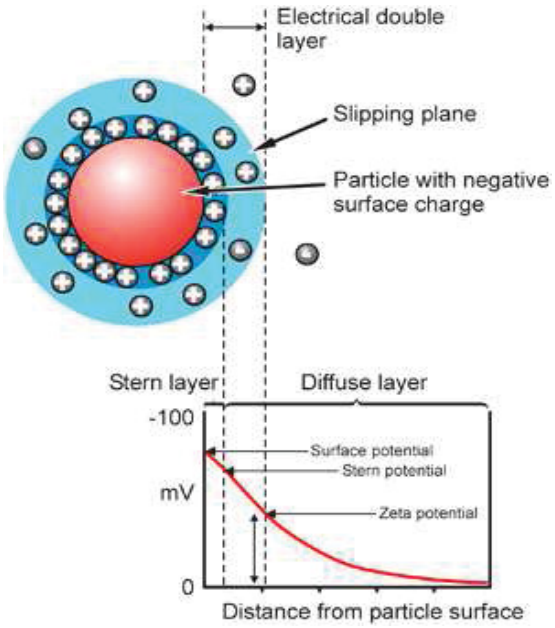

Figure 3.2: Electrical double layer on the particle surface and zeta potential (source: Zetasizer Nano manual)**.**

3.2.2.1.3 Polydispersity index

The polydispersity index exhibits the heterogeneity of sizes of polymers or particles within a suspension. This parameter can be determined by dynamic light scattering with the Zetasizer Nano. According to the the definition of IUPAC (International Union of Pure and Applied Chemistry), the dispersity of molecular weight ($Đ_M$) is the ratio of weight-average molecular weight (M_w) to the number-average molecular weight (M_n):

$$Đ_M = M_w/M_n.$$

3.2.2.2 Particle characterisation by NanoSight

The particles were also analysed by NanoSight using the nanoparticle tracking analysis (NTA) approach. This method is based as well on the measurement of the Brownian motion behaviour of nanoparticles within a liquid. In contrast to the dynamic light scattering (DLS) principle of the Zetasizer apparatus, which measures the time dependent scattering intensity fluctuations, the NTA is based on a laser illuminated microscope technique. With this tool individual particle motions can be analysed in real-time by a charge-coupled device (CCD) camera. The individual positional changes of each particle are tracked by the NanoSight sysyem in two dimensions and the size is determined from the analysis of the average speed of movement (Saveyn et al., 2010).

3.2.2.3 Particle characterisation by Transmission electron microscopy

The morphology of the curcumin loaded PLGA nanoparticles were analysed by a Philips CM200 transmission electron microscope (TEM) equipped with a Schottky cathode using an accelerating voltage of 200 kV. The detection principle of transmission electron microscopy is based on the scattering absorption effect at the atomic shells forming a light-dark contrast which reveals the particle shape. With this microscopic method a resolution of 0.1 nm can be achieved. To analyse the PLGA encapsulated curcumin morphology, the nanoparticles were resuspended in H_2O. The particle suspension was dropped on a copper grid coated with amorphous carbon serving as a semitransparent substrate. The suspension was dried in air and then transferred into the vacuum chamber of the TEM electron microscope. The shape of the particles was imaged with the use of a CCD camera (Gatan Multiscan Kamera Modell 794).

3.2.3 Curcumin release kinetics of PLGA-encapsulated curcumin

For the evaluation of the release of curcumin from the PLGA vehicle, the PLGA-encapsulated nanocurcumin (NC) was suspended in phosphate buffered saline (PBS)-Tween buffer to represent a physical environment. Twenty mg of the particles were suspended in 4 ml PBS with 1% Tween 80, and then 2 ml were transferred into a dialysis membrane. The membrane was placed in 200 ml PBS with 1% Tween 80. Under stirring conditions, after 1, 2, 3, 4, 6, 8, 10, 16, 24, 28, 32 and 48 hours, 1 ml aliquots were taken from the 200 ml buffer tank and immediately replaced with 1 ml buffer. The curcumin concentrations in the buffer samples were analysed by measurement of the curcumin auto fluorescence using a plate reader (λ_{Ex}= 420 nm; λ_{Em}= 530 nm). A curcumin standard in ethanol with PBS-Tween (1:1) was prepared with serial dilutions from 10 µM to 0.1 µM, and the curcumin release kinetics were then determined by calculation from the regression curve. The percentage of released curcumin was estimated from the initial concentration of curcumin which was contained in the inserted particle amount.

3.2.4 Curcumin encapsulation efficiency of nanocurcumin with D-sorbitol

To analyse the encapsulation efficiency nanocurcumin with D-sorbitol (NC-S) was dissolved in a mixture of ethanol/Milli Q water (1/1 v/v) under stirring at room temperature for two days to remove the encapsulate curcumin.

A curcumin stock solution of 5 mg curcumin in 100 ml ethanol/Milli Q water (1/1 v/v) was used to prepare a standard with different concentrations in ethanol/Milli Q water (1/1 v/v) and to design a calibration curve. The encapsulation efficiency was determined by measuring of absorbance of 100 µl of the standards and the samples at 432 nm using a plate reader. The encapsulation efficiency is defined in following equation:

encapsulation efficiency % = *m(curcumin encapsulated)*/ m(*curcumin initial*) x 100.

3.2.5 Caco-2 cell line culture

The human colon adenocarcinoma cell line Caco-2 was obtained from the Deutsche Sammlung von Mikroorganismen und Zellkulturen GmbH (DSMZ), Germany. The cells were cultured in minimal essential medium (MEM) with Earle´s salts and Non Essential Amino Acids supplemented with 20% Foetal Calf Serum (FCS), 30 IU/ml penicillin-streptomycin and 1% L-glutamine. The cells are grown and maintained in a cell incubator at 37°C with 95% air and 5% CO_2 in the atmosphere as well as 100% relative humidity. Cells were trypsinized at near confluence and for experiments 4 x 10^4 cells per cm^2 were seeded into six-well tissue culture plates or 96-well tissue culture plates, respectively. Cells were then grown overnight, thereby achieving approximately 50% - 60% confluence prior to treatment.

3.2.6 Nanocurcumin and curcumin treatment of Caco-2 cells

For treatment of the Caco-2 cells, nanocurcumin was suspended in starvation culture medium (i.e. culture medium without FCS) whereas curcumin was suspended in 100% ethanol followed by sonication (Sonorex TK52 water-bath; 60 Watt, 35 kHz) for 10 minutes. The indicated concentrations of nanocurcumin and curcumin, respectively, were diluted in starvation culture medium and then directly added to the cells. The final ethanol concentration in the curcumin samples was 0.15%, except for the glutathione assay experiments. Here, the ethanol concentration was 0.5%. After treatment, the cell monolayers were rinsed repeatedly with PBS to remove detached cells and their debris as well as to remove excess of extracellular nanocurcumin particles that might interfere with the various assays.

3.2.7 Caco-2 co-incubation with neutrophils

3.2.7.1 Isolation of neutrophils

Peripheral blood from healthy donors was used to isolate polymorphonuclear neutrophils (PMNs). Ten ml of the heparinized blood was diluted 1:1 with cold Hanks´ balanced salt solution ($HBSS^{+/+}$) and 20 ml of the diluted blood was slowly layered on the top of 15 ml lymphoprep (Axis Shield). After centrifugation for 20 minutes at 660 x g and 4°C, the white cell band, containing the lymphocyte-and monocyte fraction was carefully removed with a sterile pipette. The lymphoprep phase and the rest of the supernatant were also removed before the erythrocyte pellet was carefully resuspended in 40 ml lysis buffer (155 mM NH_4Cl, 10 mM $KHCO_3$, 10 mM EDTA, pH 7.4). The erythrocytes were lysed on ice for approximately

20 to 30 minutes till the suspension got a clear dark-red colour and every 5 minutes the cells were carefully shaken. This was followed by centrifugation at 150 x g and 4°C for 5 minutes. The red coloured supernatant was decanted and the pellet was lysed again for 5 minutes on ice. After the next centrifugation (150 x g, 4°C for 5 min) the pellet was washed twice in $HBSS^{+/+}$, and PMNs were counted by a hemocytometer from Neubauer.

3.2.7.2 Co-incubation

Caco-2 cells were cultured in 6 well-plates as described above and pre-treated with indicated concentrations of nanocurcumin or curcumin for 24 hours. Afterwards Caco-2 cells were co-cultured with freshly isolated and phorbol myristate acetate (PMA)-activated neutrophils in a ratio 1:1 for 30 minutes in $HBSS^{+/+}$. Following incubation, the Caco-2 cells were rinsed twice with cold PBS to remove the attached PMNs.

3.2.8 *In vivo* models of colitis to address the therapeutic potential of nanocurcumin and curcumin

In this project two murine models of colitis were used to investigate the potential therapeutic effects of nanocurcumin, and by comparison of curcumin: the DSS model, representing a widely applied chemically induced colitis model and the Winnie model, which is characterised by a spontaneous mutagenesis driven model.

3.2.8.1 *in vivo* models of colitis

3.2.8.1.1 DSS model

This colitis model based on the principle of dextran sulphate sodium (DSS) treatment as described in 1.1.8. The sulphated polysaccharide is directly toxic to the intestinal epithelial cells of the basal crypts and affects thus the integrity of the mucosal barrier (Wirtz and Neurath, 2007). Depending on the dose and duration of the treatment an acute (i.e. one 7 day treatment) or chronic (i.e. several treatment intervals) colitis can be induced with typical features like weight loose, bloody diarrhoea, ulceration and infiltration of granulocytes (Westbrook et al., 2009). The mice used for this study were C57BL/6, aged at least 8 weeks, using age matched animals for the different treatment groups. Colitis was induced by providing 3% DSS via drinking water for 7 of days. The animals were accommodated in a specific pathogen-free facility under 12 hours light/dark cycles and fed autoclaved food and water ad libitum.

3.2.8.1.2 Winnie model

The second model was the so called *Winnie* model, which represents a murine model of spontaneous colitis generated by mutagenesis (see 1.1.8). As described in Heazelwood *et al*., 2008, 8- to 15-week-old male C57BL/6 mice were treated three times at weekly intervals with 85 mg/kg *N*-ethyl *N*-nitrosourea in 10% ethanol in citrate buffer (pH 5.0). This random mutagenesis treatment caused a single nucleotide polymorphism (SNP) in the D3 domain of *Muc2* leading to a replacement of cysteine with tyrosine (Heazlewood et al., 2008). Due to the resulting aberrant Muc2 protein expression, ER stress and spontaneous intestinal inflammation are induced in the Winnie model with the typical symptoms such as diarrhoea and rectal bleeding. Severe clinical symptoms are developed after 1 year typically.

In the present study 6- to 8-weeks-old *Winnie* mice were used and compared with wild type C57BL/6 mice of similar age. The *Winnie* and wild-type C57BL/6 mice were accommodated in a specific pathogen-free facility under 12 hours light/dark cycles and fed autoclaved food and water ad libitum.

3.2.8.2 Experimental design and treatment of the *in vivo* models of colitis

3.2.8.2.1 Experimental design and treatment in the DSS colitis model study

This study contained 7 different groups with respectively 6 mice. The DSS treated C57BL/6 mice were orally treated with 40 mg/kg or 80 mg/kg nanocurcumin, 40 mg/kg or 80 mg/kg curcumin or 80 mg/kg PLGA every day for a period of 7 days. Further, a DSS control group without drug treatment as well as control mice with normal drinking water were included in this study.

The nanocurcumin particles were suspended in PBS by vortexing, whereas curcumin had to be solved in olive oil by heating at 100 °C for 10 minutes, followed by 10 minutes sonication. The drugs were orally administered by gavage. The mice in the control group, the DSS group and the curcumin group received the vehicle olive oil respectively the according amount of curcumin in oil in one treatment step, whereas the mice in the nanocurcumin and PLGA group achieved first the according nanocurcumin or PLGA amount in PBS, followed directly by a second gavage only with the curcumin vehicle olive oil.

3.2.8.2.2 Experimental design and treatment in the *Winnie* model study

Winnie mice, as model of spontaneous colitis, and wild-type C57BL/6 mice were orally treated with 80 mg/kg nanocurcumin or 80 mg/kg curcumin every other day for a time interval of 14 days.

The mice were divided in 3 groups, respectively a control group, a nanocurcumin group and a curcumin group. Whereas the Winnie groups consisted of 3 female mice and 3 to 4 male mice, the C57BL/6 groups had 4 females and 4 males for each.

The nanocurcumin particles were suspended in PBS by vortexing, whereas curcumin had to be solved in olive oil by heating at 100°C for 10 minutes, followed by 10 minutes sonication. The drugs were orally administered by gavage. The mice in the control group and the curcumin group received the vehicle olive oil respectively the according amount of curcumin in oil in one treatment step, whereas the mice in the nanocurcumin group achieved first the according nanocurcumin amount in PBS, followed directly by a second gavage only with the curcumin vehicle olive oil.

3.2.8.3 Evaluation of body weight changes and macroscopic evaluation of colitis

In both studies the body weight change and the macroscopic evaluation of colitis were determined. The body weight of the mice was measured by placing the mice in a box on the scales followed by the calculation of the percentage compared to the body weight of day 0. The body weight measured on day 0 was set 100%. The macroscopic colitis evaluation was split in the score of colitis symptoms such as diarrhoea and rectal bleeding during the experiment and the measurement of colon weight and colon length immediately after sacrificing. In presence of severe inflammation, the intestine becomes significant shorter and the weight is increased due to the massive infiltration of immune cells and changes in permeability. The diarrhoea level and the level of rectal bleeding were determined by a ranking order from 0 to 3, whereas the severest symptoms are evaluated with 3 and no symptoms with 0. So the highest score in presence of very severe colitis symptoms would be 6. If no faeces could be observed within 1 hour, it also became the highest colitis score 6 due to very severe colitis symptom.

In both studies, the determination of the body weight and the evaluation of colitis symptoms have been started one day before the experiment begin and then always immediately before the orally treatment. Thus, in the DSS study it happened every day and in the Winnie study the body weight was measured every second day, whereas the score of colitis symptoms was only evaluated on day 0, 7 and 14 of the treatment.

3.2.8.4 Microscopical evaluation

3.2.8.4.1 Histological colitis score

As assessment of the severity of colitis, the inflammation and intestinal permeability was analysed. Therefore, formalin-fixed, paraffin-embedded swiss role tissue sections of cecum, proximal colon, mid colon and distal colon/rectum of DSS treated and Winnie mice, respectively were individually analysed after H&E staining using light microscopy.

The severity of colitis in DSS treated mice were evaluated by scoring of inflammation severity (score range 0-3), infiltration extend (0-4), epithelial damage (0-5), and percentage involvement of epithelial damage (includes crypt abscessed, crypt loss or ulceration) (0-4).

In Winnie mice, the histological colitis analysis was performed by scoring of aberrant crypt architecture (score range 0-5), increased crypt length (0-3), goblet cell depletion (0-3), general leukocyte infiltration (0-3), lamina propria neutrophil counts (0-3), crypt abscesses (0-3), and epithelial damage and ulceration (0-3).

Table 3.1: Assessment of DSS colitis: scoring system adapted from others (Nel et al., 2006; van Berlo et al., 2010)

Inflammation Severity (IS) 0 = none 1 = mild 2 = moderate 3 = severe	**Infiltration Extent (IE)** 0 = no infiltrate 1 = infiltrate around crypt base 2 = infiltrate reaching to muscularis mucosae 3 = extensive infiltration reaching the muscularis mucosae and thickening of the mucosa with abundant oedema 4 = infiltration of the submucosa.
Epithelial Damage (ED) 0 = normal morphology 1 = some loss of goblet cells /some crypt abscesses or damage 2 = loss of goblet cells in large areas /extensive crypt abscesses or damage 3 = loss of crypts <5 crypt widths 4 = loss of crypts > 5 crypt widths, < 20% ulceration 5 = > 20% ulceration	**Percentage Involvement of Epithelial Damage (PD) (crypt abscessed, crypt loss or ulceration)** 0 = 0% 1 = 1-25% 2 = 26-50% 3 = 51-75% 4 = 76-100%

Table 3.2: Assessment of Winnie colitis: scoring system adapted from others (Heazlewood et al., 2008)

Crypt Architecture 0 = normal 1 = irregular 2 = moderate crypt loss (10-50%)/mild villous atrophy 3 = severe crypt loss (50-90%)/moderate to severe villous shortening 4 = small/medium sized ulcers (<10 crypt widths) 5 = large ulcers (>10 crypt widths)
Crypt Abscesses (not applicable to small intestine) 0 = none 1 = 1-5 2 = 6-10 3 = >10
Crypt Length (not applicable to small intestine) **Caecum –** 0 = < 130 uM, 1 = 130-150 um, 2 = 150-200, 3 = 200-250, 4 = >250 **PC –** 0 = < 150 uM, 1 = 150-200 um, 2 = 200-250, 3 = 250-300, 4 = >300 **MC –** 0 = < 250 uM, 1 = 250-300 um, 2 = 300-400, 3 = 350-400, 4 = >400 **DC –** 0 = < 200 uM, 1 = 200-250 um, 2 = 250-300, 3 = 300-350, 4 = >350
Tissue Damage 0 = no damage 1 = discrete lesions 2 = mucosal erosions 3 = extensive mucosal damage
Goblet Cell Loss 0 = normal <10% loss 1 = 10-25% 2 = 25-50% 3 = >50%
Inflammatory Cell Infiltration 0 = occasional infiltration 1 = increasing leukocytes in lamina propria 2= confluence of leukocytes extending to submucosa 3 = transmural extension of inflammatory infiltrates
Lamina Propria Neutrophils (PMN) 0 = 0-5 PMNs/HPF 1 = 6-10 2 = 11-20 3 = >20

3.2.8.4.2 PAS/Alcain blue staining

The histological phenotype of the Winnie mice with Muc2 mutations can be marked by Periodic Acid-Schiff (PAS)/Alcain blue staining. Whereas the Muc2 filled thecae in the wild type mice exhibit a deep Alcain blue staining, in the Winnie goblet cells magenta coloured PAS-positive/Alcain blue negative accumulations are present (Heazlewood et al., 2008). Alcain blue is a large planar pthalocyanine molecule with a copper atom in the centre and four positively charged basic isothiouronium groups. Thus, at pH 2.5 Alcain blue stains all acidic mucins whose carboxyl groups in the predominately contained carboxylated carbohydrates are ionised under these conditions. However, neutral mucins are not stained by Alcain blue, but via PAS reagent. This technique based on the reactivity of free aldehyde groups within the monosaccharide units of the mucins with the Schiff reagent, initiated by oxidation of the hydroxyl groups. Thus, the PAS staining detects both neutral and acidic mucins with sialic acids.

The histological swiss role slides from Winnie colon were first deparaffinised by using a descending alcohol line with xylol, 100%, 95% and 70% ethanol. Upon the wash step in distilled water, the slides were stained with 1% Alcain blue (1% Alcain blue from Merck in 3% acetic acid, pH 2.5) for 30 minutes. Afterwards, the slides were washed for 5 minutes in distilled water, before the pre-treatment with 1% periodic acid was performed for 10 min to oxidise the hydroxyl groups to aldehydes. After 3 wash steps in distilled water slides were stained with Schiff's reagent (Merck) for 15 minutes, followed by 3 times 2 minutes washing in sulphite water. Subsequently, slides were washed for 15 minutes in distilled water and incubate 1 minutes in haematoxylin (Meyens Hämalaunlösung, Merck) to stain nuclear structures. After washing under tap water for 5 min, an ascending alcohol line with 70%, 95%, 100% ethanol and xylol was used to dehydrate the tissue. Finally, the slides were covered using DEPEX mounting medium (Serva).

3.2.8.5 Cytokine expression profiling in distal colon

The Bio-Plex cytokine assay (Bio-Rad) was used to analyse the cytokine expression profile in the distal colons from DSS-treated mice and Winnie mice with and without treatment. This assay system based on the Luminex xMAP technology and is able to quantify the level of multiple cytokines in a single well. The multiplex assay is designed like a capture sandwich immunoassay containing antibodies which are covalently coupled to colour-coded polystyrene beads. Up to 100 beads, stained with different fluorescent dyes, can be used as solid phase for simultaneously quantification of up to 100 different analytes. Upon binding of the capture antibody-coupled beads to their target molecules, the second biotinylated detection antibody is in its turn able to conjugate specifically with a different epitope of the

particular cytokine. By addition of the reporter streptavidin-phycoerythrin (streptavidin-PE), which binds to the biotinylated detection antibody, the quantity of each specific cytokine can be analysed by a Luminex detection system. This system uses two different lasers, a classification laser to detect the bead colour and a reporter laser to detect the fluorescence intensity of the reporter. The unknown cytokine concentrations in the sample are automatically calculated by Bio-Plex Manager software using a standard curve derived from a recombinant cytokine standard. In the current study the Luminex100 IS 2.3 system coupled to the Bio-Plex Manager 4.1.1 software were used.

To analyse the cytokines IL-1α, IL-1β, IL-6, IL-17, G-CSF, GM-CSF, KC, MCP-1, MIP-1α, MIP-1β and RANTES in the distal colon tissue homogenates, the Bio-Plex murine cytokine 11-plex panel (Biorad) was used.

The distal colon tissue was homogenised in RIPA buffer (1% NP-40 (Igepal), 0.5% Sodium deoxycholate and 0.1% sodium dodecyl sulphate (SDS)) with protease inhibitor (Complete Protease Inhibitor tablets from Roche) using a mortar. The homogenates were incubated for 30 minutes on ice before centrifugation by maximal speed for 20 minutes at 4°C. The supernatants were transferred in a new eppendorf tube and stored at -20°C until the luminex analysis was performed.

The Bio-Plex assay was performed according to the manufacturer's instructions.

Upon washing the wells of a 96 well plate with Bio-Plex wash buffer, 50 µl of the 1x multiplex bead working solution were added per well, followed by 2 wash steps. Then 50 µl of the standard or sample were placed per well. Therefore, serial dilutions of the cytokine master standard (32 ng/ml) were prepared by 4-fold dilution steps in standard diluent. The used sample concentration was 1 µl/ml (according to 1 µl/mg protein). The filter plate was covered with plate sealing tape and aluminium foil before the shaking on the microplate shaker for 30 seconds and 30 minutes incubation at room temperature. After 3 wash steps with Bio-Plex wash buffer, 25 µl of the 1x detection antibody was put in each well followed by shaking as and 30 minutes incubation at room temperature. Upon further 3 wash steps, 50 µl 1x streptavidin-PE were added per well, followed by shaking and incubation for 10 minutes at room temperature. Other 3 wash steps were performed before the beads were resuspended with 125 µl Bio-Plex assay buffer in each well and shaked for 30 seconds immediately before the measurement.

3.2.9 Measurement of cytotoxicity (WST-1 assay)

Cytotoxicity was determined by using the commercial *water-soluble tetrazolium salt (WST-1) diagnostic kit* (Roche). This colorimetric assay can be used to assess the metabolic activity of cells based on the ability of mitochondrial dehydrogenases in viable cells to cleave the tetrazolium salt (WST-1) into a dark-red formazan dye which can be detected spectrophotometrically. For this assay, Caco-2 cell were incubated with 5, 10 or 20 µM nanocurcumin, PLGA and curcumin in a 96-well tissue culture plate for 24 hours. As a positive control 1 mM of the oxidant hydrogen peroxide (H_2O_2) was used. After the incubation time, 10 µl WST-1 solution was added into the wells, and the cells were incubated for additional 2 hours at 37°C. The colour change was measured at 450 nm using a plate reader. For each individual experiment, each sample was tested in a 96 well plate in quintuplicate in the presence of the WST-1 as well as in triplicate in the absence of WST-1. The average of the latter three values was subtracted from the average of the former five values. The same procedure was performed in the same 96 well plate for the control incubations (untreated cells). The values of the samples per experiment were accordingly expressed as % of the controls.

3.2.10 Analysis of DNA strands breaks and oxidative DNA damage by Fpg-modified comet assay

The formamidopyrimidine glycosylase (Fpg)-modified comet assay was used to establish the potential DNA damaging properties of the different cell treatments. While the conventional comet assay measures DNA strand breaks and alkali labile sites, the Fpg-modified assay allows in addition for the determination of specific oxidative DNA lesion which are considered as an indicator of the presence of oxidative stress. The Fpg enzyme specifically detects oxidative DNA damage by its ability to cleave oxidative DNA lesions, particularly 8-OH-dG sites.

After indicated treatments and time points, cells were rinsed twice with PBS, detached by trypsinization and suspended in 1 ml culture medium. Afterwards, the cells were centrifuged at 150 x g for 10 minutes at 4 °C and resuspended in starvation medium at a concentration of 1.5 x 10^6 cells/ml. Ten µl aliquots of the cell suspensions were added to 120 µL 0.5% low melting point (LMP) agarose and the mixture was put onto 1.5% agarose precoated slides. The slides, prepared in duplicates, were solidified for 10 min on ice before incubation in lysation buffer (2.5 M NaCl, 100 mM EDTA, 10 mM Tris-base, pH 10, containing 10% DMSO and 1% Triton X-100) at 4°C over night. Afterwards, the slides were washed in Fpg-enzyme buffer (40 mM HEPES, 100 mM KCl, 0.5 mM EDTA, 0.2 mg/ml BSA, pH 8) three times for 5 minutes, covered with 100 µl of Fpg containing or free buffer incubated at 37°C for 30 min.

After transfer of the slides in an electrophoresis tank alkaline unwinding followed in denaturation buffer (0.3 M NaOH, 1 mM EDTA, pH 13) for 20 minutes before the electrophoresis was performed at 270 mA and 26 V for 10 minutes. The slides were neutralised three times for 5 minutes in neutralisation buffer (0.4 M Tris, pH 7.5) before they were dried on air for 10 minutes and stained with ethidium bromide (10 µg/ml, 40 µl per slides) for analysis. The formation of DNA strand breaks and oxidative DNA damage were investigated by using an fluorescence microscope (Olympus BX60) at 400 x magnification and a comet image analysis software program (Comet Assay II, Perceptive Instruments, Haverhill, UK). The DNA damage is detectable as a "tail" of DNA fragments (tail moment) behind the cell core and is scored by determination of the percentage of DNA in tail. The amount of specific oxidative DNA damage results from the calculation of delta (Δ) +/- Fpg:

$$\Delta \text{ +/- Fpg} = (\text{+Fpg (DNA in tail [\%])}) - (\text{-Fpg (DNA in tail [\%])}).$$

A total amount of 50 cells was analysed per slide per experiment.

3.2.11 Oxidative DNA damage repair kinetics in Caco-2 cells after Ro19-8022 treatment in presence of light

To investigate the ability of Caco-2 cells to repair oxidative DNA damage, the photosensitizer Ro19-8022 ([R]-1-[(10-chloro-4-oxo-3-phenyl-4H-benzo[*a*]quinolizin-1-yl)-carbonyl]-2-pyrrolidine-methanol), synthesized by Widmer and Hoffman-La Roche and characterised in Fischer *et al.,* 1990, was used as initiator of oxidative DNA modifications. In presence of light the polar compound Ro19-8022 induces oxidative DNA damage via generation of reactive oxygen species, in particular singlet oxygen (Will et al., 1999). The dominated base modifications are 8-hydroxyguanine (8-oxo-dG) residues which are sensitive to the repair endonuclease Fpg protein, as described above (Boiteux et al., 1990). Therefore, for analysis of oxidative DNA damage repair and determination of the repair kinetic, the Fpg-modified comet assay was used. The Caco-2 cells were seeded in 6-well plates as mentioned before. On the next day, the culture medium was replaced with serum-free medium for further 24 hours. After two wash steps with PBS, the cells were treated with 400 µM Ro19-8022 in PBS-G buffer (10% 10x PBS, 1 mM $CaCl_2$, 0.5 mM $MgCl_2$, 0,1% glucose in water) for 3 minutes with irradiation (1000 W lamp) at the same time. To avoid overheating of the cells, they were kept on ice for the whole procedure. After induction of oxidative DNA damage, cells were further incubated after different recovery time intervals, i.e. 0, 0.5, 1, 2, 4 and 6 hours. Cells were then trypsinized and used for Fpg-modified comet assay as described

before. By detection of the recovery-time dependent remaining amount of oxidative DNA lesions, the kinetics of oxidative DNA damage repair can be calculated for the Caco-2 cells.

3.2.12 Total glutathione content measured by GSH assay

Glutathione (GSH) is a tripeptide thiol (γ-glutamyl cysteinyl glycine) and serves as a co-factor for several enzymes in metabolic processes. It is also an important antioxidant and the measurement of changes in its intracellular concentration is used as an indicator for oxidative stress in cells and tissues (Pastore et al., 2003). Therefore, the total glutathione content in Caco-2 cells was analysed after 24 hours treatment with the indicated concentrations of nanocurcumin and curcumin, respectively. For the quantitative determination of the reduced glutathione content, the so-called enzymatic recycling method was used, a modification of the method described by Tietze (Tietze, 1969). This assay based on the catalytic reaction of GSH with 5,5'-dithio-bis(2-nitrobenzoic acid) (DTNB, also named as Ellman's reagent) that forms the yellow derivate 5-thionitrobenzoic acid (TNB) with a maximal absorbance at 412 nm and oxidized glutathione-TNB adduct (GS-TNB) (see Figure 3.3). The concentration of GSH in a sample is proportional to the rate of formation of TNB, measured at 412 nm. The GS-TNB is subsequently reduced by glutathione reductase (GR) in presence of β-nicotinamide adenine dinucleotide phosphate (NADPH) and therefore the GSH is recycled back into the reaction and amplifying the response. In addition, any oxidized GSH (GSSG) is rapidly reduced in two GSH by glutathione reductase and NADPH.

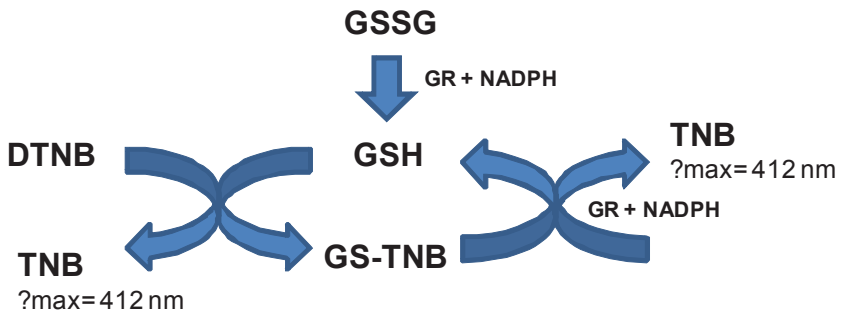

Figure 3.3: Principle of GSH assay.

The GSH concentration in samples is determined by calculation from the regression curve generated from several GSH standards.

For the GSH assay, after treatment, cells were rinsed twice with cold PBS and scraped in 1 ml KPE-buffer containing phosphate buffer A [0.1 M KH_2PO_4] and phosphate buffer B [0.1 M K_2HPO_4*3 H_2O] in a ratio of 1:6.25, 0.1% Triton-X-100 and 0.6% SSA. The samples were

alternate sonicated and vortexed three times for 30 seconds each, followed by centrifugation at 4,100 x g for 5 minutes at 4°C. The supernatants were directly used for analysis. Therefore, 50 µL of the sample or GSH standard was transferred in a 96-well plate, followed by the immediate addition of 100 µl of 0.8 mM NADPH and 0.6 mM DTNB mixture (1:1) as well as 50 µl GSH reductase (4 units/ml). The GSH standard was in a range of 0 to 26 nmol/ml glutathione with 1:1 dilution steps in between. The absorbance was measured at 412 nm five times during 2 minutes and the values were adjusted to the total protein content as determined by bicinchoninic acid (BCA)-assay (Bio-Rad).

3.2.13 The bicinchoninic acid assay

The bicinchoninic acid (BCA) assay is a high sensitive method to determine the total protein concentration in a sample. The principle is based on the reduction of Cu^{2+} to Cu^{1+} by proteins in alkaline medium (i.e. biuret reaction) and the capability of the chromogenic reagent bicinchonic acid to chelate the reduced copper, forming a purple complex (Valko et al., 2007). The intensity of the purple colour is proportional to the amount of proteins in the sample, which can be determined by calculation from the regression curve from a protein standard. A bovine serum albumin (BSA) protein standard was prepared with serial dilutions from 0 to 15 µg/µl and 10 µl of each dilution or sample was pipetted in duplicates in a 96-well plate. BCA solution and copper (II) sulphate solution were mixed in a 1:50 ratio and 200 µl of the mixture was added in each well. After 30 minutes incubation at 37°C absorption of the purple BCA/copper complex was measured at 540 nm in a plate reader (Labsystems Oy, Helsinki Finland).

3.2.14 Quantitative PCR

3.2.14.1 RNA isolation from Caco-2 cells and murine intestinal tissue

3.2.14.1.1 Caco-2 cells

To analyse the influence of nanocurcumin and curcumin on altered gene expression on the mRNA level in Caco-2 cells, the cells were treated with 20 µM nanocurcumin or curcumin for the indicated time points as described above. Afterwards, the cell monolayer was washed two times with PBS, before the cells were trypsinized. The cell suspension was centrifuged at 150 x g for 10 minutes at 4°C and the cell pellet was then resuspended in 0.5 ml TRIzol reagent (Invitrogen) and stored at -20°C until RNA extraction. The RNA extraction was performed by the isolation method based on the phenol-chloroform method as introduced by Chomczynski and Sacchi (Chomczynski and Sacchi, 1987). The commercial reagent TRIzol

contains guanidinium thiocyanate and phenol which lyses the cells and inactivates RNases and other enzymes by protein denaturation. After subsequent addition of 100 µl ice cold chloroform to the samples with a briefly vortex-mixing, followed by incubation at room temperature for 5 min and centrifugation at 12,000 x g for 15 minutes at 4°C a three phase separation is present. Herein, the RNA is in the upper aqueous phase, the interphase contains DNA and the lower chloroform phase contains proteins. Approximately 200 µl of the aqueous phase was transferred into a new eppendorf tube and the RNA was precipitated by isopropanol and ethanol. Therefore, 250 µl isopropanol was added to the aqueous phase, mixed and incubated for 10 minutes at room temperature. Samples were then centrifuged at 12,000 x g for 10 minutes at 4°C, before the supernatants were discarded and the pellets washed in 1 ml 75% ethanol. After the centrifugation at 7,500 x g at 4°C for 5 minutes, the supernatant was discarded again and the pellet was dissolved in 30 µl RNase free water, and stored at -80°C. To increase the RNA solubility the samples were heated at 60°C for 10 minutes, before the RNA concentration was quantified spectrophotometrically (see 3.2.14.2).

3.2.14.1.2 Murine intestinal tissue

The isolation of RNA from tissue started with the tissue homogenization. The tissue samples were thawed on ice and transferred into a 2 ml eppendorf tube containing a steel ball and 1 ml TRIzol reagent. Using a Tissue Lyser the tissue was homogenized by shaking two times for 3 minutes with maximal power (30 x / seconds). To the homogenate, 200 µl chloroform was added and mixed followed by incubation for 5 min at room temperature and centrifugation at 12,000 x g for 15 minutes at 4°C. As described above for the Caco-2 cells (see 3.2.14.1.1), the aqueous upper layer was transferred in a new tube and washed with the equal amount of 75% ethanol. For RNA purification the *High Pure RNA Isolation Kit* from Roche was used according to the protocol provided by the manufacturer. This method is based on the fact that nucleic acids bind to the solid phase, like glass fibre fleece on a minicolumn, depending on the pH and salt content in the buffer. Therefore, the RNA mixture was transferred into the upper reservoir of the filter tube which was inserted in a collection tube. After centrifugation at 8,000 x g at 4°C for 15 seconds, the RNA binds to the glass fibre fleece and the flowthrough liquid was discarded. After re-inserting the filter tube 90 µl DNase incubation buffer with 10 µl DNase I was pipetted into the filter tube and incubated for 15 minutes at room temperature. Following three washing steps, the RNA was eluted in 30 - 50 µl RNase free water. The eluted RNA was stored at -80°C until further use.

3.2.14.2 RNA Quantification by UV- Spectroscopy

RNA quantity and purity were analysed by ultraviolet spectrophotometry. This method is based on the fact that nucleic acids absorb wavelength at the ultraviolet field and possess an absorption maximum at 260 nm due to the aromatic ring structure of the bases. A single-stranded RNA solution with a concentration of 40 µg/ml contained in a quartz cuvette with 1 cm layer thickness corresponds to an optical density (OD) of 1. Therefore the RNA concentration can be calculated via the Beer-Lambert law which indicates a linear change of the absorbance with concentration:

Concentration of RNA sample [µg/ml] = 40 x OD260 x dilution factor.

To determine the RNA purity the ratio of the absorbance at 260 nm and 280 nm is calculated since at 280 nm the absorption maximum for proteins exists because of the aromatic amino acid residues. The optimal value of the OD260 /OD280 ratio is within the range of 1.8 and 2 and indicates RNA samples of high purity. To measure the optical density at 260 nm and 280 nm of RNA samples in a UV spectrophotometer, 5 µl of the isolated RNA sample was diluted in 95 µl RNase free water and transferred in a quartz cuvette.

3.2.14.3 Synthesis of complementary DNA (cDNA)

For the synthesis of complementary DNA (cDNA) the *iScript cDNA Synthesis kit* from Bio-Rad was used. The iScript reverse transcriptase is a modified MMLV (Moloney Murine Leukemia Virus) – derived reverse transcriptase with ribonuclease H activity which provides a great sensitivity in quantitative PCR. The RNA-dependent DNA polymerase can use the messenger RNA (mRNA) as template to generate cDNA by means of oligo(dT) primers (15 – 25 desoxythymidine) which bind complementary to the poly(A) tail of eukaryotic mRNA. For the reverse transcription 0.5 µg mRNA of each sample was assembled in following mixture with a total reaction volume of 20 µl:

- 4 µl 5x iScript reaction mix
- 1 µl iScript reverse transcriptase
- 15 µl RNA template in RNase free water (0.5 µg RNA in total)

For an optimal transcription process a program with following temperature steps was adjusted in the thermal cycler:

- 5 min at 25°C (priming step)
- 30 min at 42°C (reverse transcription step)
- 5 min at 85°C (inactivation step of reverse transcriptase)
- Hold at 4°C (optional cooling step)

The cDNA was directly used in semi-quantitative Real-time PCR or alternatively stored at -20°C until PCR analysis.

3.2.14.4 Analysis of gene expression by Semi-quantitative Real-Time Polymerase Chain Reaction

The semi-quantitative real-time polymerase chain reaction (real-time PCR) is a commonly used method to analyse gene expression. It based on the amplification and simultaneously quantification of a target gene via fluorescence dye, in this case SYBR green, which binds to double-strained DNA. The SYBR green fluorescence signal (λ_{ex}= 495 nm; λ_{em}= 520 nm) increases in proportion to the amplified amount of DNA. The relative quantification is based on internal reference genes to allow for the analysis of fold-change in mRNA expression of the target gene under investigation. Therefore a housekeeping gene is used which has to be stable and independent of treatments. For the present investigations, the fluorescence amount of the gene of interest was compared to the fluorescence amount of the housekeeping gene β-actin. The amplification reaction was initiated by the hot-start iTaq-DNA polymerase.

In the reaction mix following components were contained:

- 12.5 µl iQ SYBR green supermix (containing SYBR green, iTaq-DNA polymerase, dNTPs)
- 2.5 µl Primer (forward); 0.375 µM
- 2.5 µl Primer (reverse); 0.375 µM
- 2.5 µl RNase free water
- 15 µl cDNA (1:15 diluted in RNase free water)

For gene expression analysis the iQ5 real-time PCR detection system was used under following conditions:

- 95°C 3 min
- 95°C 15 sec
- 60°C 45 sec

} x 40

To ensure primer specify and to exclude non-specific products and primer-dimers, a melting curve analysis was performed. Therefore a melting curve was generated by increasing temperature in 0.5°C increments over a temperature range of 56°C to 95°C and the fluorescent signal was monitored at each step.

The quantification of the gene expression is based on the determination of a threshold for the DNA-based fluorescence detection which is set slightly above background. The number of cycles at which the fluorescence exceeds the threshold is defined as the Ct value.
A convenient way to calculate the relative changes in gene expression of a target gene X, and thus used in the present investigations, is the $2^{-\Delta\Delta Ct}$ method, described by Livak & Schmittgen (Livak and Schmittgen, 2001):

Relative gene expression of gene X from sample A compared to sample B

$$= 2^{-\{[Ct(\text{gene X, A}) - Ct(\text{HKgene, A})] - [Ct(\text{gene X, B}) - Ct(\text{HK gene, B})]\}}$$

3.2.15 Statistical analyses

Statistical analysis was performed using IBM SPPS version 20 software.

For the evaluation of the *in vitro* results, the one way Analysis of Variance (ANOVA) with Dunnett post hoc was performed for dosimetric analysis to compare every mean of the different treatment groups to the control. The one way ANOVA with Tukey post hoc was used for multiple comparisons between different groups. To compare just one treatment with the control, the two-tailed Student's t-test was used. In all cases, statistical significance was defined as $p<0.05$.

In the *in vivo* study, comparisons between two animal groups were made by Student's T-test. One way Analysis of Variance (ANOVA) with LSD post hoc comparison evaluations was used for multiple group comparisons. Colitis score results were evaluated using the nonparametric Mann Whitney U-test. A $p<0.05$ was considered as statistically significant.

4. Results

4.1 Preparation and physical characterisation of PLGA-encapsulated curcumin nanoparticles and PLGA vehicles

To analyse the potential therapeutic effect of curcumin in a nano-drug delivery approach towards inflammatory bowel disease, PLGA-encapsulated curcumin nanoparticles, (nanocurcumin, NC) were prepared by the emulsification-diffusion-evaporation technique. PLGA particles without curcumin were prepared in parallel as vehicle control. For the *in vitro* study, three different batches of NC and two different batches of PLGA vehicles were produced as described in the methods section (see paragraph 3.2.1), whereas three batches of NC with sorbitol (NC-S) and one batch of PLGA with sorbitol (PLGA-S) were manufactured for the *in vivo* study. Upon their preparation, the size, size distribution (polydispersity index) and the zeta potential of the nanoparticles were measured by Zetasizer Nano and Nanosight methods. In addition, the release kinetics of curcumin from the PLGA-carrier particles was analysed. For the NC-S particles also the curcumin encapsulation efficacy was determined.

4.1.1 Characterisation of particle size, polydispersity index and zeta potential

The particle size, the polydispersity index (PDI) and the zeta potential (ZP) were measured by Zetasizer Nano, which is based on the dynamic light scattering. Figure 4.1 (panel A) gives a tabulate overview of the mean particle size, PDI and ZP, as calculated from all measurements of all prepared batches. The three batches of NC had an average particle size of 309 nm, with an average polydispersity index of 0.48 and an average zeta potential of - 33.2 mV. These findings are indicative of the relative stability of the particles in aqueous solution. The size of the particles, as evaluated for the PLGA batches, was found to be relatively smaller with 190 nm. These particles also possessed a lower PDI (0.04) and a zeta potential (– 30.0 mV). The nanocurcumin and PLGA particles that were freeze dried with D-sorbitol showed a rather similar particle size, i.e. 205 nm and 206 nm, respectively. The PDI was 0.33 for NC-S and 0.02 for PLGA-S, and had a zeta potential of – 25.0 mV and – 18.6 mV, respectively.

To exclude potential interferences in the determination of the particle size with the applied dynamic light scattering approach, size was also evaluated by Nanosight as an independent approach. With this nanoparticle tracking based method, a particle size of 139 nm was measured (see Figure 4.1 B). The prepared nanocurcumin was also evaluated by transmission electron microscopy (TEM), a representative picture is show in Figure 4.1 C. When solved in distilled water the nanocurcumin particles revealed the typical structure for PLGA particles (Cheng et al., 2008).

A.

sample	Size [nm]	PDI	ZP [mV]
In vitro			
Nanocurcumin (NC)	309	0.48	- 33.2
PLGA	190	0.04	- 30.0
In vivo			
Nanocurcumin with sorbitol (NC-S)	206	0.33	- 25.0
PLGA with sorbitol (PLGA-S)	205	0.02	- 18.6

C.

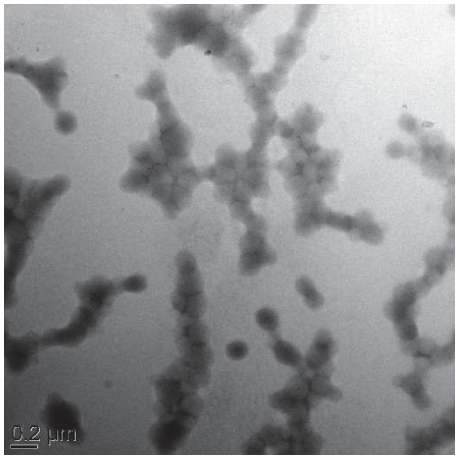

B.

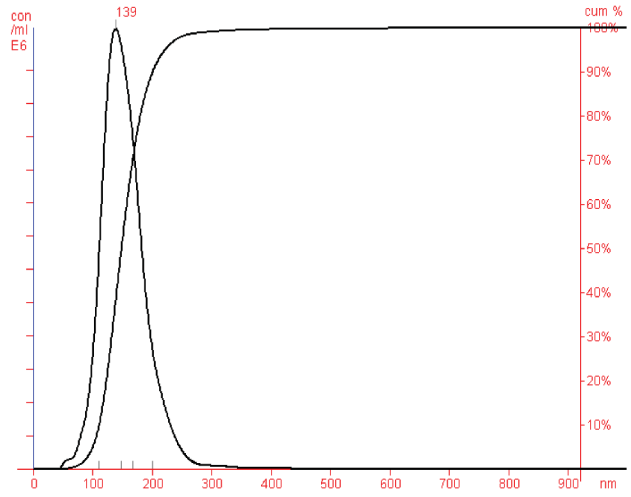

Particle Size / Concentration

Figure 4.1: Physical characteristics of PLGA-encapsulated curcumin nanoparticles and PLGA vehicle. Size, polydispersity index (PDI) and zeta potential (ZP) of nanocurcumin (NC), PLGA, nanocurcumin with sorbitol (NC-S) and PLGA with sorbitol (PLGA-S) were measured by Zetasizer Nano. Each sample was measured three times. A: Average measurements of three, respectively two independent batches of NC, PLGA and NC-S. For PLGA-S only one batch was prepared. B: Analysis of NC size by Nanosight. C: Representative transmission electron microscopy (TEM) picture of NC.

4.1.2 Curcumin release kinetics of PLGA-curcumin particles

To evaluate the release kinetics of the curcumin from the PLGA-encapsulated curcumin particles, a known amount of the freeze dried particles was suspended in PBS with 1% Tween 80 and transferred in a dialysis membrane as described in the methods section. The membrane was placed in PBS-Tween 80 for 48 hours, whereupon after different time intervals samples were taken. The curcumin release was evaluated on the basis of its autofluorescence properties. Over the measured time interval, a consistent increase of released curcumin could be observed (see Figure 4.2). After 48 hours, about 13% of the particle-containing curcumin amount was released, which equates to a released concentration of 3.5 µM.

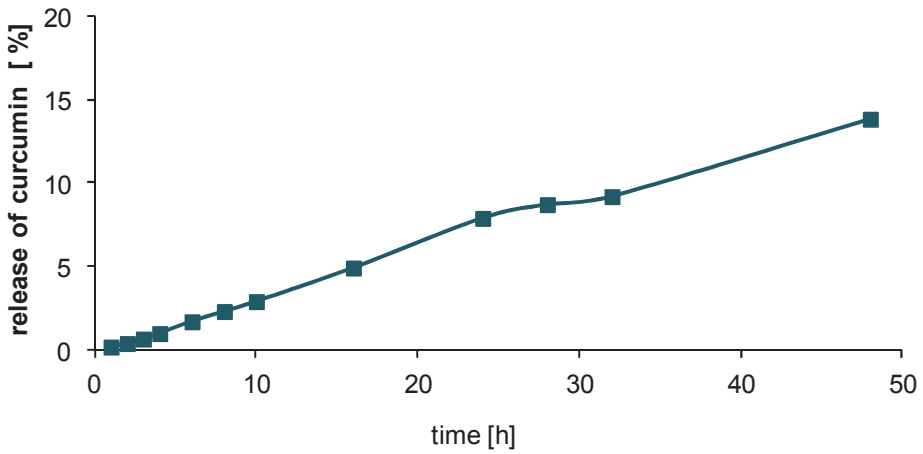

Figure 4.2: Kinetics of curcumin release from the PLGA-encapsulated particles.
The curcumin release from the PLGA-curcumin particles into PBS with 1% Tween 80 was determined at different time points over a time interval of 48 hours. The curcumin concentrations in the buffer samples were analysed by measurement of the curcumin autofluorescence (λ_{Ex}= 420nm; λ_{Em} = 530nm) and expressed as % of the initial curcumin amount contained in the particles.

4.1.3 Curcumin encapsulation efficiency in nanocurcumin with sorbitol

The curcumin encapsulation efficacy of nanocurcumin with sorbitol particles was tested by removing the curcumin encapsulation. Therefore, the particles were dissolved in an ethanol/ distilled water mixture and stirred for two days, before the released curcumin amount was determined by measurement of the curcumin auto fluorescence at 420 nm. The encapsulation efficacy of the two NC-S batches was on average 91.6%. This indicates a high efficiency of curcumin encapsulation in PLGA particles by emulsion-diffusion-evaporation technique.

4.2 *In vitro study*: Effects of nanocurcumin in the human epithelial colorectal adenocarcinoma cell line Caco-2

Curcumin is considered as a promising therapeutic agent because of its anti-oxidant and anti-inflammatory effects. It has been discussed to exhibit potent clinical effects against various diseases including cancer, cardiovascular diseases and Crohn's diseases (Aggarwal et al., 2003; Ramassamy, 2006; Shishodia et al., 2005b). However, curcumin possesses a rather limited therapeutic efficacy due to its minimal systemic bioavailability, rapid metabolism and systemic elimination. Therefore, different strategies are tested to improve bioavailability of curcumin. One of the possible strategies herein, namely the use of curcumin in PLGA encapsulated preparations (Bisht et al., 2007), was applied in the framework of the present thesis. A first step herein, was the concurrent evaluation of nanocurcumin and native (non-encapsulated) curcumin in the well established human intestinal epithelial cell line Caco-2. To address potential side effects of the prepared nanocurcumin, initial investigations concentrated on the evaluation of cytotoxicity. This was done by measurement of changes in metabolic competence and evaluation of oxidative stress induction and DNA damage. Subsequently, the potential therapeutic relevance of nanocurcumin was analysed in the Caco-2 cells, specifically by evaluation of its potential beneficial effects towards oxidant induced cellular stress and damage.

4.2.1 Cytotoxicity of NC, PLGA and curcumin

After the manufacturing of nanocurcumin, the first step in the *in vitro* analysis of the particles was to determine their cytotoxic properties towards the Caco-2 cells. Therefore, cells were incubated with different concentrations (5 µM, 10 µM and 20 µM) of nanocurcumin or their corresponding vehicle particles (PLGA) for a period of 24 hours. For comparison with the native substance, also the toxicity of curcumin was tested as well as of its solvent, i.e. 0.15% ethanol. As a positive control, 1 mM hydrogen peroxide (H_2O_2) was used. The results of these experiments are shown in Figure 4.3. It could be observed that neither NC nor curcumin, in their corresponding range of concentrations were toxic to the Caco-2 cells, i.e. no significant reduction in metabolic activity was measured. Also the corresponding vehicles (i.e. PLGA and ethanol) did not cause toxicity. In contrast, with the known oxidant H_2O_2, the viability of the cells became significantly reduced.

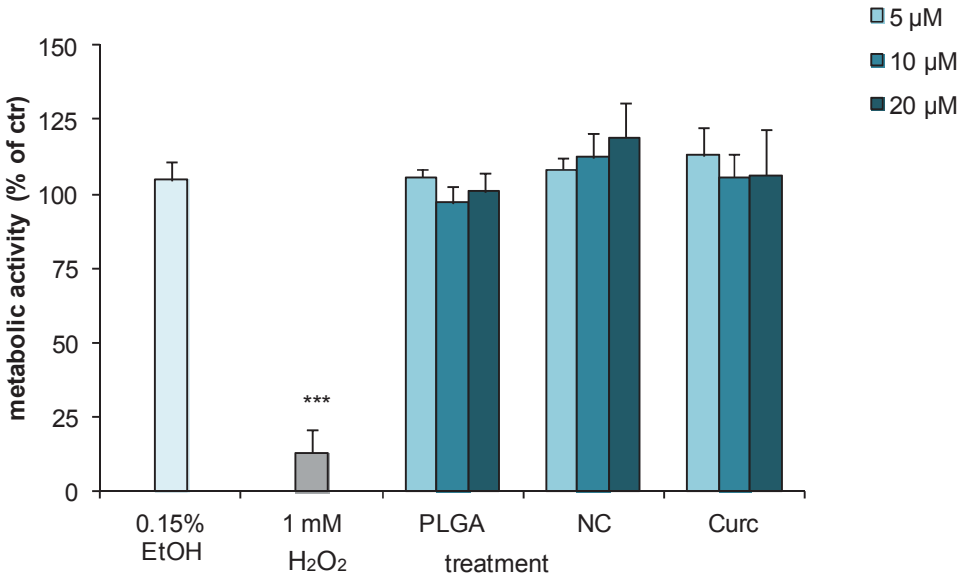

Figure 4.3: Cytotoxic effects of PLGA (vehicle), nanocurcumin (NC) and curcumin (Curc) on Caco-2 cells. Cells were incubated with 5 µM, 10 µM and 20 µM of curcumin, NC or PLGA, respectively. As positive control 1 mM H_2O_2 was used. In addition, cells were treated with 0.15% ethanol (EtOH) to control the solvent of curcumin. Cells were treated for 24 hours, before the cytotoxicity was evaluated by WST-1. The data are expressed as metabolic activity, in percentage of control (i.e. untreated cells) and assay represent mean and standard deviations of three independent experiments (n=3). ***p<0.001 versus control, ANOVA with post hoc Dunnett test.

4.2.2 Evaluation of the DNA damaging properties of NC and curcumin

Although no notable cytotoxictity could be observed in the Caco-2 cells, as a next step potential DNA damaging effects of NC and curcumin were investigated. Therefore, the cells were exposed to 20 µM NC or curcumin, respectively for short (30 minutes) and long (24 hours) time interval. Again, 0.15% ethanol (EtOH) was included as additional curcumin solvent control. After treatment, DNA strand breakage and the specific induction of oxidative DNA damage was analysed in the Caco-2 cells using the Fpg-modified comet assay. The results, shown in Figure 4.4 represent the mean and standard deviation of three independent experiments (n=3) with duplicates in each experiment. NC as well as curcumin did not induce DNA strand breaks after short or long incubation (Figure 4.4 panel A.). However, 30 minutes exposure with curcumin resulted in a highly significant increase of oxidative DNA damage induction, an effect which was not observed with NC or the ethanol control (Figure 4.4 panel B.). Surprisingly, after 24 hours no increased oxidative DNA damage was detectable anymore in the curcumin-treated cells. In general, after 24 hours treatment, the DNA strand breaks and the oxidative DNA damage tended to be lower for all treatment groups.

A.

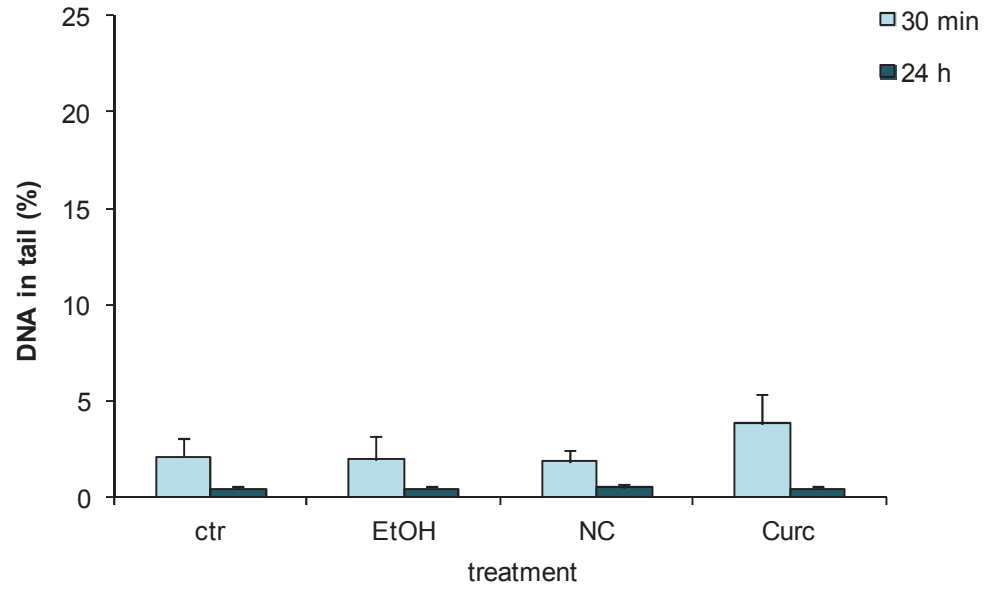

B.

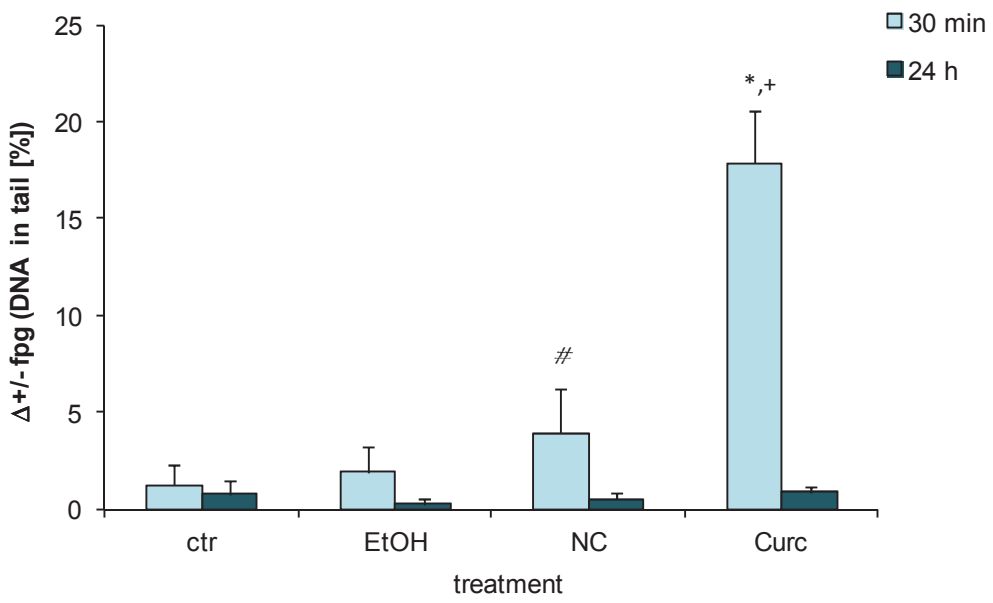

Figure 4.4: Evaluation of DNA damage in Caco-2 cells by nanocurcumin (NC) and curcumin (Curc). The Caco-2 cells were incubated with 20 µM curcumin, with NC containing the corresponding curcumin amount, with 0.15% ethanol (EtOH) or with cell culture medium used as negative control (ctr) for 30 minutes or 24 hours, respectively. The DNA strand breaks (shown in panel A.) and the oxidative DNA damage (Δ+/-fpg(DNA in tail [%])) (show in panel B.) were analysed by Fpg- modified comet assay. The data represent three independent experiments (n=3), each with duplicate treatments. *p<0.001 versus control, +p<0.001 versus EtOH, #p<0.001 versus Curc, ANOVA with post hoc Tukey.

4.2.3 Oxidative DNA damage repair kinetic in Caco-2 cells

Curcumin induced oxidative DNA damage after 30 minutes treatment of the Caco-2 cells, but after 24 hours no damage were visible anymore, indicative of efficient oxidative DNA repair. The ability of Caco-2 cells to repair oxidative stress-induced DNA lesions was therefore further explored. Caco-2 cells were incubated with the photosensitizer Ro19-8022 ([R]-1-[(10-chloro-4-oxo-3-phenyl-4H-benzo[*a*]quinolizin-1-yl)-carbonyl]-2-pyrrolidine-methanol) and irradiated with light as described in detail in the method section (paragraph 3.2.11). The polar compound Ro19-8022 causes oxidative base modifications and particularly 8-hydroxyguanine (8-oxoG) residues via the formation of reactive oxygen species (Will et al., 1999). The oxidative DNA damage repair capacity was evaluated by measurement of remaining oxidative DNA damage after different recovery time after treatment of the cells with Ro19-8022 plus light, using the Fpg-modified comet assay. Results of these kinetic investigations are shown in Figure 4.5. In line with published observations (Gerloff et al., 2012a), the Ro19-8022 compound did not induce a significant amount of DNA strand breaks (see Figure 4.5 panel A.). However, this treatment caused an immediate, highly significant increase of oxidative DNA damage (Figure 4.5 panel B.). Already after 30 minutes recovery time, a marked reduction of oxidative DNA damage levels could be observed, and its decline continued in a clear time-dependent manner. The half-life of the oxidative DNA damage lesions that were induced by the Ro19-8022/light treatment was found to be approximately 4 hours, which is well in line with literature data for several human cell lines (Lorenzo et al., 2009).

A.

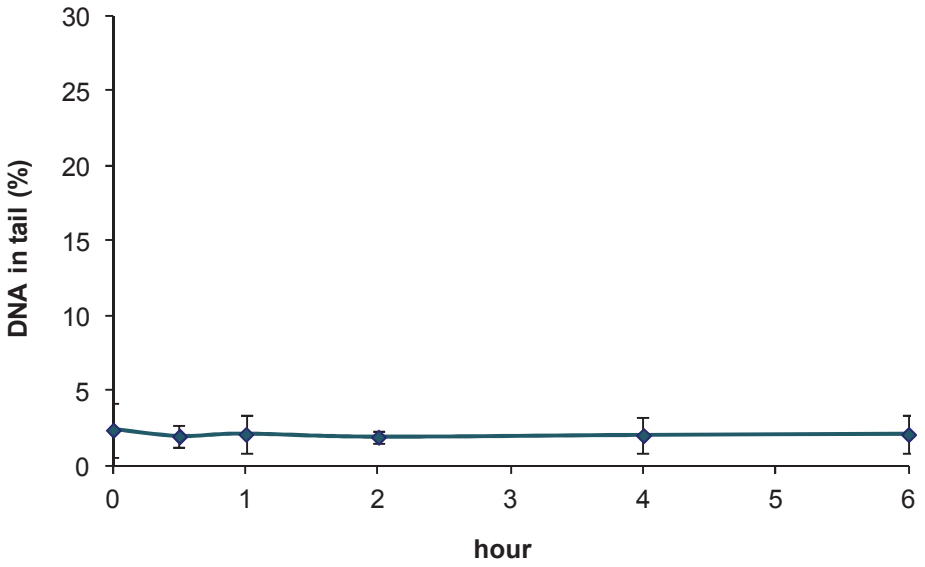

B.

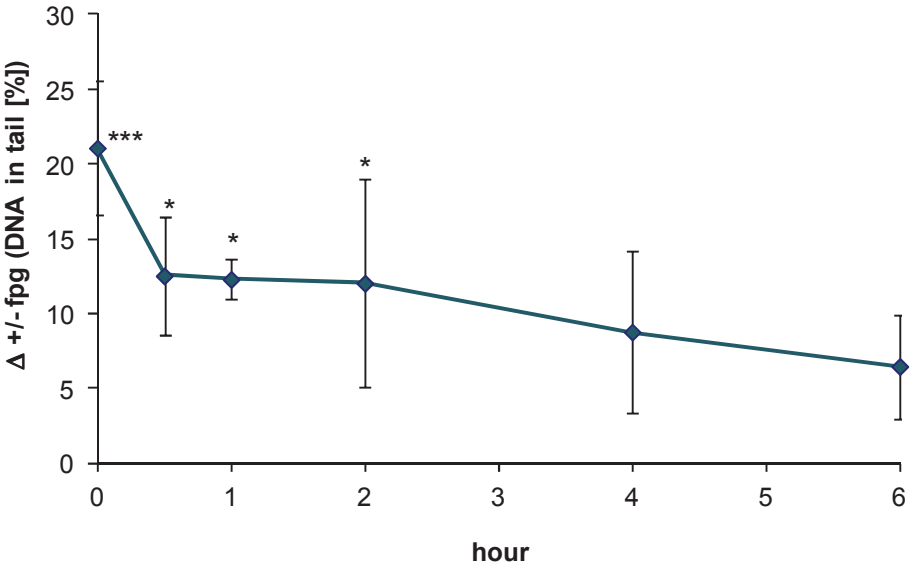

Figure 4.5: Oxidative DNA repair kinetics in Caco-2 cells after incubation with Ro19-8022 and light. The cells were incubated with the photosensitizer Ro19-8022 (400 µM) in PBS-G buffer in the presence of light (1000 W) for 3 minutes. Cells were then allowed to recover for different periods of time (as indicated in the graph) at 37°C prior to evaluation of DNA damage by Fpg-modified comet assay. Three independent experiments were performed (n=3). Panel A. shows DNA strand breakage, expressed as % DNA in tail, while panel B. shows oxidative DNA damage, expressed as ∆+/-fpg(DNA in tail[%]). DNA strand breakage levels and oxidative DNA damage in the untreated control cells for these experiments were 3.4 ± 1.91 and 1.2 ± 0.42, respectively. *p<0.05, ***p<0.001 versus control (n=3), ANOVA with post hoc Dunnett test.

4.2.4 Oxidative stress-related gene expression after NC and curcumin treatment

Antioxidants, like curcumin are agents which inhibit oxidative stress and scavenge free radical intermediates produced by oxidation reactions. By doing this, the reducing agents become oxidized themselves. Thus, paradoxically, antioxidants can also act as prooxidants and may cause an increase of oxidative stress. The hypothesis is that an endogenous response is induced by free radicals which protects against exogenous radicals (Valko et al., 2007). However, in contrast to curcumin, NC did not induce oxidative DNA damage induction after short term incubation which indicates that the NC did not trigger strong pro-oxidative effects in the cells. To analyse the differences between NC and curcumin more in detail in matters of the potential mechanism of antioxidant capacity, the treatment time dependent expression of oxidative stress-related genes was analysed. Therefore, Caco-2 cells were treated with NC, curcumin or the solvent ethanol (0.15%) for 2, 4, 8 and 24 hours. After RNA isolation and the transcription to cDNA, the expression of the oxidative stress-related genes heme oxygenase-1 (HO-1) and gamma-glutamylcysteine synthetase (γ-GCS) was detected by semi-quantitative real-time polymerase chain reaction (qRT-PCR) as described in detail in paragraph 3.14. The expression of HO-1 is related to oxidative stress responses within cells, specifically also in relation to it characteristic function to degrade heme which is released from damaged erythrocytes and can act as prooxidant (Jeney et al., 2002). The stress marker γ-GCS was chosen as it is one of the major determinants of glutathione homeostasis, which serves as a key endogenous antioxidant system. The gene expressions of HO-1 and γ-GCS were expressed as fold change to their expression in untreated cells. In concordance with the DNA damaging effect, curcumin was found to increase the HO-1 mRNA expression in a significant manner at 2, 4 and 8 hours incubation (Figure 4.6 panel A.). After 24 hours treatment, the HO-1 expression did not differ from the control expression. The NC incubation did not result in a significant change of HO-1 mRNA expression, although there was also a slight increase over time with a similar pattern as observed with curcumin. Also the expression of the oxidative stress marker γ-GCS was increased significantly in curcumin-treated Caco-2 cells at 8 hours (Figure 4.6 panel B.). The NC, again did not show a significant difference over the time when compared to the untreated controls. Ethanol, used as solvent control, did not influence the HO-1 and γ-GCS gene mRNA expression in the Caco-2 cells.

A.

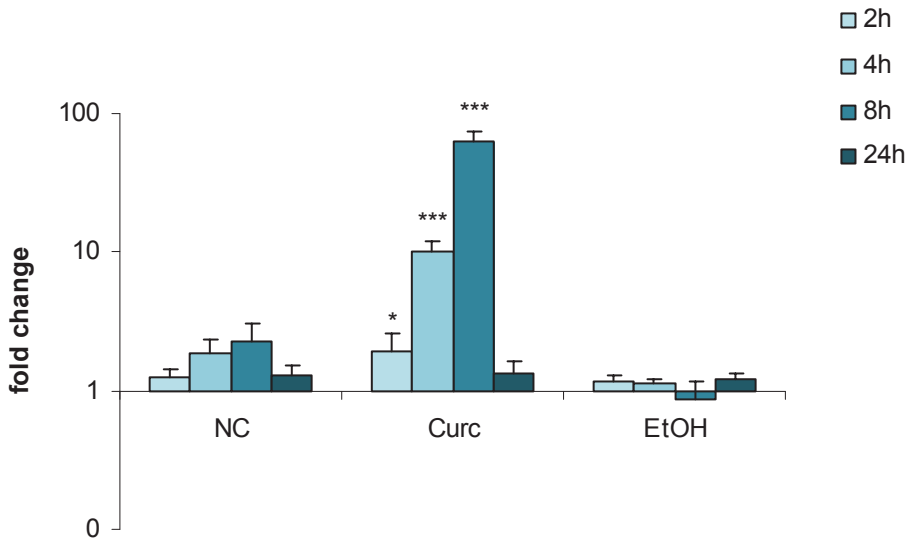

B.

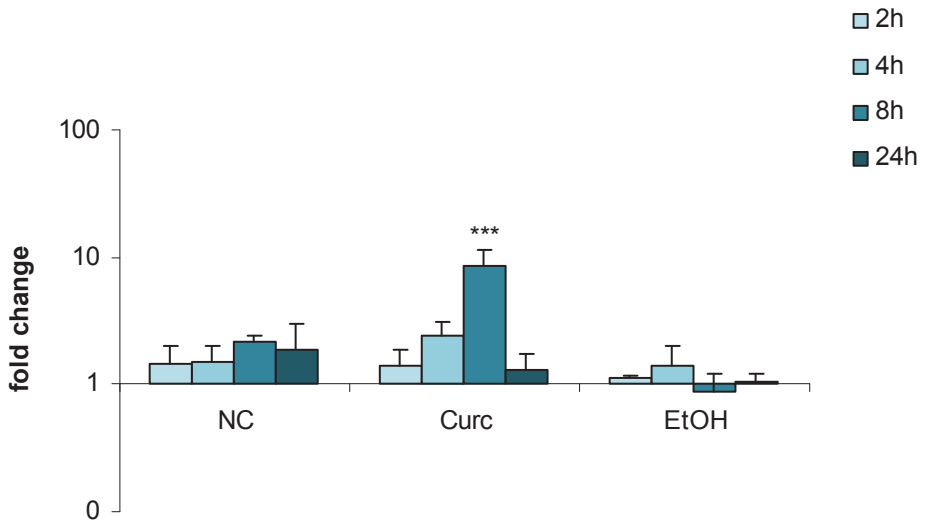

Figure 4.6: Effects of nanocurcumin (NC) and curcumin (Curc) on stress related gene expression. The Caco-2 cells were treated with 20 µM NC or curcumin or 0.15% ethanol (EtOH) as solvent control for the indicated time intervals. The mRNA amounts of HO-1 (panel A.) and γ-GCS (panel B.) were analysed by qRT-PCR in ratio to control and are indicated in the graphs as fold change to untreated controls. Three independent experiments were performed (n=3). *p<0.05, ***p<0.001 versus control of the same treatment time, ANOVA with post hoc Dunnett test.

4.2.5 Effect of NC and curcumin on total glutathione content in Caco-2 cells

Glutathione is a very important intracellular antioxidant with the crucial role to protect cellular components from damage induced by reactive oxygen species (Pompella et al., 2003). The

concentration of intracellular glutathione can be used as marker for oxidative stress. The rare limiting factor in the glutathione homeostasis is the availability of γ-GCS (Griffith, 1999). Due to the fact that curcumin affected the γ-GCS gene expression in contrast to NC, the question raised up whether the intracellular glutathione content would differ after NC and curcumin incubation. Therefore, the Caco-2 cells were treated with NC or curcumin in a concentration range from 5 µM up to 80 µM for 24 hours, before the cells were harvested in ice cold KPE buffer supplemented with Triton-X100 and SSA to lyse the cells. The total glutathione content in the cell lysates was detected as described in paragraph 3.12. The results of the experiments are shown in Figure 4.7. A concentration-dependent increase of total glutathione amount could be observed in the cells that were treated with curcumin as well as the cells that were treated with NC. However, in both cases, these increases were not statistically significant different from the controls. Interestingly however, curcumin incubation tended to cause a slightly higher increase in glutathione synthesis compared to NC.

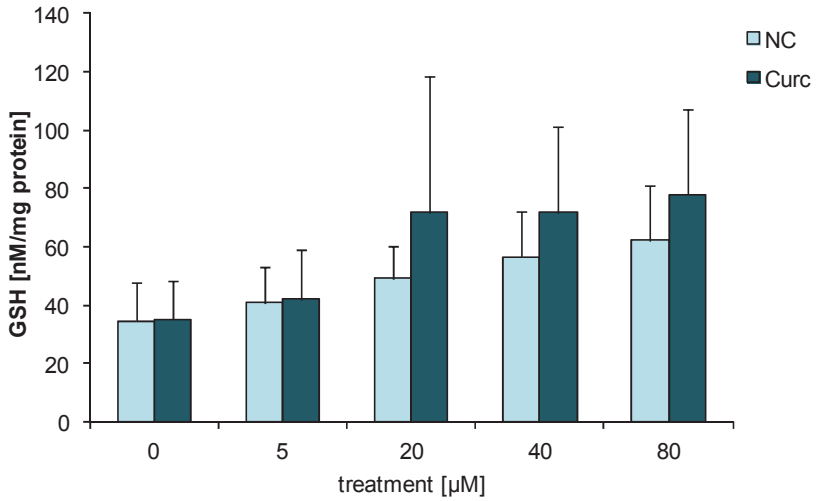

Figure 4.7: Effect of nanocurcumin (NC) and curcumin (Curc) on total glutathione content in Caco-2 cells. The cells were treated with 0, 5, 20, 40 and 80 µM of Curc or the corresponding amounts of NC for 24 hours. The total glutathione content is expressed as nM/mg protein. Three independent experiments were performed (n=3).

4.2.6 Effects of buthionine sulphoximine (BSO) on total glutathione levels

It is already well established that buthionine sulphoximine (BSO) can cause a cellular depletion of glutathione due to its ability to inhibit the synthesis of γ-GCS (Drew and Miners, 1984). In the context of the present investigations with NC and curcumin, the effect of BSO was investigated in the Caco-2 cells. Specifically, the Caco-2 cells were incubated with BSO

for 24 hours in a concentration range of 6.26 µM to 100 µM, followed by glutathione measurement. The results of these experiments are shown in Figure 4.8. As expected, BSO incubation resulted in a high significant decrease of total glutathione content in a concentration-dependent manner. The lowest used BSO concentration (6.26 µM) already reduced the total intracellular glutathione level in a significant manner in the Caco-2 cells and 50 µM BSO appeared to cause a maximal inhibition of glutathione production.

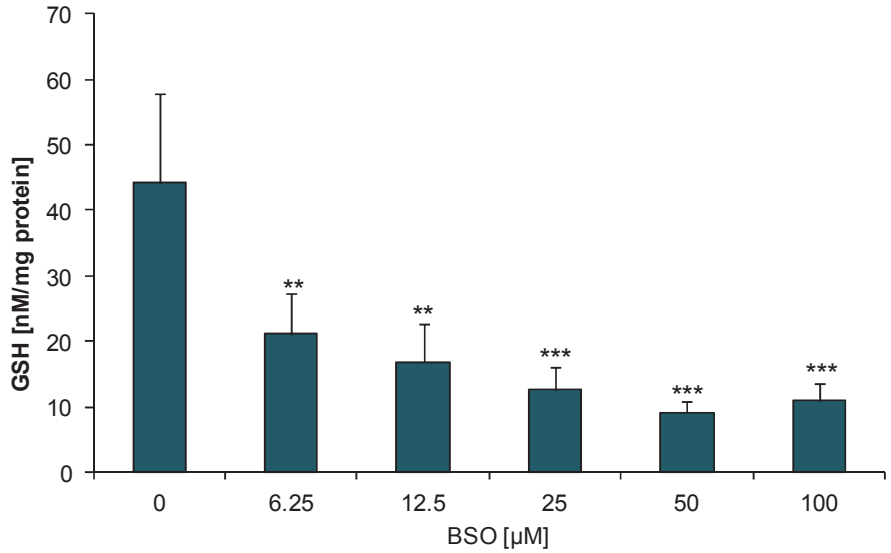

Figure 4.8: Effect of buthionine sulphoximine (BSO) on total glutathione content in Caco-2 cells. The cells were incubated with 0, 6.25, 12.5, 25, 50 or 100 µM BSO for 24 hours, followed by measurement of the intracellular glutathione content, which is expressed as nM/mg protein. Three independent experiments were performed (n=3). **p< 0.01, ***p<0.001 versus untreated cells, ANOVA with post hoc Dunnett test.

4.2.7 Influence of the cellular glutathione status on oxidant-induced DNA damage in Caco-2 cells

To analyse the importance of the cellular glutathione status in the defence against oxidant-induced DNA damage in Caco-2 cells, the cells were pre-treated with a low (5 µM) or a high (100 µM) concentration of BSO to reduce the amount of glutathione at different levels. To induce oxidative stress, hydrogen peroxide (H_2O_2) was used. After 24 hours pre-treatment with BSO, the Caco-2 cells were incubated with 100 µM H_2O_2 for 30 minutes. Afterwards, DNA strand breaks as well as oxidative DNA adducts were analysed in Caco-2 cells by comet assay. As shown in Figure 4.9 panel A., H_2O_2 induced a significant increase in DNA strand breaks compared to the untreated cells. In addition, with increasing BSO concentration, and thus decreasing glutathione amount, the H_2O_2 induced DNA damage tended to increase further, however this effect was not significant. The effect of BSO

pretreatment on H_2O_2 induced oxidative DNA damage induction was also determined with the use of the Fpg-modified comet assay protocol. As shown in (Figure 4.9 B.), H_2O_2 did not cause a significant increase in oxidative DNA lesions in Caco-2 cells that were not pre-treated with BSO. However, in the Caco-2 cells that were pre-exposed to BSO, the ability of H_2O_2- to induce oxidative damage increased, becoming significant at the high dose BSO pre-treatment (100 µM). Interestingly, the BSO pre-treatments alone, did not cause significant changes in global DNA strand breakage levels of oxidative DNA adducts in the Caco-2 cells.

A.

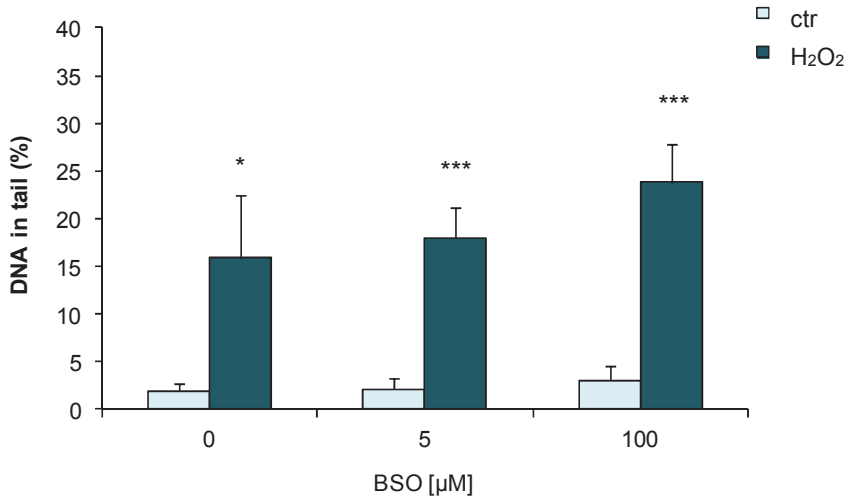

B.

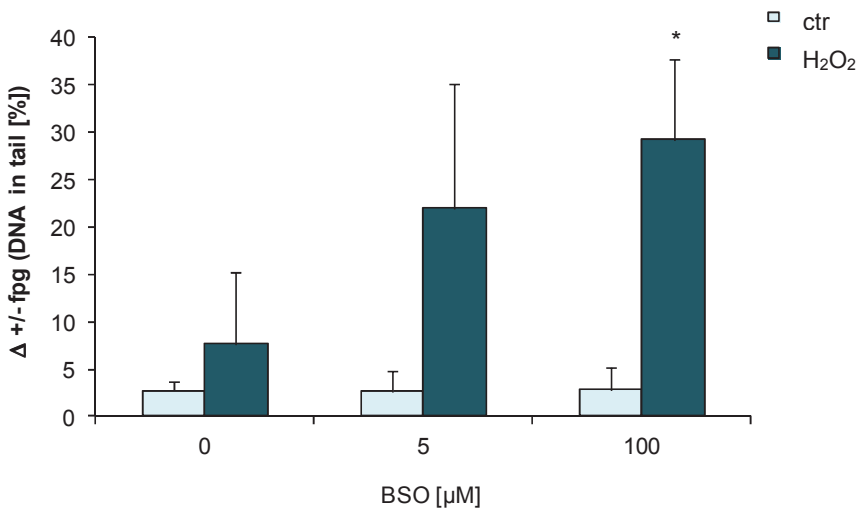

Figure 4.9: Influence of the cellular glutathione status on oxidant-induced DNA damage in Caco- 2 cells. For the analysis of H_2O_2 induced DNA strand breaks (panel A.) and oxidative DNA damage (panel B.) after glutathione depletion, Caco-2 cells were pre-incubated with 0, 5 or 10 µM buthionine sulphoximine (BSO) for 24 hours, and subsequently treated with 100 µM H_2O_2 for 30 minutes. The DNA damage was detected by Fpg-modified comet assay. Three independent experiments were performed. *$p<0.05$ versus current BSO control, ***$p<0.001$ versus concurrent BSO control, t-test.

4.2.8 Effect of NC and curcumin on H_2O_2-induced cytotoxicity in Caco-2 cells

To evaluate the potential protective effects of curcumin and NC towards oxidative stress, Caco-2 cells were pre-incubated with the indicated NC or curcumin concentrations for 24 h, followed by the H_2O_2 treatment for 30 minutes. Afterwards the WST-1 assay was performed to detect the metabolic activity of the cells as an indicator of cytotoxicity. In Figure 4.10 panel A. the effect of NC is shown and in Figure 4.10 B. the effect of curcumin pre-treatment.

A.

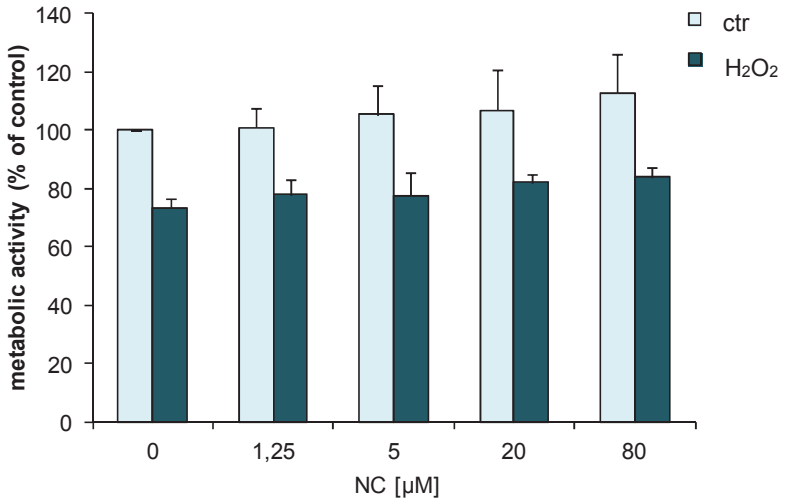

B.

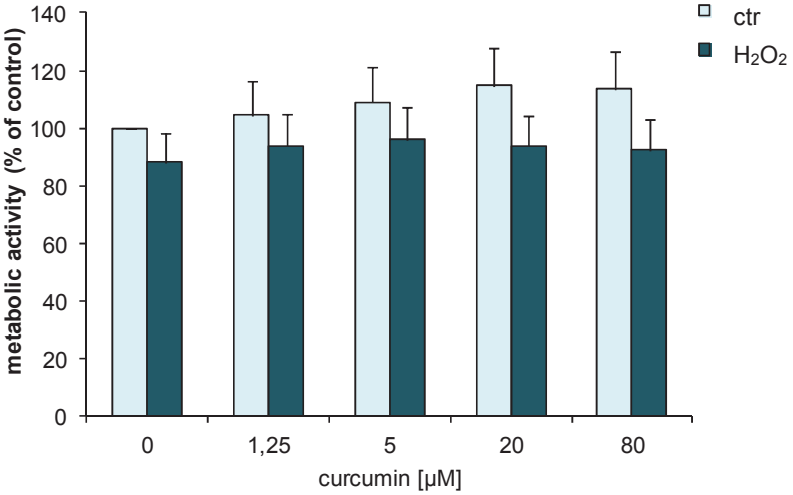

Figure 4.10: Effect of nanocurcumin (NC) and curcumin on H_2O_2-induced cytotoxicity. Caco-2 cells were pre-incubated with the indicated NC and curcumin concentrations (0, 1.25, 5, 20 and 80 µM) for 24 hours, followed by H_2O_2 treatment (100 µM) for 30 minutes. The cytotoxicity was determined by measuring the metabolic activity using the WST-1 assay. The results show the metabolic activity of the cells in percentage of activity as determined for the untreated controls. Three (panel A.) respectively two (panel B.) independent experiments were performed.

In concordance with the results observed earlier (see paragraph 4.2.1 and Figure 4.3), neither NC nor curcumin incubation was cytotoxic up to a concentration of 80 µM. However, the H_2O_2 treatment caused a reduction of the metabolic activity in Caco-2 cell of approximately 10 to 30% from control levels. Neither curcumin, nor NC was found to restore this oxidant associated metabolic activity loss. Thus, neither curcumin nor NC appeared to have a protective effect towards H_2O_2-induced cytotoxicity in Caco-2 cells.

4.2.9 Effect of NC on H_2O_2-induced DNA strand breakage

Although NC and curcumin were not found to protect Caco-2 cells against H_2O_2-induced cytotoxicity in general, the potential anti- DNA damaging effect of NC was evaluated. Specifically, it was explored whether NC could protect the Caco-2 cells from H_2O_2-induced DNA damage as, in contrast to non-encapsulated free curcumin, the NC did not cause oxidative DNA damage itself in these cells (as shown in paragraph 4.2.2 and Figure 4.4). Therefore, the Caco-2 cells were pre-incubated with different NC concentrations for 24 hours, followed by a 30 minutes treatment with H_2O_2 at a concentration of 0 µM, 25 µM or 100 µM. DNA strand breakage was evaluated by comet assay, and shown in Figure 4.11.

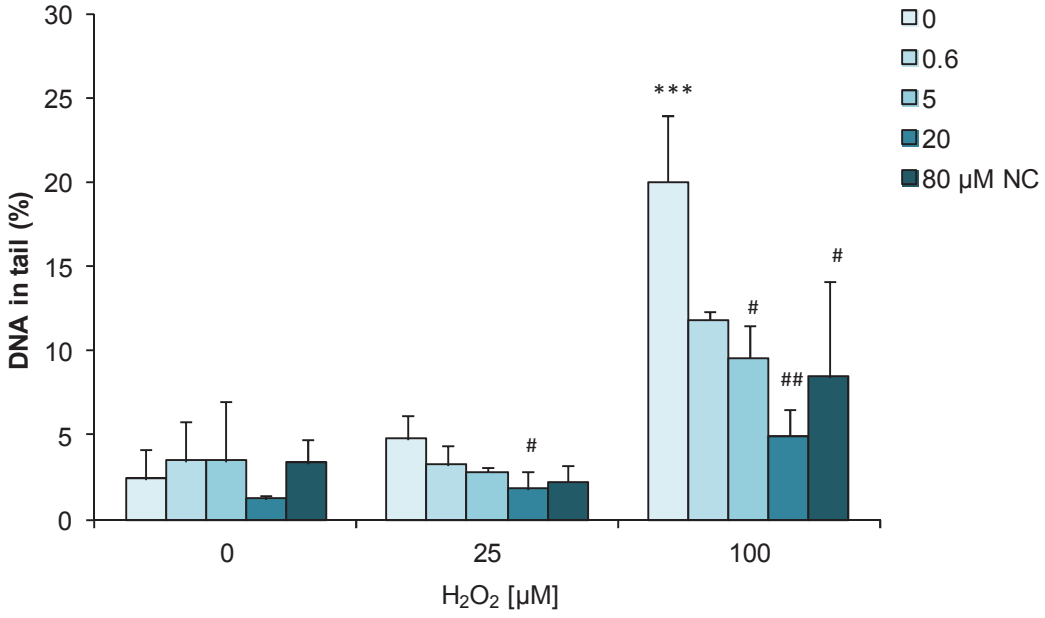

Figure 4.11: Influence of nanocurcumin (NC) on H_2O_2-induced DNA strand breaks. Caco-2 cells were pretreated with 0, 0.6, 5, 20 or 80 µM NC for 24 hours followed by H_2O_2 treatment (0, 25 or 100 µM) for 30 minutes. DNA strand breakage was analysed by comet assay. Three independent experiments were performed (n=3). #p<0.05 versus respective control [25 µM H_2O_2; 0 µM NC] or [100 µM H_2O_2; 0µM NC], ##p<0.01 versus control [100 µM H_2O_2; 0µM NC], ***p<0.001 versus control [0 µM H_2O_2; 0µM NC].ANOVA with post hoc Tukey.

The highest H_2O_2 dose caused a marked and significant increase of DNA damage, however, only in the Caco-2 cells that were not pre-treated with the NC. Pre-incubation of the cells with NC was found to cause a clear concentration-dependent protection against oxidant induced DNA stand breakage. Except for the lowest NC concentration, this effect was significant. The lower H_2O_2 concentration (25 µM) as well as the NC itself did not affect the DNA. Independent of the presence of oxidative stress, 20 µM NC seems to be the optimum concentration to reduce DNA damage levels in the Caco-2 cells.

4.2.10 Effect of NC on oxidative DNA damage induced by PMA-activated neutrophils

To analyse the protective effect of NC in matters of (oxidative) DNA damage under more biologically relevant treatment conditions, phorbol myristate acetate (PMA)-activated neutrophils (PMN) were used to induce oxidative stress as it occurs in inflammation. Therefore, the PMN were isolated from peripheral blood from young healthy volunteers by density gradient centrifugation and erythrolysis as described in detail in paragraph 3.7. The Caco-2 cells were pre-incubated with 0 µM, 5 µM and 20 µM NC for 24 hours, before the freshly isolated and PMA-activated immune cells were added to the epithelial cells in a ratio of 1:1. After 30 minutes of co-culture, the PMN were removed again by several washing steps and the oxidative DNA damage in Caco-2 cells was analysed by Fpg-modified comet assay. The results of these experiments are shown in Figure 4.12. The PMA-activated neutrophils were found to cause a significant induction of oxidative DNA damage in the Caco-2 cells. In the cells that were pre-treated with NC lower levels of oxidative DNA adduct were detected, that did not reach a statistical significance. However, the oxidative lesions were still higher than in the control cells, and there was also no clear concentration dependent effect visible for the NC. Treatment of PMA alone did not affect the oxidative DNA levels of the Caco-2 cells.

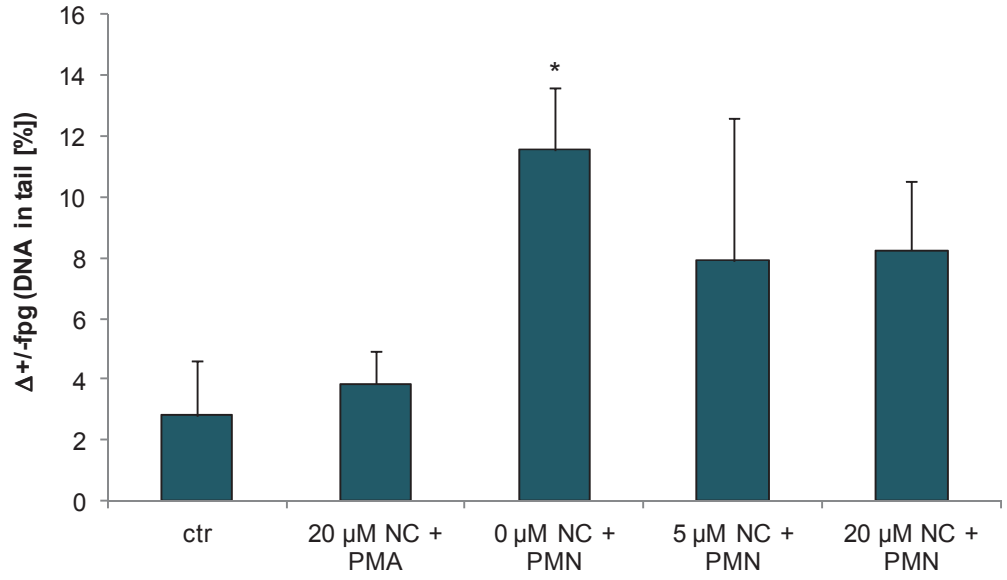

Figure 4.12: Effect of nanocurcumin (NC) on oxidative DNA damage induction in Caco- 2 cells upon co-incubation with phorbol myristate acetate (PMA)-activated neutrophils. Neutrophils (PMN) were isolated from peripheral blood from young healthy volunteers. Prior to co-incubation with the PMA-activated PMN, the Caco-2 epithelial cells were pre-treated with 0 µM (0 µM NC+PMN), 5 µM (5 µM NC+PMN) and 20 µM NC (20 µM NC+PMN) for 24 hours. The Caco-2 cells and the PMN were co-cultured for 30 minutes. Afterwards the PMN were removed and the oxidative DNA damage in Caco- 2 cells was analysed by Fpg-modified comet assay. Oxidative damage is expressed as Δ+/-fpg (DNA in tail [%]). The following controls were included in the experiments: Untreated Caco-2 cells (ctr) and Caco-2 cells that were pre-treated with 20µM NC and subsequently treated with PMA in the absence of PMN (20 µM NC+PMA). Three independent experiments were performed (n=3). * $p<0.05$ versus control, ANOVA with post hoc Tukey.

4.3 *In vivo study*: Investigations of the therapeutic efficacy of NC in the DSS induced colitis model

The aim of the current study was to evaluate the potential therapeutic efficacy of NC, also compared to bulky curcumin, in inflammatory bowel diseases, like ulcerative colitis. In the *in vitro* study, an anti-oxidative effect of NC could be determined in the Caco-2 cells in the presence of oxidative stress, as may occur in inflammation. Subsequently, the potential preventive effects of NC were assessed *in vivo* in two independent murine colitis models. First, the most commonly applied, i.e. chemically induced colitis model was used, the Dextran Sodium Sulphate (DSS) model. The results of this study are described in this paragraph. In the second step, a study was performed using the genetically induced colitis model *Winnie*. The results of this study are described from paragraph 4.4 onwards.

The DSS induced colitis is based on the chemical disruption of the mucosal barrier. DSS is directly toxic to intestinal epithelial cells and thereby causes massive infiltration of inflammatory cells in the lamina propria resulting in severe inflammation. In the DSS studies mice were treated with 3% DSS in the drinking water for 7 consecutive days. At the same time, 40 or 80 mg/kg NC, 80 mg/kg PLGA, or 40 or 80 mg/kg curcumin were administered orally every day to the different treatment groups of mice as described in paragraph 3.8.2.1. The control group, having normal drinking water, as well as the DSS control group received the curcumin solvent olive oil. The body weight change and the clinical colitis score, divided in diarrhoea score and rectal bleeding score were determined every day, always immediately before the oral application. After the sacrifice on day 8, the colon weight and the colon length were measured. For histological analysis, Swiss roles were prepared and the cytokine expression profile in the distal colon was evaluated by luminex assay.

4.3.1 Body weight change in DSS treated C57BL/6 mice after PLGA, NC or curcumin application

The body weight of the mice was used as a first indicator for the health of the mice and the severity of the developed inflammation. Results are shown in Figure 4.13. On day 0, the body weight of each individual animal was set as 100%. The measured body weights during the experiment were compared to day 0 and the percentage change was calculated. Until day 4 all animals gained weight, but upon day 5 all animals, except of the controls with normal drinking water began to lose body weight with increasing severity. On day 7 and day 8 the (percent) body weight of the DSS control mice was significant reduced to the control mice.

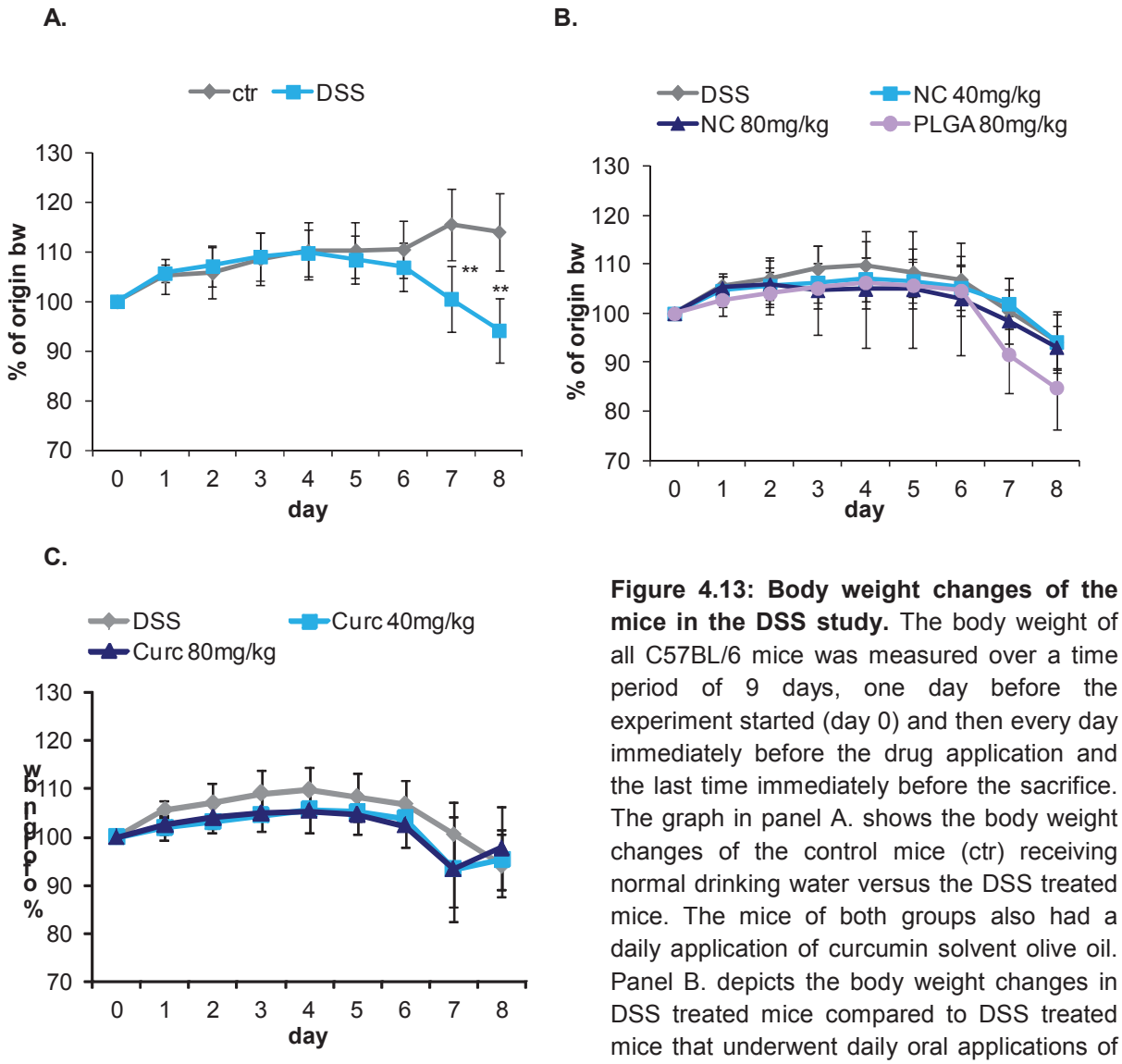

Figure 4.13: Body weight changes of the mice in the DSS study. The body weight of all C57BL/6 mice was measured over a time period of 9 days, one day before the experiment started (day 0) and then every day immediately before the drug application and the last time immediately before the sacrifice. The graph in panel A. shows the body weight changes of the control mice (ctr) receiving normal drinking water versus the DSS treated mice. The mice of both groups also had a daily application of curcumin solvent olive oil. Panel B. depicts the body weight changes in DSS treated mice compared to DSS treated mice that underwent daily oral applications of 40 or 80 mg/kg NC, or 80 mg/kg PLGA respectively. In panel C., the body weight changes of DSS treated mice with and without curcumin (40 mg/kg or 80 mg/kg) application are shown. **p<0.01; t-test: ctr versus DSS, n=6 for all groups.

Overall the DSS-treated mice of the PLGA co-treated group tended to lose most weight with -15 % of the original body weight on day 8. However, this effect was not significantly different from the DSS only treatment group. Taken together, beyond an obvious effect of DSS in the mice, no beneficial effects of curcumin or NC could be observed for whole body weight.

4.3.2 Colitis score in DSS treated C57BL/6 after PLGA, NC and curcumin application

In the current DSS study, the degree of diarrhoea and rectal bleeding was determined from day 4 onwards and is shown in Figure 4.14. The colitis score of the DSS control mice was already significantly increased versus the control group at this day and showed a raising tendency until day 7. On day 5, 6 and 7 the severity of colitis was increased in all DSS treated groups. Again, neither for curcumin nor for NC a beneficial effect was apparent.

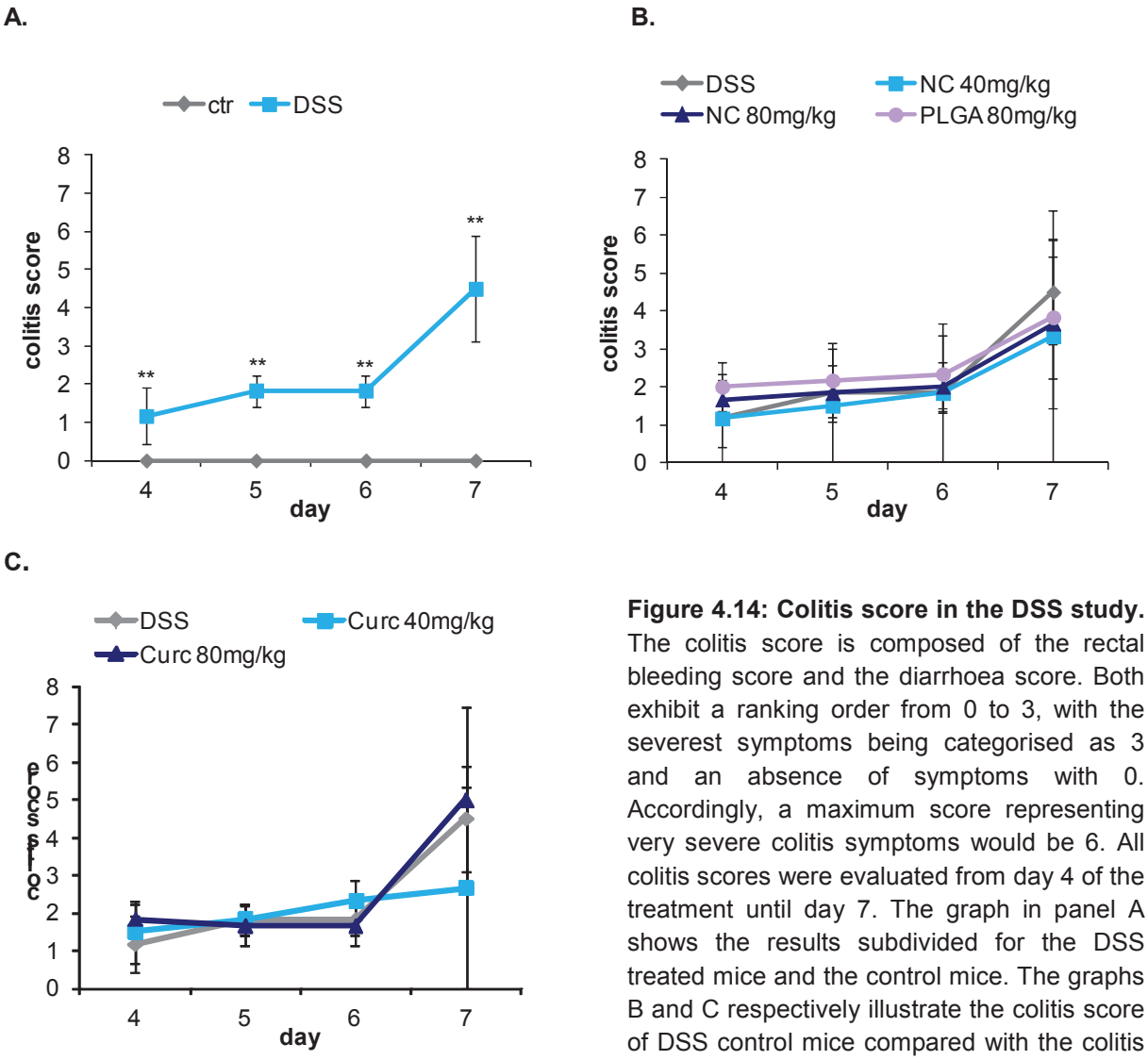

Figure 4.14: Colitis score in the DSS study. The colitis score is composed of the rectal bleeding score and the diarrhoea score. Both exhibit a ranking order from 0 to 3, with the severest symptoms being categorised as 3 and an absence of symptoms with 0. Accordingly, a maximum score representing very severe colitis symptoms would be 6. All colitis scores were evaluated from day 4 of the treatment until day 7. The graph in panel A shows the results subdivided for the DSS treated mice and the control mice. The graphs B and C respectively illustrate the colitis score of DSS control mice compared with the colitis score of DSS mice treated with NC or PLGA (panel B) or compared with curcumin (panel C). The DSS control group and the control group with normal drinking water received by gavage the curcumin solvent olive oil and the other DSS treated mice were grouped respectively of the oral drug application in 40 or 80 mg/kg NC, 40 or 80 mg/kg curcumin and 80 mg/kg PLGA. **p<0.01, Mann-Whitney test: DSS versus control, n=6 for all groups.

4.3.3 Colon length and colon weight in DSS treated C57BL/6 after PLGA, NC or curcumin application

The colon length and the colon weight were examined as an indicator of inflammation. In presence of inflammation, many inflammatory cells are recruited to the site of injury and oedema are formed, explaining why the colon weight is rising (Izcue et al., 2008). In contrast, the colon length typically is diminished with a higher degree of inflammation due to fibrosis (Feldherr and Akin, 1997). The results of these evaluations are shown in Figure 4.15. After DSS treatment for 7 days, the colon weight was not significantly changed in any of the treatment groups (panel A.), whereas the colon length (panel B.) was significantly reduced in the DSS control compared to the control with normal drinking water. However, the daily application of PLGA, NC or curcumin in DSS treated mice for 7 days did not affect colon weight or colon length, when compared to DSS treatment only. Also the ratio of colon weight and colon length (depicted in Figure 4.15 C.) was only changed in a significant manner in the DSS control group compared to the untreated control. Again, none of the other treatments significantly modified the DSS effect.

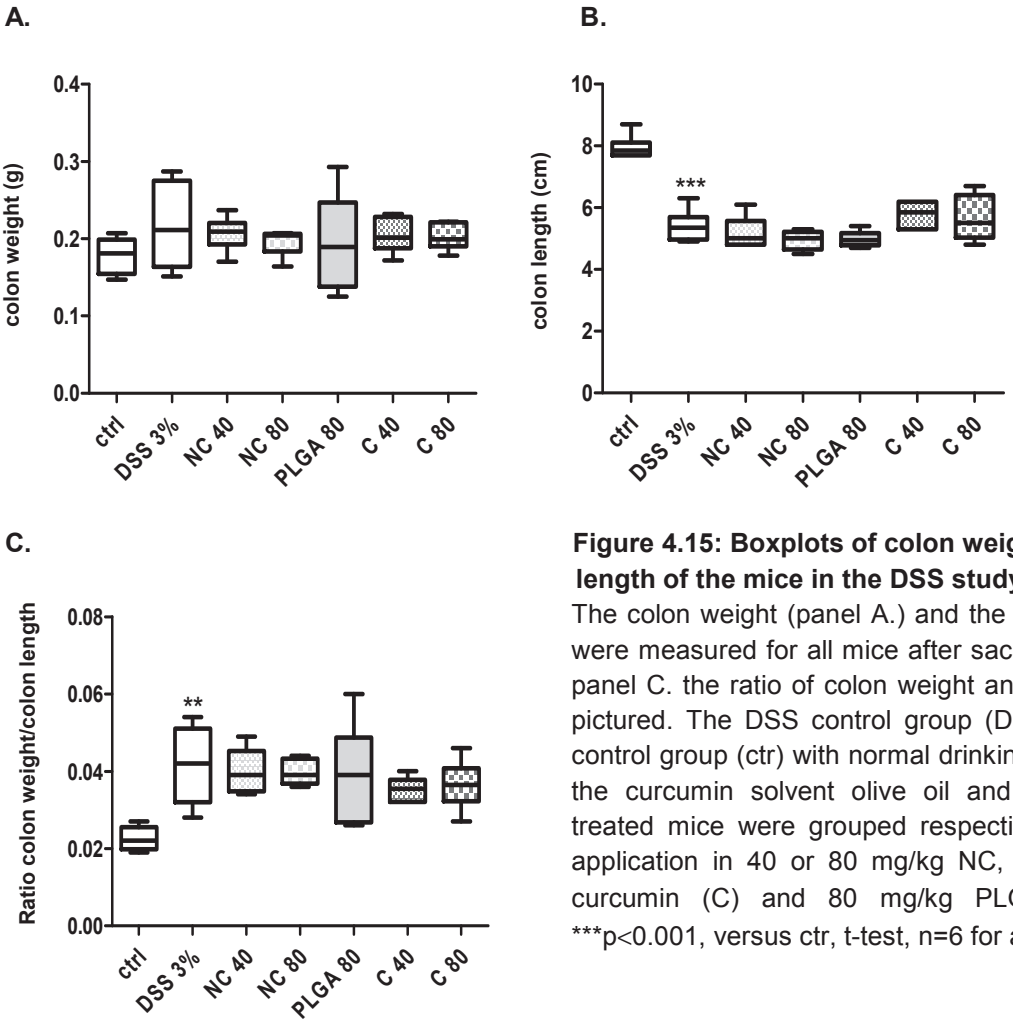

Figure 4.15: Boxplots of colon weight and colon length of the mice in the DSS study.
The colon weight (panel A.) and the colon length (B.) were measured for all mice after sacrifice at day 7. In panel C. the ratio of colon weight and colon length is pictured. The DSS control group (DSS 3%) and the control group (ctr) with normal drinking water received the curcumin solvent olive oil and the other DSS treated mice were grouped respectively of the drug application in 40 or 80 mg/kg NC, 40 or 80 mg/kg curcumin (C) and 80 mg/kg PLGA**$p<0.01$ and ***$p<0.001$, versus ctr, t-test, n=6 for all groups.

4.3.4 Histological colitis score

To determine the clinical severity in DSS induced colitis, the histological colitis score was evaluated by scoring of inflammation severity (score range 0-3), infiltration extend (0-4), epithelial damage (0-5), and percentage involvement of epithelial damage (includes crypt abscessed, crypt loss or ulceration) (0-4). Using intestinal Swiss role tissue sections, the individual colon parts were analysed under the light microscope. The findings of these evaluations are shown in Figure 4.16. In all colon parts evaluated, namely cecum (panel A.), proximal colon (B.), mid colon (C.) and distal colon/rectum (D.) the histological colitis score was found to be significantly increased in the DSS treated animals compared to the untreated control mice. Interestingly, the daily application of 40 mg/kg curcumin reduced the colitis symptoms significantly in cecum, mid colon and distal colon. In the distal colon also the higher curcumin concentration (80 mg/kg) led to a significantly improved histological colitis score compared to the DSS treated group, similar to 80 mg/kg NC. However, in all other colon parts NC had no influence, neither with 40 mg/kg curcumin concentration nor with 80 mg/kg curcumin concentration. Furthermore, PLGA did not affect the intestinal histological colitis score in DSS-induced colitis.

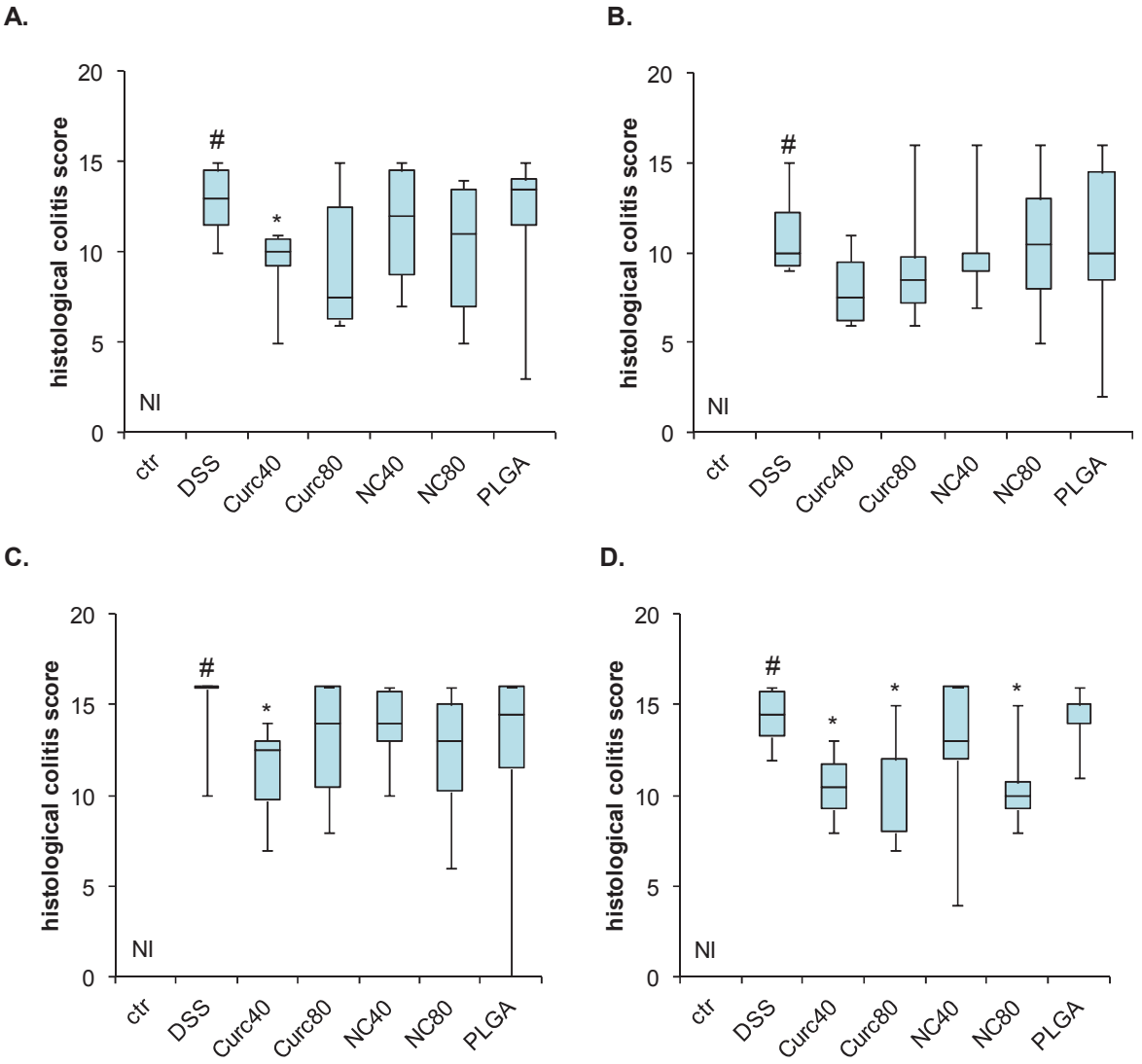

Figure 4.16: Boxplots of histological colitis score data in the DSS study.

The histological colitis score in DSS treated mice was analysed in cecum (panel A.), proximal colon (B.), mid colon (C.), and distal colon/rectum (D.) using intestinal Swiss role tissue sections. The control mice (ctr), fed with normal drinking water and the DSS treated control mice (DSS) received by gavage the curcumin solvent olive oil. The other DSS treated mice were grouped respectively for the oral drug application in 40 or 80 mg/kg NC, 40 or 80 mg/kg curcumin or 80 mg/kg PLGA vehicle. The severity of colitis in DSS treated mice was evaluated by scoring of inflammation severity (score range 0-3), infiltration extent (0-4), epithelial damage (0-5), and the percentage involvement of epithelial damage (includes crypt abscesses, crypt loss or ulceration) (0-4). *$p<0.05$ versus DSS; #$p<0.01$ versus control; Mann-Whitney test; n=6 for all groups. NI: not induced

4.3.5 Luminex analysis to detect cytokine and chemokine protein expression level in DSS treated mice after PLGA, NC and curcumin application

After 7 days treatment, the cytokine and chemokine expression levels were analysed in the distal colon tissue of the mice by luminex assay. Hereby, the protein levels of six different cytokines (IL-1α, IL-1β, IL-6, IL-17, G-CSF and GM-CSF, shown in Figure 4.17) and five different chemokines (MCP-1, MIP-1α, MIP-1β, RANTES and KC, shown in Figure 4.18) were measured. Because the distal colon, which is mostly involved in UC, is also mainly affected by the DSS-induced epithelial damage, the luminex analysis was performed for this tissue part. After homogenization of the distal colon tissue, equal protein amounts were used in the luminex assay and the cytokine concentrations were denoted as pg/mg protein. Next to the untreated control and the DSS group, the DSS groups with 80 mg/kg PLGA, 80 mg/kg NC and 80 mg/kg curcumin application were investigated in this assay. As can be seen in Figures 4.17 and 4.18, no significant differences in distal colon tissue levels were found for IL-1α, IL-17, GM-CSF, MCP-1, MIP-1β and RANTES. The most pronounced treatment related differences were observed for IL-1β (Figure 4.17 panel B.). After DSS feeding as well as after DSS feeding together with PLGA or NC application, a significantly higher tissue level was found for this cytokine. Moreover, in the DSS-induced colitis, the curcumin caused a significant reduction of IL-1β compared to the DSS group, as well as compared to the NC group. This indicates a beneficial effect of curcumin in DSS induced colitis, even in comparison to NC. Moreover, IL-6 was significantly elevated in the distal colon tissues of the NC group (Figure 4.17 panel C.) and G-CSF was elevated in the PLGA group (Figure 4.17 panel E.) compared to the control. Marked effects were also observed with the chemokines MIP-1α and KC. The colon tissue level of MIP-1α (Figure 4.18 panel B.) was significantly increased in the DSS, DSS-PLGA and DSS-NC treatment groups in comparison to the control group, in the DSS-PLGA group the level was even further increased than in the DSS only group. Moreover, PLGA and NC application in DSS fed mice enhanced the KC expression significantly compared to control and in addition, the NC group even showed a significantly higher KC level than the DSS only group (Figure 4.18 panel E.). Altogether, the luminex data indicates that the curcumin offered some-anti-inflammatory features to the DSS-induced colitis, whereas the treatment of the nanoparticles (i.e. NC and PLGA) rather tended to enhance specific pro-inflammatory markers in this experimental model.

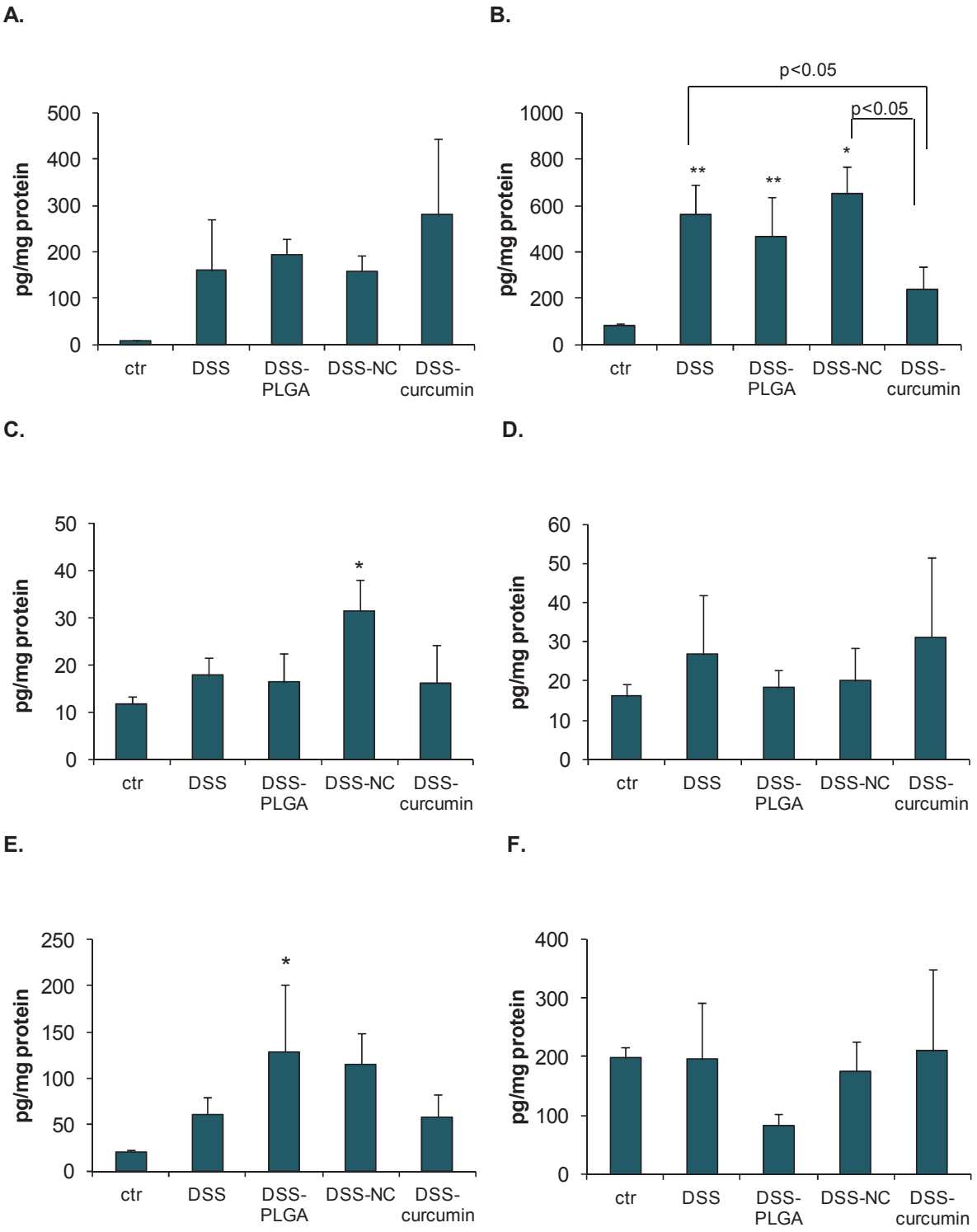

Figure 4.17: Cytokine protein expression levels in the DSS colitis model after treatment with PLGA, NC and curcumin. Analysis of the protein expression level of a panel of cytokines was determined by luminex assay in the distal colon of control mice (ctr) or Dextran sulfate sodium (DSS) treated mice after the daily application of PLGA, nanocurcumin (NC) or curcumin for 7 days. The following cytokines were detected by Bio-Rad luminex assay and illustrated as pg/mg protein: Interleukin (IL)-1α (panel A.), IL-1β (B.), IL-6 (C.), IL-17 (D.), G-CSF (E.) and GM-CSF (F.). *p<0.05, **p<0.01 versus ctr, ANOVA with post hoc LSD; n=5 for ctr, n=5 for DSS, n=4 for DSS-PLGA, n=6 for DSS-NC, n=6 for DSS-Curc

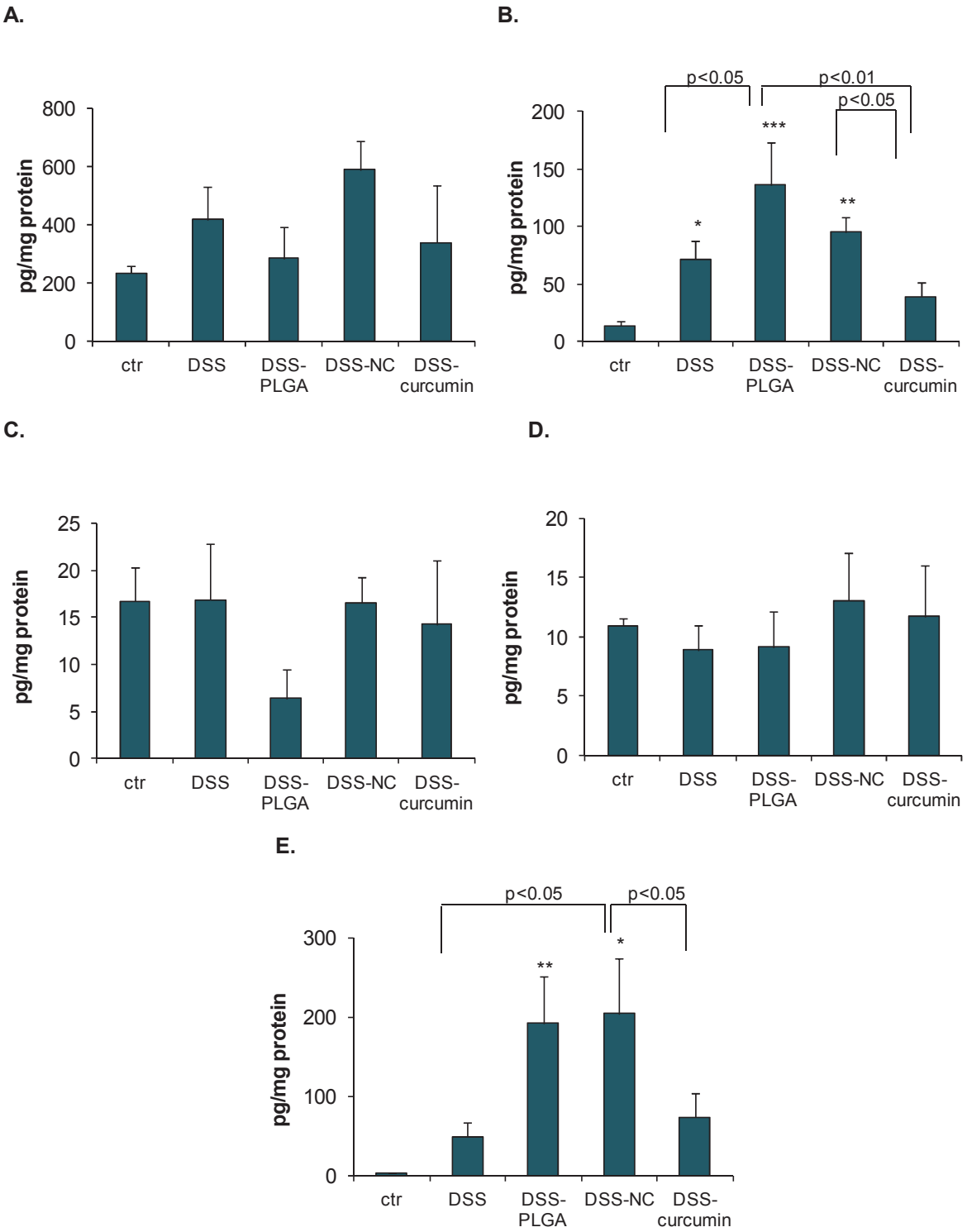

Figure 4.18: Chemokine level in the DSS model after treatment with PLGA, NC and curcumin. Analysis of the protein expression level of a variety of chemokines in the distal colon of Dextran sulfate sodium (DSS) treated mice after the daily application of PLGA, nanocurcumin (NC) and curcumin for 7 days. Following chemokines were detected by Bio-Rad luminex assay and illustrated as pg/mg protein: MCP-1 (A.), MIP-1α (B.), MIP-1β (C.), RANTES (D.) and KC (E.). *p<0.05, **p<0.01, ***p<0.001 versus ctr, ANOVA with post hoc LSD; n=5 for ctr, n=5 for DSS, n=4 for DSS-PLGA, n=6 for DSS-NC, n=6 for DSS-Curc.

4.4 *In vivo study*: Investigations of the therapeutic efficacy of NC in the mutagen generated colitis model- the *Winnie* model

The *Winnie* model, generated by mutagenesis, has a single nucleotide polymorphism in the Muc2 gene, and as a consequence the mice develop spontaneous colitis (Heazlewood et al., 2008). The severity of the disease increases with the age of the mice. The mucin expression in both mouse models was evaluated by PAS/Alcain blue staining. The *Winnie* mice and the wild type mice (C57BL/6) received 80 mg/kg NC or curcumin, respectively by oral application as described in detail in the methods section (see paragraph 3.8.2.2). The control group animals only obtained the curcumin solvent, olive oil. For the whole treatment period, the body weight and the colitis score were monitored. After 14 days the mice were sacrificed, colon weight and colon length were determined and the severity of effects was also evaluated by histology after preparation of Swiss rolls. Using luminex analysis the protein expression of cytokines and chemokines was evaluated in distal colon tissues, similar to the DSS study. In addition, in the present in vivo study, mRNA was isolated from proximal as well as distal colon tissue of the Winnie and C57BL/6 mice to evaluate expression differences of various genes. These included Muc2 as well as a number of markers of oxidative stress, ER stress and oxidative DNA damage repair.

4.4.1 Pas/Alcain Blue staining

Winnie mice have been shown to display an aberrant mucin expression caused by the mutation in their Muc2 gene. To verify the mucin expression defect in this model for the present investigations, intestinal Swiss role tissue sections from both the *Winnie* mice and wild type mice were stained with Pas/Alcain blue. Alcain blue stains all acidic mucins intensively blue in normal mice. In contrast, the neutral immature mucins in the *Winnie* mice intestine are not stained by Alcain Blue, but only by Periodic Acid-Schiff (PAS) reagent. As shown in Figure 4.19, tissues from the C57BL/6 wild type mice display clearly blue stained goblet cell thecae, from proximal to distal colon, based on the storage of mature mucins. Furthermore, the Pas/Alcain blue staining in these mice established the characteristic goblet cell locations in the different parts of the colon. In the proximal colon the most (blue stained) goblet cells were present in the base of the crypts, whereas in the mid colon, the goblet cells were found to reside in the whole crypt from the base to the top. In the distal colon only a few goblet cells were detectable in the top of the crypt. In the tissues from the *Winnie* mice, in contrast, a strongly reduced Alcain blue staining was present in all three colon parts, indicating a reduced amount of mature mucin. Furthermore, no explicit goblet cell position was observed in *Winnie* mice. However, Pas-positive/Alcain blue negative magenta coloured mucin accumulations were detectable, particularly in the proximal and mid colon.

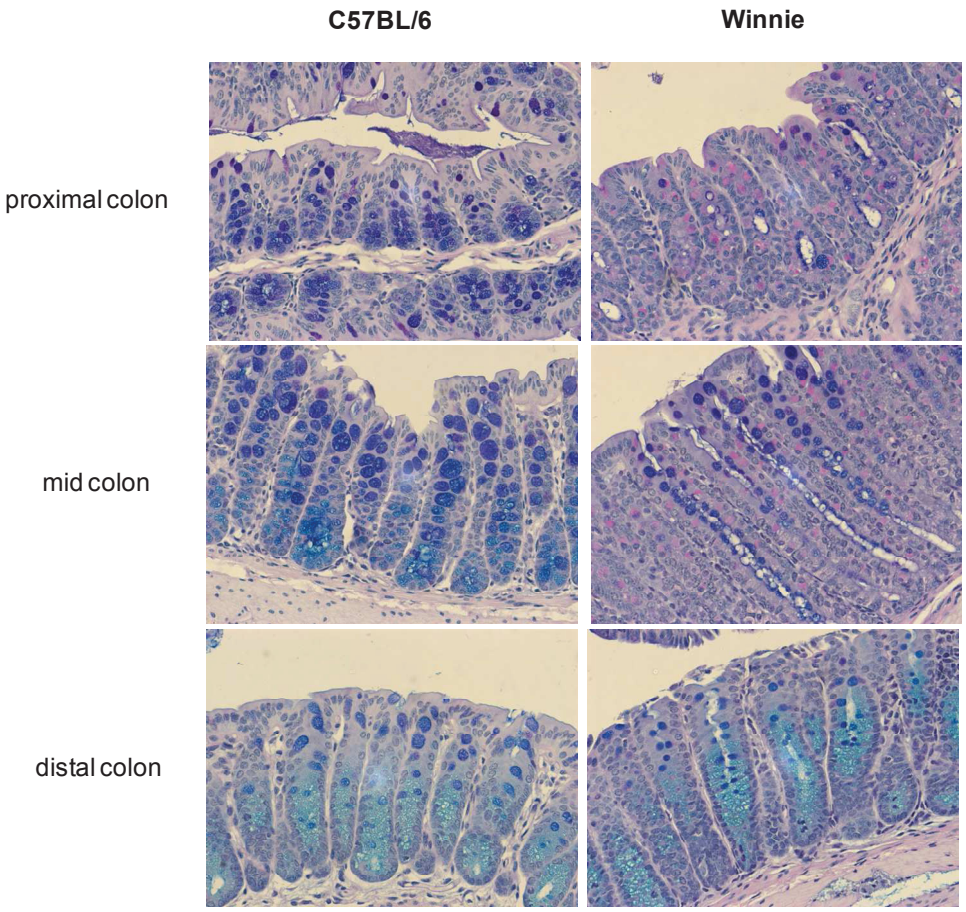

Figure 4.19: Pas/Alcain blue stained intestinal sections from *Winnie* versus wild type mice. The Pas/Alcain blue staining was performed to verify the histological phenotype of the Muc2 mutation-containing *Winnie* mice. Representative stainings of Swiss rolls from wild type C57BL/6 mice (left panels) and *Winnie* mice (right panels) are shown at 400x magnification, for proximal, mid and distal colon respectively. In the C57BL/6 wild type mice the Alcain blue stained mucin was present, typically stored in the goblet cell thecae. As shown here, in the proximal colon most goblet cells are in the base of the crypts. The mid colon has longer crypts with goblet cells from the top to the base of the crypt. In the distal colon the goblet cells are only in the top of the crypts. In the *Winnie* mice, reduced blue stained mucins were present, and instead also Pas-positive/Alcain blue negative magenta coloured mucin accumulations. These were detectable in the proximal colon, mid colon and distal colon.

4.4.2 Body weight change in *Winnie* mice and C57BL/6 after NC and curcumin application for 14 days

The body weights of *Winnie* and wild type mice were evaluated every other day, always immediately before the drug application. The body weight was used as a global indicator for the good health of the animals. In general, the *Winnie* mice in this present study were smaller and lighter than the C57BL/6. In the control group the average weight of the *Winnies* at the study start was 16.47 g and at day 14 the average weight was 19.33 g (Figure 4.20 panel

C.). The wild type mice at day 0 already had an average weight of 21.4 g which increased to an average of 23.25 g after 2 weeks. However, the two drugs, NC and curcumin did not affect the body weight, neither in the Winnie mice nor in wild type mice. Notably also, the colitis symptoms in the *Winnie* mice were not yet so severe that they lost weight. In all *Winnie* groups the body weight increased over the 2 weeks in a range from 12 to 17% of the original weight (panel A.). The animals in the three C57BL/6 groups also gained weight during the experimental time (range 8 to 15%) (panel B.).

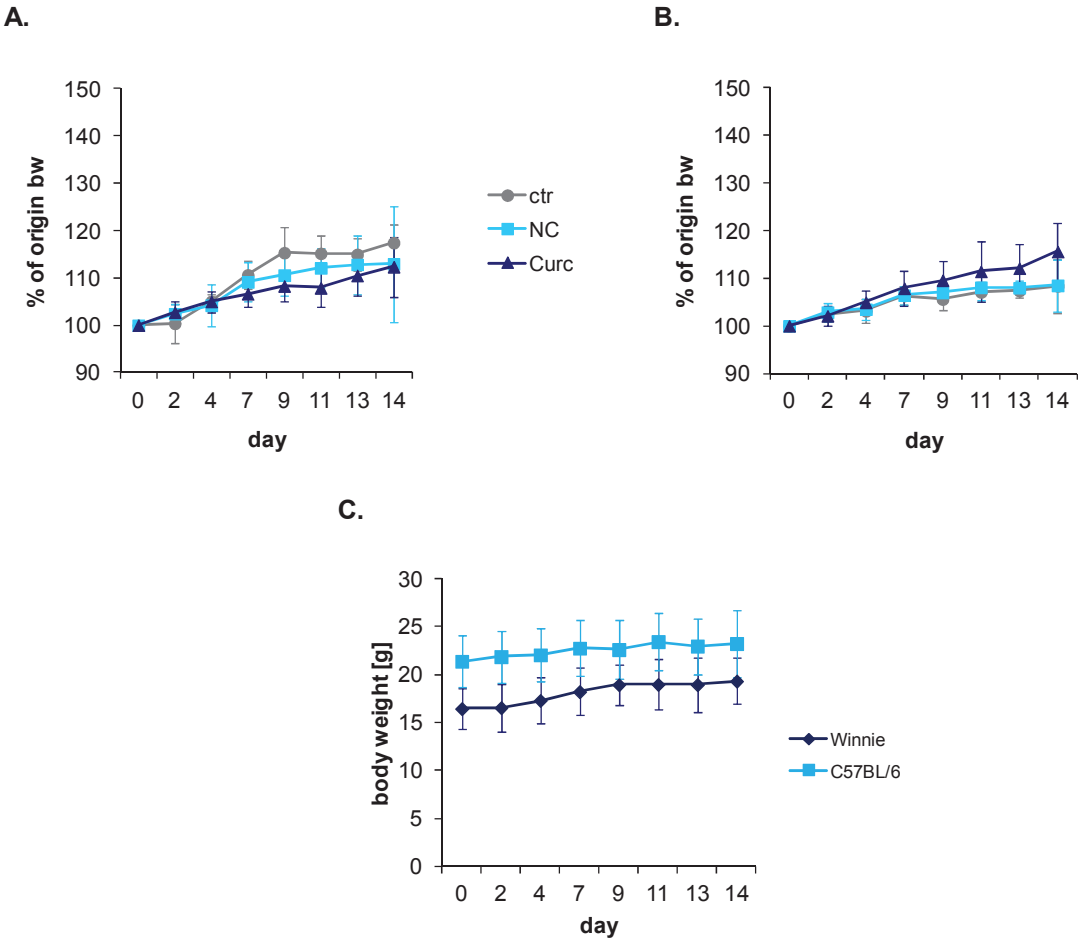

Figure 4.20: Body weights of *Winnie* and C57BL/6 mice. Analysis of the body weight (bw) change in *Winnie* mice (panel A.) and C57BL/6 mice (panel B.) after oral application of curcumin solvent olive oil (ctr), 80 mg/kg nanocurcumin (NC) or 80 mg/kg curcumin (Curc) respectively every other day for a total duration of 2 weeks. The body weight change is illustrated as percentage of origin body weight and represents the average (and standard deviation) of each group. In Panel C. the average body weights in grams (g) of the untreated *Winnie* and wild type mice are shown as well as their changes during the experimental time. n=6 for *Winnie* ctr, n=7 for *Winnie* NC, n=7 for *Winnie* Curc, n=8 for C57BL/6 ctr, n=8 for C57BL/6 NC, n=8 for C57BL/6 Curc.

4.4.3 Colitis score in *Winnie* and C57BL/6 after NC and curcumin application for 14 days

The colitis score was performed in the same way as in the DSS study. As shown in Figure 4.21 panel A., the 6 to 8 weeks old *Winnie* mice had already at day 0 some notable colitis symptoms in a score between 2 and 3. Notably, this score was principally due to diarrhoea, as at this time point no rectal bleeding was noticeable. After NC and curcumin treatment a mild decrease of the colitis symptoms was detected in *Winnie* mice. After 14 days the colitis score of the NC group was found to be significantly reduced compared to the colitis score in the control group and the curcumin group. In all groups of the wild type mice, no significant colitis symptoms were visible over the whole experimental time (panel B.).

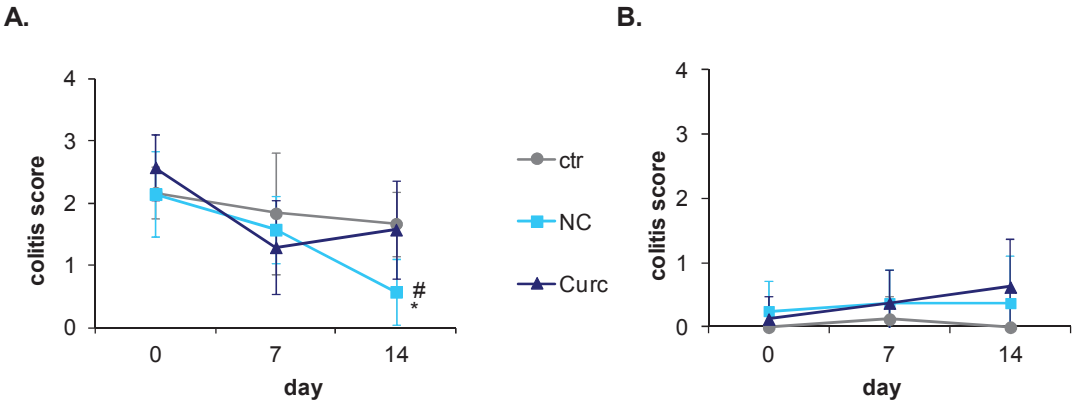

Figure 4.21: Colitis Score in *Winnie* and C57BL/6 mice. Evaluation of the colitis score, as evaluated by rectal bleeding and diarrhoea, in the *Winnie* mice (panel A.) and C57BL/6 mice (panel B.) after day 0, day 7 and day 14. The mice were treated with 80 mg/kg nanocurcumin (NC), 80 mg/kg curcumin (Curc) or just with the curcumin solvent olive oil (ctr) every other day. Both categories have a ranking order from 0 to 3, so the maximal score can be 6 in presence of very severe symptoms. *$p<0.05$ versus ctr day 14, #$p<0.05$ versus curcumin day 14, Mann-Whitney test; n=6 for *Winnie* ctr, n=7 for *Winnie* NC, n=7 for *Winnie* Curc, n=8 for C57BL/6 ctr, n=8 for C57BL/6 NC, n=8 for C57BL/6 Curc

4.4.4 Colon length and colon weight in *Winnie* and C57BL/6 after 14 days NC or curcumin application

Similar to the DSS study, colon lengths and weights were also measured in the present study as an indicator of inflammation. As can be seen in the Figure 4.22 panel A., the colons of the colitis developing *Winnie* mice had a significantly increased weight. However, the colitis in the *Winnie* mice was not yet so severe that their colon length was affected (panel B.). The *Winnie* mice in the NC group had a significantly reduced colon weight compared to the untreated control mice. A trend was also observed for the non-encapsulated curcumin, but

this effect did not reach a statistical significance. The ratio of colon weight to colon length was also significantly increased in Winnie mice compared to C57BL/6. However, no further differences were detectable between the different treatment groups.

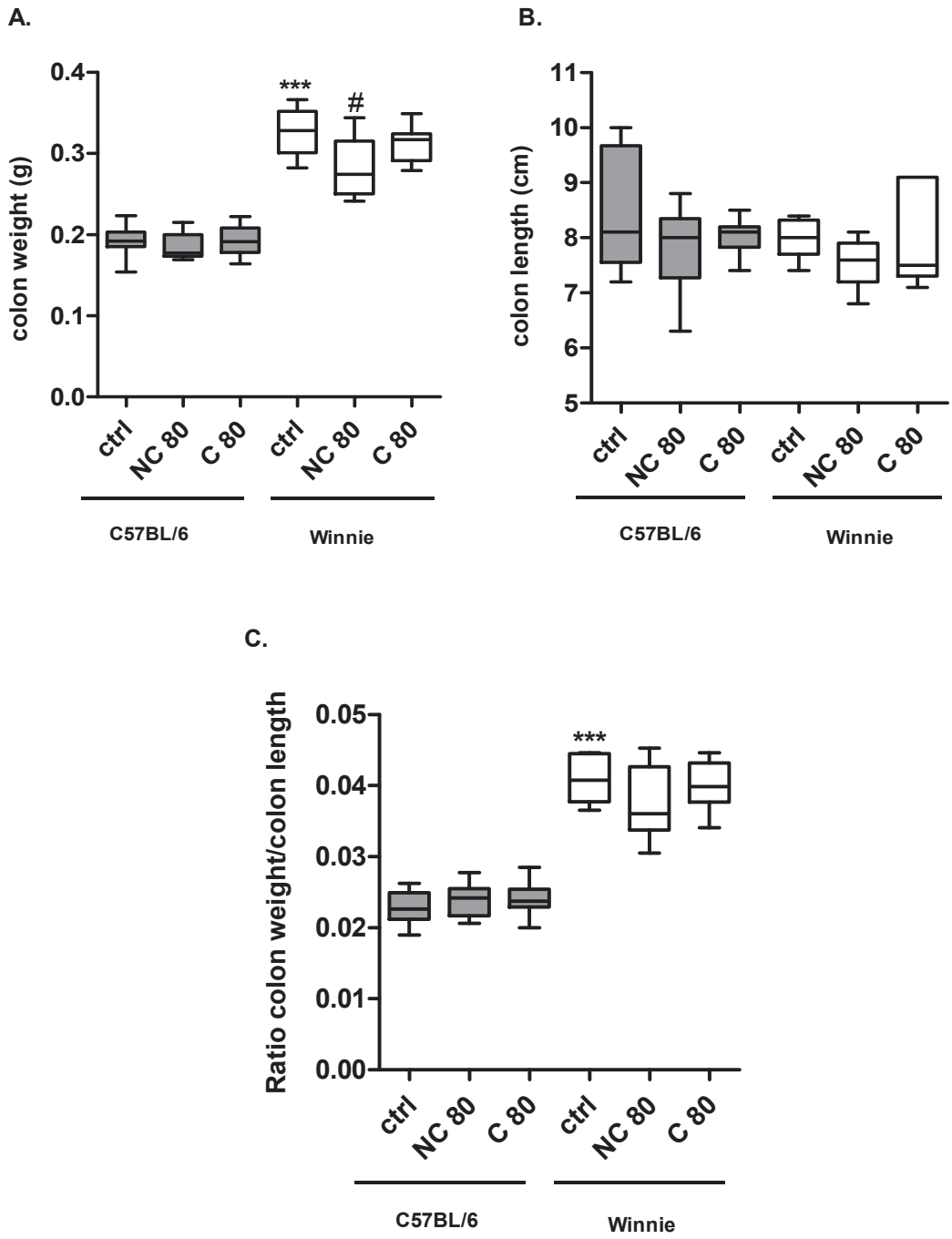

Figure 4.22: Boxplots of colon weight and length measurements in the *Winnie* and C57BL/6 mice. *Winnie* mice and C57BL/6 mice were treated with 80 mg/kg nanocurcumin (NC 80), 80 mg/kg curcumin (C 80) or just with olive oil, used as vehicle (ctrl). The colon weight (panel A.) and the colon length (panel B.) were measured, and the ratio of colon weight to length was calculated (panel C.). #$p<0.05$ versus *Winnie* ctrl,***$p<0.001$ versus C57BL/6 ctrl, t-test; n=6 for *Winnie* ctr, n=7 for *Winnie* NC, n=7 for *Winnie* curcumin, n=8 for C57BL/6 ctr, n=8 for C57BL/6 NC, n=8 for C57BL/6 curcumin.

4.4.5 Histological colitis score

For the determination of the severity of colitis in *Winnie* mice, histological colitis symptoms were evaluated by scoring of aberrant crypt architecture (score range 0-5), increased crypt length (0-3), goblet cell depletion (0-3), general leukocyte infiltration (0-3), lamina propria neutrophil counts (0-3), crypt abscesses (0-3), and epithelial damage and ulceration (0-3). The results are shown in Figure 4.23. In contrast to the wild type mice, the *Winnie* mice possessed colitis symptoms in all colon parts, namely cecum (panel A.), proximal colon (panel B.), mid colon (panel C.) and distal colon/rectum (panel D.). The treatment with NC and curcumin did not improve the histological symptoms score in the *Winnie* mice. In contrast, the wild type mice did not exhibit any colitis symptoms. Interestingly, in some of the C57BL/6 mice the NC caused a slight increase of inflammation in the cecum, while curcumin did so in the proximal colon.

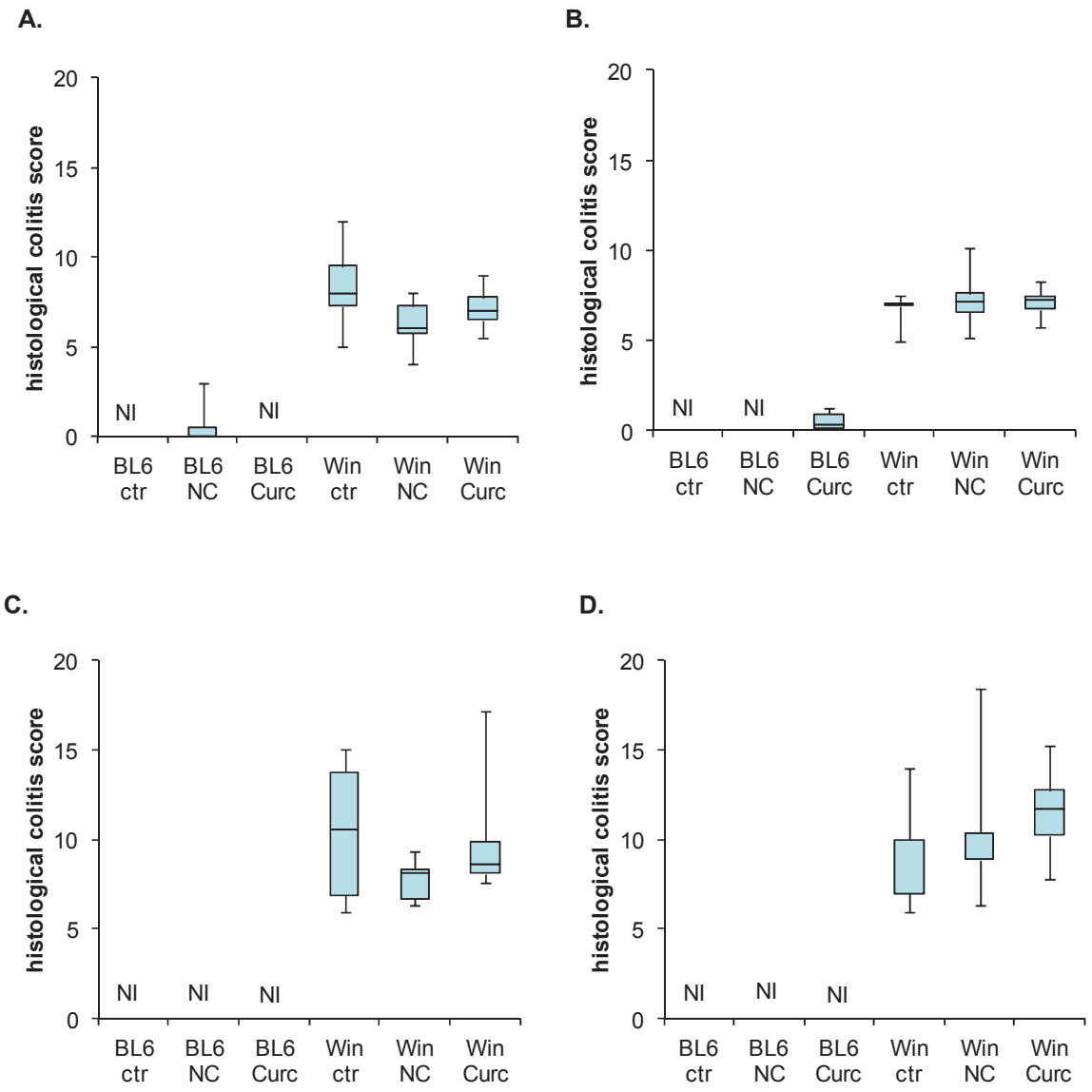

Figure 4.23: Boxplots of histological colitis score data in the *Winnie* and C57BL/6 mice. The histological colitis score in *Winnie* mice and wild type mice (C57BL/6) was analysed in cecum (A.), proximal colon (B.), mid colon (C.), and distal colon/rectum (D.) by microscopical evaluation of intestinal Swiss role tissue sections. The mice were treated every other day for 14 days with NC or curcumin (both 80 mg curcumin/kg). The control mice (ctr) received the curcumin solvent olive oil. The severity of colitis was evaluated by scoring of the aberrant crypt architecture (score range 0-5), increased crypt length (0-3), goblet cell depletion (0-3), general leukocyte infiltration (0-3), lamina propria neutrophil counts (0-3), crypt abscesses (0-3), and epithelial damage and ulceration (0-3). n=8 for all wild type groups (BL6), n=6 for *Winnie* ctr, n=7 for *Winnie* NC, n=7 for *Winnie* Curc. Ni: not induced

4.4.6 Analysis of gene expression in proximal and distal colon tissue of *Winnie* and C57BL/6 mice after NC or curcumin application for 14 days

As described in Heazlewood *et al*., the *Winnie* mice possess a mutation in the mucin gene Muc2, which results in their aberrant Muc2 biosynthesis. This impairment has been associated with ER stress in these animals and intestinal inflammation. To analyse whether these effects can be influenced by oral NC or curcumin application, the mRNA expression of Muc2 gene, and as well as of markers of ER stress were examined in *Winnie* and C57BL/6 mice by qRT-PCR after 2 weeks treatment. Moreover, the expression of a number of markers of inflammation and of oxidative stress/oxidative DNA damage repair was evaluated. The results are shown in Figures 4.24, 4.25, 4.26 and 4.27.

As visualised in Figure 4.24, the Muc2 mRNA expression was found to be significant lower in *Winnie* mice than in the in wild type mice. This difference was visible both in proximal and distal colon, but in the proximal tissue the contrast was more pronounced (Figure 4.24 B.). However, the NC and curcumin application did not significantly influence the Muc-2 mRNA expression.

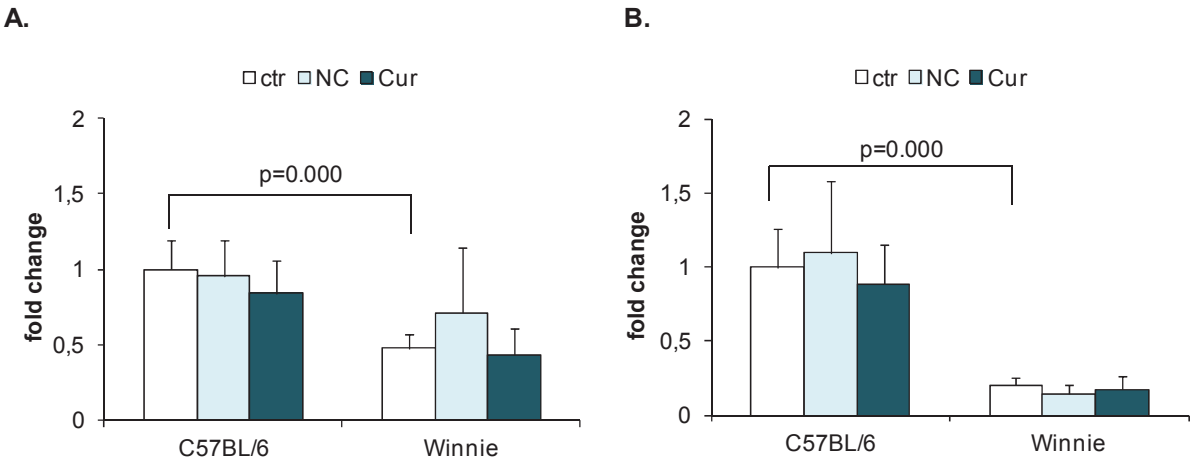

Figure 4.24: Muc2 gene expression in proximal and distal colon tissues of *Winnie* versus C57BL/6 wildtype mice. The mRNA expression of Muc2 was measured by qRT-PCR in distal (panel A.) and proximal (B.) colon of *Winnie* versus C57BL/6 mice after 14 days treatment with NC, curcumin (Cur) or vehicle control (ctr). The gene expression is expressed as fold change of the expression in C57BL/6 control mice. ANOVA with post hoc LSD; n=6 for *Winnie* ctr, n=7 for *Winnie* NC, n=7 for *Winnie* Cur, n=8 for C57BL/6 ctr, n=8 for C57BL/6 NC, n=8 for C57BL/6 Cur.

To further evaluate the inflammatory state in the spontaneous colitis model *Winnie* and its potential modification of NC and curcumin application, the mRNA expression levels of IL-1β, IL-23 and TNF-α were measured (see Figure 4.25). Interestingly, the expression level of IL-1β tended to be increased in the distal colon tissue of the *Winnie* control mice in

comparison to the wild type controls, while NC and, to a lesser extent also curcumin, tended to reduce this effect (Figure 4.25 A.). However, due to the large variability of expression in the *Winnie* mice these effects did not reach a statistical difference. In the C57BL/6 wild type mice, a small but statistically significant lower mRNA expression of IL-1 β was observed in the curcumin treated group. No significant differences were found in the proximal colon tissues for both mouse backgrounds (Figure 4.25 B.). Surprisingly, IL-23 was expressed to a significantly lower extent in the *Winnie* mice than in the healthy mice. However, the NC or curcumin treatment had neither distal nor proximal an influence on the IL-23 mRNA expression (Figure 4.25 C. & D.). Also for the mRNA expression of the pro-inflammatory cytokine TNF-α, no particular trends was visible (Figure 4.25 E. & F.).

Due to the Muc2 protein misfolding, ER stress is induced in *Winnie* mice. Therefore, the mRNA expression of both the spliced and the unspliced XBP1 was analysed in the various treatment groups of this study. The spliced version of XBP1 is considered to represent a specific ER stress marker which induces UPR (unfolded protein response) target genes. Those represent a network of signal transduction pathways that are activated in response to ER stress. In contrast, the unspliced form of XBP1 encodes a transcription factor which represses UPR target genes (Heazlewood et al., 2008). The observed mRNA expression patterns for both genes is shown in Figure 4.26. Surprisingly, less spliced XBP1 was found in the *Winnie* mice compared to C57BL/6 mice, while in the literature (Heazlewood et al., 2008) no difference was predicted in those two animal models. Nevertheless, in the distal colon of *Winnie* mice curcumin treatment was associated with a diminished mRNA expression level of this ER stress marker, also when compared to the NC group (Figure 4.26 A.). In the proximal part, NC and curcumin significantly influenced the gene expression of spliced XBP1 (panel B.). The unspliced XBP1 mRNA expression was found to be reduced in both colon parts of the *Winnie* mice when compared to the respective tissues of the wild type (Figure 4.26 C. & D.). This is in support of the presence of ER stress in the *Winnie* model, in accordance with published findings (Heazlewood et al., 2008). Interestingly, the NC application was found to cause a significant mRNA increase of the ER stress repressor in the proximal colon of C57BL/6 compared to the curcumin treated group (panel D).

In relation to the observed effects for both mRNAs, the resultant calculated ratio of spliced and unspliced XBP1, which is considered as indicator for UPR activation was higher in the colitis model than in the wild type (Figure 4.26 E. & F.). In the NC treated C57BL/6 mice the ratio was significant decreased in proximal colon compared to the control and the curcumin group.

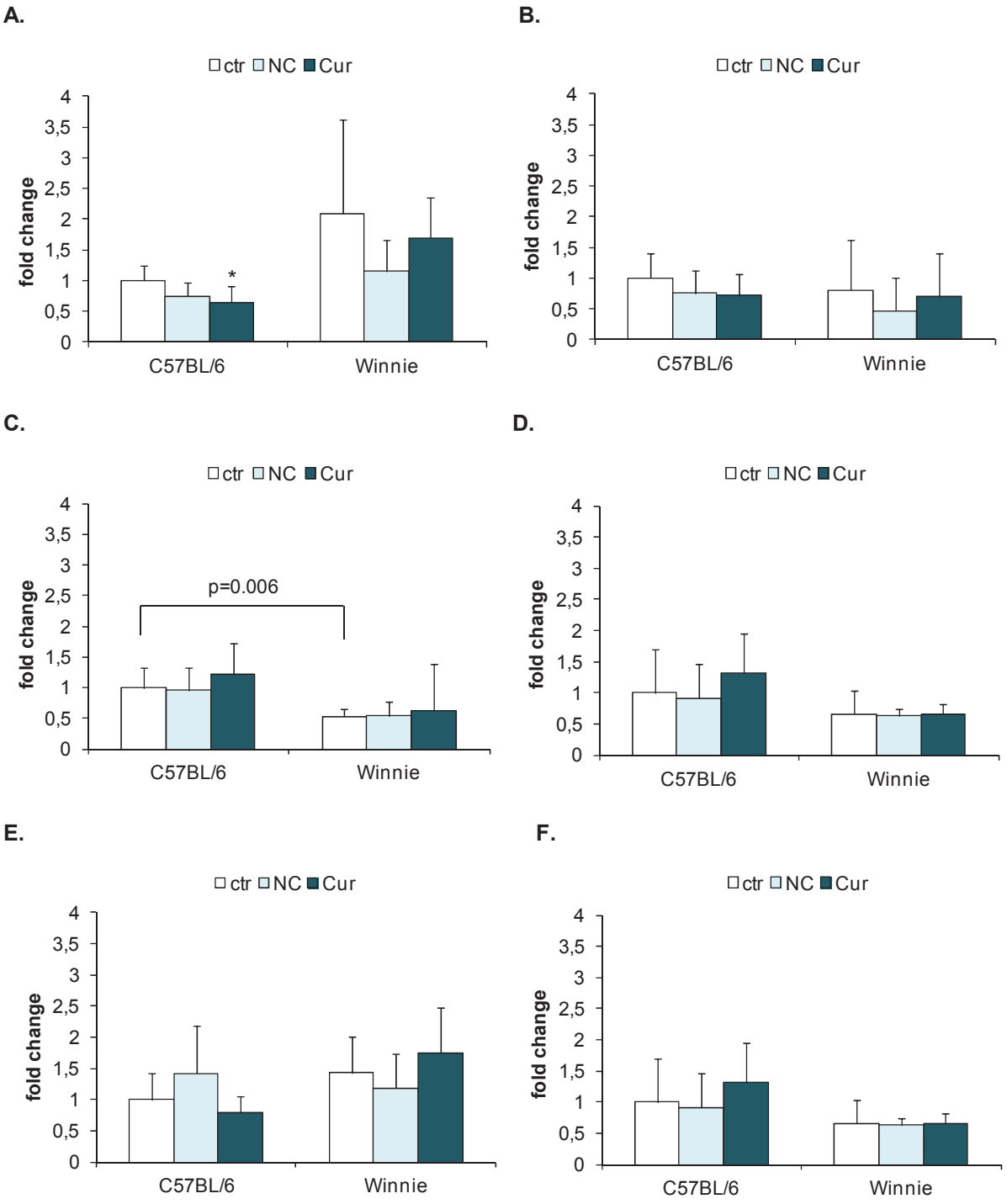

Figure 4.25: Inflammatory gene expression in colon tissues of *Winnie* versus C57BL/6 wild type mice. The mRNA expression of IL-1β (A. & B.), IL-23 (C. & D.) and TNF-α (E. & F.) was measured by qRT-PCR in distal (A, C and E.) and proximal (B, D and F.) colon of *Winnie* versus C57BL/6 mice after 14 days treatment with NC, curcumin (Cur) or vehicle control (ctr). The gene expression is expressed as fold change of the expression in C57BL/6 control mice.*p<0.05 versus ctr C57BL/6; ANOVA with post hoc LSD; n=6 for *Winnie* ctr, n=7 for *Winnie* NC, n=7 for *Winnie* Cur, n=8 for C57BL/6 ctr, n=8 for C57BL/6 NC, n=8 for C57BL/6 Cur.

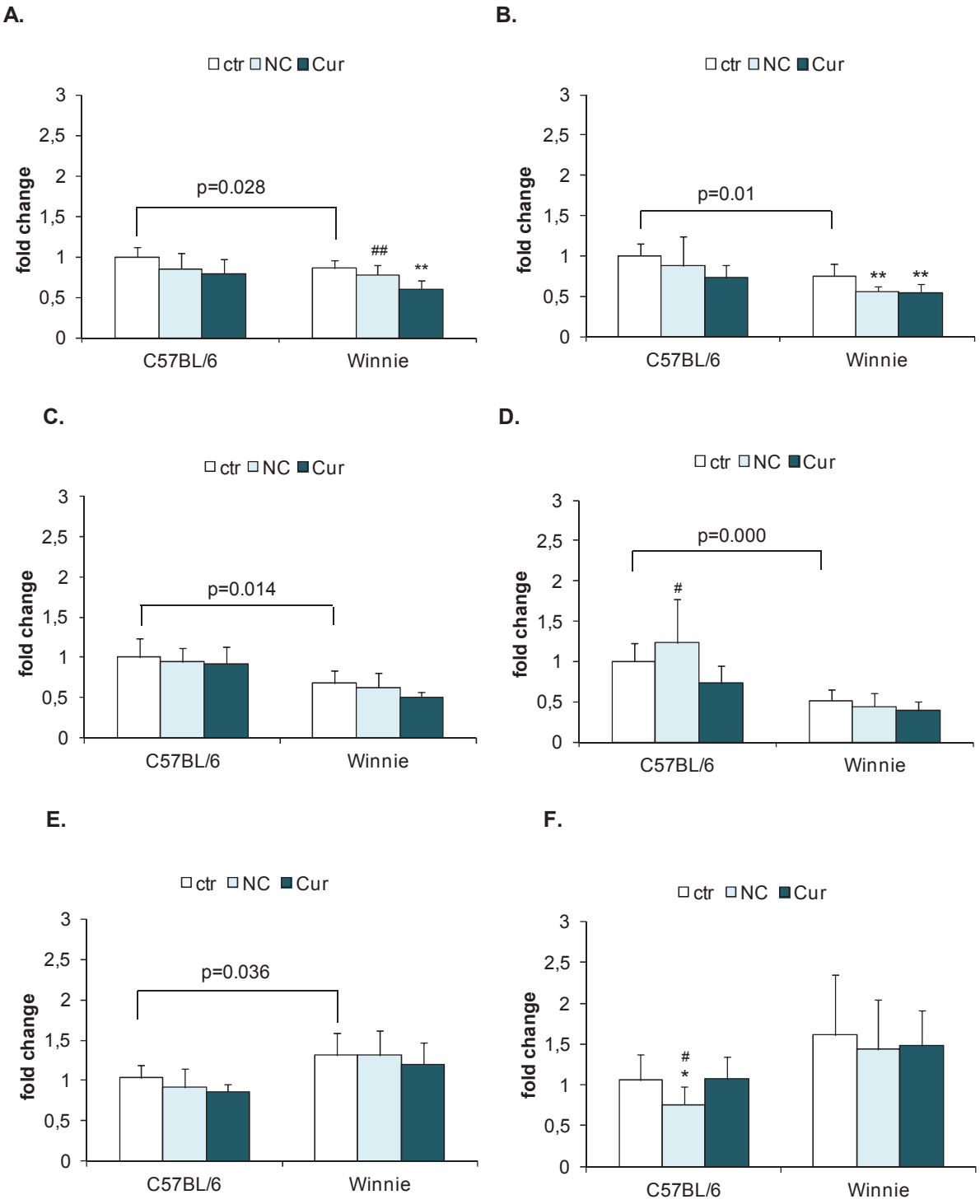

Figure 4.26: ER stress related genes in colon tissues of *Winnie* versus C57BL/6 wild type mice. The mRNA expression of spliced XBP1 (A. & B.), unspliced XBP1 (C. & D.) and ratio spliced to unspliced XBP1 (E. & F.) was measured by qRT-PCR in distal (A, C and E.) and proximal (B, D and F) colon of *Winnie* versus C57BL/6 mice after 14 days treatment with NC, curcumin (Cur) or vehicle control (ctr). The gene expression is expressed as fold change of the expression in C57BL/6 control mice. *p<0.05 versus ctr C57BL/6 and *Winnie* respectively, # p<0.05 versus curcumin C57BL/6, *p<0.05 versus ctr C57BL/6, #p<0.05 versus curcumin C57BL/6, **p<0.01 versus ctr *Winnie*, ##p<0.01versus curcumin *Winnie*; ANOVA with post hoc LSD; n=6 for *Winnie* ctr, n=7 for *Winnie* NC, n=7 for *Winnie* Cur, n=8 for C57BL/6 ctr, n=8 for C57BL/6 NC, n=8 for C57BL/6 Cur.

To address the role of oxidative stress and possibly associated DNA damage induction, the proximal and distal colon tissues were also evaluated for the mRNA expression of DNA base excision repair genes OGG1 and APE/Ref-1. The results of these measurements are shown in Figure 4.27. Neither in the wild type mice nor in the *Winnie* mice, effects of curcumin or nanocurcumin could be noted. Remarkably however, both DNA repair genes showed less mRNA expression in the *Winnie* mice than in the C57BL/6. For OGG1 this effect was statistically significant. This suggests that the increased intestinal inflammation in the *Winnie* mice may lead to impaired genome integrity.

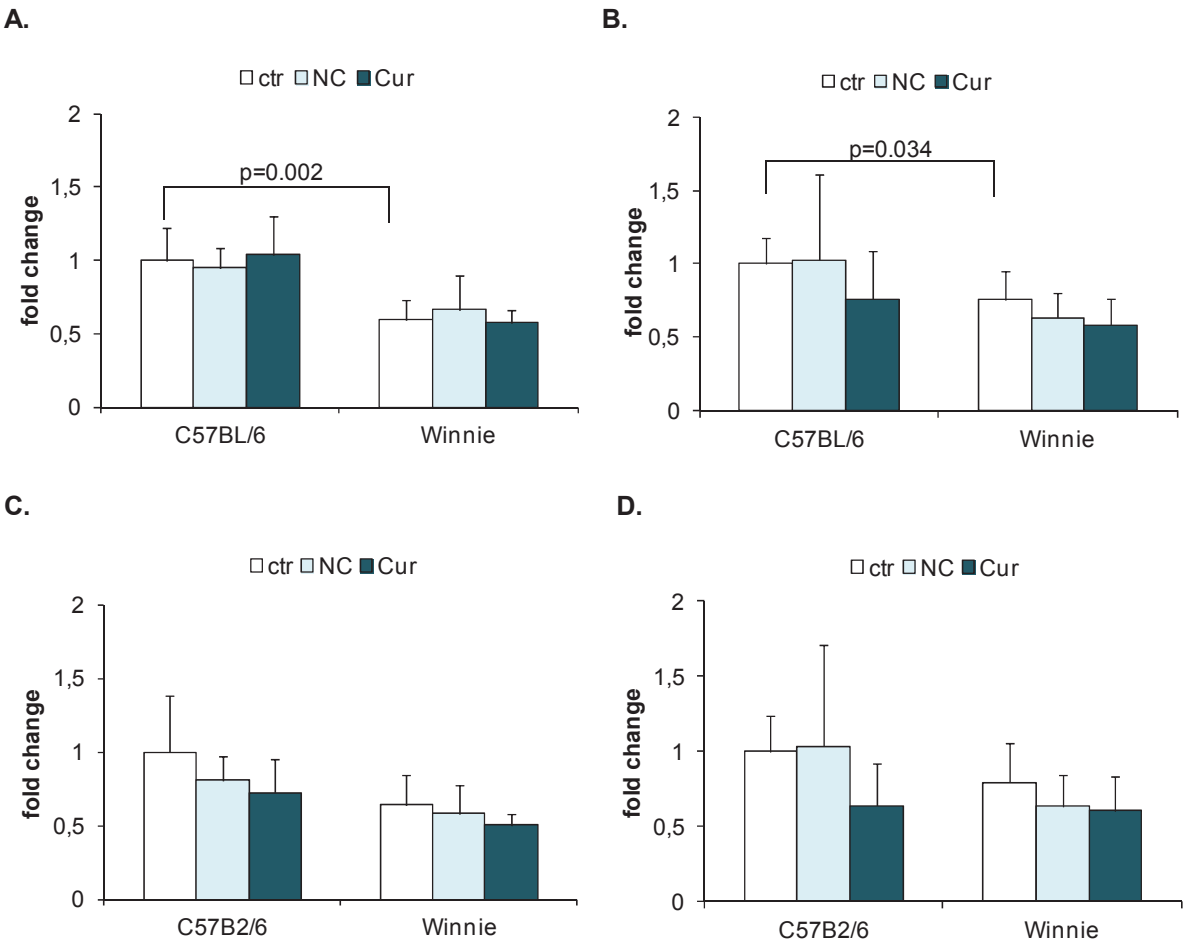

Figure 4.27: DNA damage repair genes in colon tissues of *Winnie* versus C57BL/6 wild type mice. The mRNA expression of spliced OGG1 (A. & B.), APE/Ref-1 (C. & D.) was measured by qRT-PCR in distal (A. & C.) and proximal (B. & D.) colon of *Winnie* versus C57BL/6 mice after 14 days treatment with NC, curcumin (Cur) or vehicle control (ctr). The gene expression is expressed as fold change of the expression in C57BL/6 control mice. n=6 for *Winnie* ctr, n=7 for *Winnie* NC, n=7 for *Winnie* Cur, n=8 for C57BL/6 ctr, n=8 for C57BL/6 NC, n=8 for C57BL/6 Cur.

4.4.7 Luminex analysis to detect cytokine and chemokine protein expression level in *Winnie* mice after NC and curcumin application

To analyse the influence of NC and curcumin on the cytokine and chemokine expression patterns in the distal colon tissues of the *Winnie* mice versus the wild type C57BL/6 mice, the Bio-Rad luminex assay was used. In concordance with the DSS study (see paraghaph 4.3.5), also here the protein levels of IL-1α, IL-1β, IL-6, IL-17, G-CSF and GM-CSF (Figure 4.28) and of MCP-1, MIP-1α, MIP-1β, RANTES and KC (Figure 4.29) were investigated. As can be seen in the Figures, the *Winnie* mice showed no significantly increased levels of pro-inflammatory cytokines and chemokines, when compared to the C57BL/6 mice. Moreover, in contrast to the DSS-induced colitis model, NC and curcumin treatments did not result in tissue protein expression changes in the *Winnie* model, with the exception of IL-1α. The level of this pro-inflammatory cytokine was found to be significantly increased in the NC-receiving group compared to curcumin-treated group (see Figure 4.28 A.). In line with the results from the DSS model (see paragraph 4.3.5), this suggests that the NC particles may can trigger some pro-inflammatory response in the mouse intestine. Such pro-inflammatory trend, albeit not statistically significant, we also observed for some other inflammatory mediators including IL-1β (Figure 4.28 B.), IL-6 (Figure 4.28 C.), KC (Figure 4.29 E.) and MCP-1 (Figure 4.29 A.). In the wild type C57BL/6 mice no clear treatment related effects were observed.

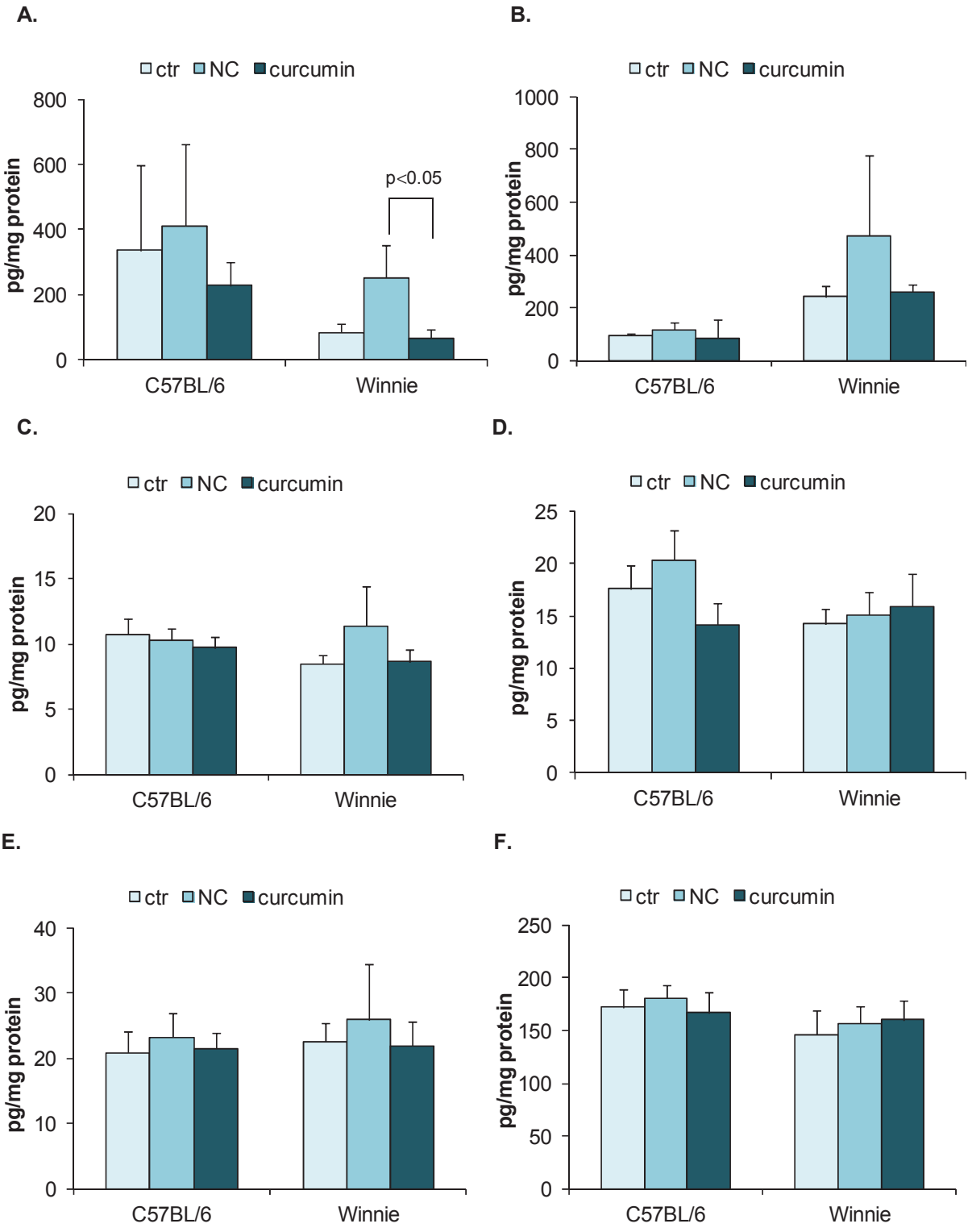

Figure 4.28: Cytokine protein expression levels in distal colons of *Winnie* or C57BL/6 mice after treatment with NC and curcumin. Protein expression level of a variety of cytokines were determined by luminex assay from the distal colon of *Winnie* mice or C57BL/6 mice following oral application of nanocurcumin (NC) or curcumin every other day for a time period of 14 days. The following cytokines were detected by Bio-Rad luminex assay and shown here in the graphs as mean and SD of levels in pg/mg protein: Interleukin (IL)-1α (A.), IL-1β (B.), IL-6 (C.), IL-17 (D.), G-CSF (E.) and GM-CSF (F.). ANOVA with post hoc LSD; n=8 for C57BL/6 ctr, n=8 for C57BL/6 NC, n=8 for C57BL/6 curcumin, n=6 for *Winnie* ctr, n=7 for *Winnie* NC, n=7 for *Winnie* curcumin.

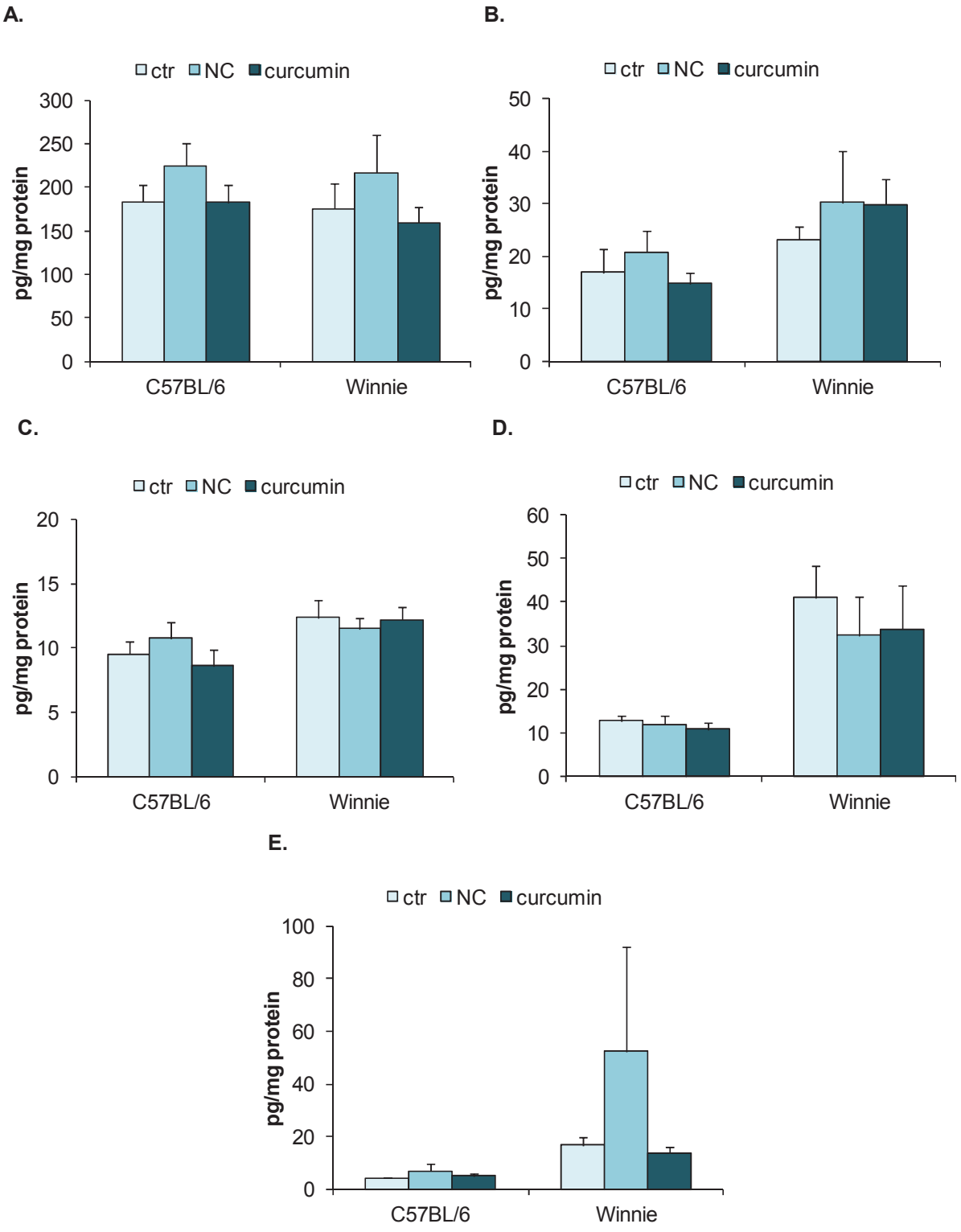

Figure 4.29: Chemokine protein expression levels in distal colons of *Winnie* or C57BL/6 mice after treatment with NC and curcumin. Protein expression level of a variety of cytokines were determined by luminex assay from the distal colon of *Winnie* mice or C57BL/6 mice following oral application of nanocurcumin (NC) or curcumin every other day for a time period of 14 days. The following cytokines were detected by Bio-Rad luminex assay and shown here in the graphs as mean and SD of levels in pg/mg protein: Interleukin MCP-1 (A.), MIP-1α (B.), MIP-1β (C.), RANTES (D.), KC (E.). n=8 for C57BL/6 ctr, n=8 for C57BL/6 NC, n=8 for C57BL/6 curcumin, n=6 for *Winnie* ctr, n=7 for *Winnie* NC, n=7 for *Winnie* curcumin.

4.4.8 Comparison of IL-1β mRNA and protein expression measurements in the *Winnie* and C57BL/6 mice

For the master-regulator of innate inflammation, i.e. IL-1β, protein expression levels as evaluated by luminex analysis were also compared to the mRNA expression measurements of this gene. As both were be determined in the available distal colon tissues of the *Winnie* study it was possible to perform a correlation analysis on the individual animal level. As shown in Figure 4.30, protein and mRNA expression were found to correlate well. The overall higher expression of IL-1β in the Winnie mice, in association with the pro-inflammatory phenotype of the *Winnie* mice is interesting in view of a potential role of aberrant Muc2 expression and/or increased ER stress in the activation of this key inflammatory mediator.

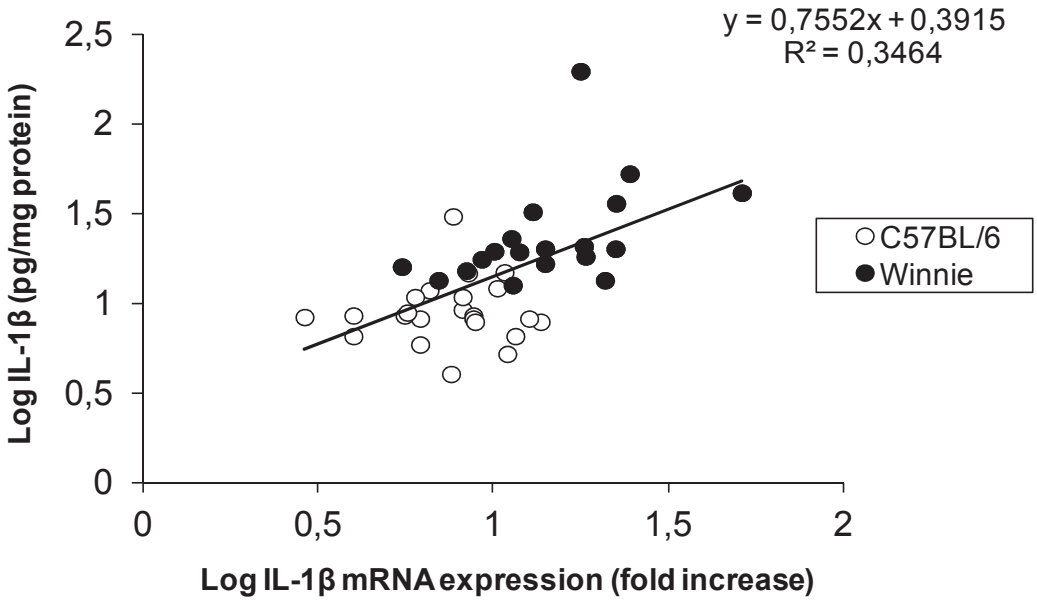

Figure 4.30: Correlation of IL-1β mRNA expression and IL-1β protein expression in the distal colon of *Winnie* mice and C57BL/6 wild type: Analysis of the IL-1β mRNA expression by quantitative real-time PCR and analysis of IL-1β protein expression level by luminex assay.

4.4.9 Comparison of the cytokine expression levels in two independent colitis models: DSS induced colitis model versus *Winnie* model

The two independent colitis models that were used in the context of the investigations for this thesis also allowed for a comparative evaluation in the basis of their cytokine expression patterns. Therefore, the results of the luminex assay from both studies are put together in Table 4.1. As illustrated in this table, the C57BL/6 control animals in both studies showed rather similar average expression patterns, except for the cytokine IL-1α. This contrast could be explained by a single outlier animal in the *Winnie* study. Taken together, the consistent findings in the control animals in both studies indicate that cytokine expression data in both studies are replicable and therefore may reflect constitutive levels in healthy intestine of this mouse background. Interestingly, therefore, it can be concluded that the DSS treatment exhibited an overall stronger increase in cytokine/chemokine protein expression levels in distal colon, than the *Winnie* spontaneous colitis model displays. Specifically, in the DSS fed animals all cytokines levels were increased by more than 50%, with the exception for GM-CSF, MIP-1 and RANTES. In contrast, the *Winnie* mice showed only for three mediators a more than 1.5 fold increase, IL-1β, KC and RANTES. In both colitis models, IL-1β and KC were significantly enhanced and therefore probably possess a role in both models of colitis. In contrast however, MIP-1α was only significantly increased in DSS induced colitis, while RANTES was only significantly increased in the *Winnie* mice. Altogether, the observed differences in quantity and quality of cytokine expression point towards differences in the underlying pathways that cause and/or maintain the inflammatory phenotype in the respective murine models.

Table 4.1: Cytokine expression pattern in the distal colon of DSS treated mice, *Winnnie* mice and C57BL/6 control mice. The cytokine expression levels in the distal colons of the DSS treated mice, the *Winnie* mice and the C57BL/6 control mice were analysed by Bio-Rad luminex assay. Following cytokines were analysed: IL-1α, IL-1β, IL-6, IL-17, G-CSF, GM-CSF, KC, MCP-1, MIP-1α, MIP-1β and RANTES. The average rate of cytokine concentration in each group with appending standard deviation is illustrated in this table as pg/mg protein. Further, the average rate of fold increase of the cytokines in the treatment groups compared to the particular control group was calculated. In the DSS study, C57BL/6 wild type mice and C57BL/6 wild type mice with 3% DSS in the drinking water for 7 days were investigated. In the *Winnie* study C57BL/6 control mice and *Winnie* mice with the missense mutation in the MUC2 gene were analysed.

	DSS study			**Winnie study**		
	n=5 control	n=5 DSS	fold increase average	n=8 C57BL/6	n=6 Winnie	fold increase average
IL-1α	8 ± 5	160 ± 249	20	77.9 ± 107	84 ± 64	1,01
IL-1b	84 ±17	**563 ± 281 ****	6,7	95 ± 20	**242 ± 108 ****	2,55
IL-6	12 ± 3	18 ± 8	1,5	11 ± 4	8 ± 2	0,73
IL-17	16 ± 7	27 ± 34	1,69	18 ± 6	14 ± 4	0,78
G-CSF	20 ± 5	61 ± 42	3,05	21 ± 9	23 ± 7	1,1
GM-CSF	198 ± 39	195 ± 214	0,98	172 ± 49	146 ± 58	0,85
KC	3 ± 1	**49 ± 42 ***	16,33	4 ± 1	**17 ± 7 ****	4,25
MCP-1	234 ± 60	418 ± 253	1,79	183 ± 58	175 ± 71	0,96
MIP-1α	14 ± 7	**71 ± 37 ****	5,07	17 ± 13	23 ±6	1,35
MIP-1b	17 ± 8	17 ±13	1	10 ± 3	12 ± 3	1,2
RANTES	10 ± 1	9 ± 5	0,9	13 ± 4	**41 ± 18 ****	3,15

*p<0.05, **p<0.01 versus control, t-test; n=5 for both groups in DSS study, n=8 for control group in *Winnie* study and n=6 for *Winnie* mice.

5. Discussion

5.1 Inflammatory bowel diseases, prevalence and current treatment strategies

Inflammatory bowel diseases, like ulcerative colitis (UC) and Crohn's disease (CD) are characterised by chronic and relapsing gastrointestinal inflammation associated with significant morbidity, which can result in cancer development. IBD has a high incidence, especially in Western countries. Only in Europe already more than 3 million people suffer from those diseases (Crohn's and Colitis Organisation 2012). The balance between immune system defence and immune tolerance, the so called intestinal immune homeostasis, is perturbed in IBD causing excessive pro-inflammatory immune response toward normal intestinal flora. Hereby, both the innate and adaptive immune systems are involved. Possible sources that are discussed amongst others include defects in mucosal barrier function and microbial clearance as well as aberrant immunoregulation (Sartor, 2006). Nevertheless, the particular aetiology and pathogenesis is still unclear. An interesting approach for therapeutics focuses on the restoration of the imbalance of pro-inflammatory (e.g. TNF-α, IFN-γ and IL-1) and anti-inflammatory (e.g. IL-4 and IL-10) cytokines. As such, IBD therapies generally include anti-inflammatory or immunosuppressive drugs such as 5-aminosalicylic acid and 6-mercaptopurine. However, their clinical efficacy is limited because of the low rate of sustained remission and the increased risk of serious infections and malignancies (Ali et al., 2012). Therefore, more research is necessary to understand the clinical mechanisms in IBD and to identify new, safe components for therapeutic approaches. Currently, phytochemicals such as phenolic compounds and flavonoids offer a great hope to improve IBD. In the last 10 years many publications suggest a pharmacological effect and clinical benefits for natural products such as curcumin, due to their ability to modulate cytokine production (Hur et al., 2012). Thus, a number of human trials could already demonstrate some clinical effects of curcumin in inflammatory diseases, amongst others in irritable bowel syndrome (Bundy et al., 2004), tropical pancreatitis (Durgaprasad et al., 2005), gastric ulceration (Prucksunand et al., 2001), and rheumatoid arthritis (Deodhar et al., 1980; Kobelt, 2006). Two human studies are preformed so far which specifically indicate beneficial effects of curcumin in IBD (Hanai et al., 2006; Holt et al., 2005). However, curcumin possesses a limited therapeutic efficacy due to the minimal systemic bioavailability, the rapid metabolism and systemic elimination.

Therefore, the aim of the present thesis was to develop PLGA encapsulated curcumin nanoparticles and to evaluate their potential therapeutic efficacy in IBD, specifically in comparison to native, non-encapsulated curcumin. Upon preparation, the NC particles were first characterised (Chapter 4.1) followed by in vitro evaluation in Caco-2 human intestinal

epithelial cells (Chapter 4.2) and in vivo investigations using the common DSS induced colitis model (Chapter 4.3) and the genetically induced colitis model *Winnie* (Chapter 4.4).

5.2 Characterisation of nanocurcumin

Currently the field of nanomedicine, and herein specifically the use of biodegradable nanoparticles as effective drug delivery devices, gains impact. The main goal in this approach is the controlled release of pharmacological active agents at a specific site of action for achieving a therapeutically optimal dose and dose rate. To improve the curcumin efficacy in IBD therapy, this advantage was to be utilized by formation of PLGA encapsulated curcumin nanoparticles. The development of polymer based nanodevices has rapidly emerged. It opens new ways for clinical applications, above all, in the field of oncology. Here, the albumin-bound paclitaxel (Abraxane) is already successfully used in breast cancer therapy (Gradishar et al., 2005). For instance, Doxorubicin loaded polyalkylcyanoacrylate nanoparticles are currently tested in clinical phase III studies for treatment of multidrug resistant hepatocarcinoma (Couvreur, 2013). Poly(lactic-co-glycolic acid) (PLGA) represents the most successfully used type of polymer due to several attractive properties such as biodegradability and biocompatibility. The two monomers of PLGA, i.e. lactid acid (PLA) and glycolic acid (PGA), are endogenous substances and can be easily metabolized by the Krebs cycle after PLGA hydrolysis in the human body (Danhier et al., 2012). Various PLGA drug-delivery systems have already been approved for use in humans by the FDA and European Medicine Agency (EMA). (Danhier et al., 2012; Kumari et al., 2010b).

The curcumin-loaded PLGA nanoparticles used in the studies described in this thesis were formed by emulsion-evaporation technique. This is the most common technique for PLGA nanoparticle preparation, and facilitates the encapsulation of hydrophobic drugs like curcumin. The particles formed with this method exhibit a nanosphere shape, in this case entrapped with curcumin in the core as well as absorbed on the surface. Under the transmission electron microscope (TEM), a typical PLGA particle morphology was detectable, similar as shown by Cheng *et al*., 2008. The used oil in water (O/W) emulsion technique results in the formation of nanosized droplets. The droplet size depends on the homogenisation intensity as well as the used stabilizer, which reduces the surface tension of the nanoparticles. Shaikh *et al*. could establish that compared to other stabilizers, poly vinyl aldehyde (PVA) induces relatively large sized curcumin loaded PLGA particles, but it also has a high entrapment efficiency (Shaikh et al., 2009). This is explained by the low solubility of curcumin in PVA, which leads to hydrophibic interaction of curcumin and the polymer. In contrast, the stabilizer cetyltrimethylammonium bromide (CTAB) offers high curcumin

solubility, but a low curcumin entrapment. Shaikh *et al*. have also shown that an increase in drug loading correlates with an increased particle size and PDI. The maximum load of curcumin in PLGA nanoparticles was about 15 % because higher entrapment resulted in precipitation (Shaikh et al., 2009). In the present study 16 % curcumin was loaded on PLGA nanoparticles with 90- 100 % entrapment efficacy using 2 % PVA as stabilizer. The PLGA encapsulated curcumin nanoparticles that were generated showed with 309 nm a mean particle size which is highly similar to the size of PLGA-curcumin particles as reported in the literature (Shaikh et al., 2009). The unloaded PLGA particles were found to be smaller (109 nm) than the drug loaded particles, but nevertheless also very much in line with the sizes as reported in literature (Danhier et al., 2012). The observed size difference between the curcumin loaded PLGA versus the empty PLGA vehicles may be explained by an influence of the drug loading. The characteristic negative surface charge of the PLGA particles is known to result from the polymeric matrix and is an indicator of a good particle preparation. In water suspension, the particles were stabile whereby the measured PDI of the curcumin loaded particles (i.e. 0.48) indicated a polydisperse appearance while the low PDI of the unloaded PLGA particles (i.e. 0.4) demonstrates monodispersity. To exclude a potential interference of curcumin autofluorescence with the DLS measurement, the size was additionally analysed in an independent manner. The Nanosight measurement is based on the tracking analysis of nanoparticles in suspensions. The PLGA-curcumin particle size as measured with this method was found to be lower on average (i.e. 139nm), but nevertheless still in the same range as for the DLS method.

For the *in vivo* experiments performed in this thesis, sorbitol was included in the preparation of the NC, since longer storage was required of the material for these investigations. To stabilize colloidal systems for a longer storage, freeze-drying is a common method. However, during this step, the prepared particles can aggregate and mechanical stress can be induced by ice crystallization causing nanoparticle destabilisation. Therefore, cryoprotectants such as sorbitol are often used in order to increase the physical stability during freeze-drying. For instance, Fonte *et al*. have shown that the ZP of insulin-loaded PLGA nanoparticles was enhanced due to the application of sorbitol during the freeze drying process (Fonte et al., 2012). For the present studies, the ZP of PLGA-curcumin particles with sorbitol was found not to be increased compared to the PLGA particles without sorbitol. However, it has to be considered that the particle batches with and without sorbitol were not prepared at the same time. Usually particle properties can be affected by several parameters during preparation. As soon as not all conditions are completely identical, it can cause different characteristics. Most importantly, for all particles prepared in the present studies, the characterisation methods indicated a stable structure. The drug release in PLGA particles depends on the polymer composition. An increase of PLA copolymer concentration is known to cause lower

degradation rates. Here a 50:50 PLGA ratio was used. Shaikh *et al*. observed a rapid curcumin release from 50:50 ratio PLGA particles, characterised as a rapid diffusion in the first 24 hours, followed by a sustained release mediated by the nanoparticle degradation (Shaikh et al., 2009). Importantly, for the evaluation of drug release, the choice of the dissolution medium is essential to ensure the solubility of the drug but to avoid enhanced degradation of the particles. In PBS Tween, 13% of the loaded curcumin amount was released from the nanoparticles within 48 hours. Obviously, this is only a first hint of an appropriate drug release kinetic under physiological conditions. For a clear confirmation, detailed pharmacological release studies are necessary, e.g. by measurement of the curcumin concentration in the blood after a certain time of application. For the specific studies that were performed in the framework of this thesis, it would be interesting to evaluate the release kinetics of the curcumin in cell culture medium as well as in model fluids that mimic gastrointestinal tract fluids.

5.3 Effects of curcumin and NC in Caco-2 cells

In Chapter 4.2 the potential therapeutic efficacy of NC, also compared to bulky curcumin in IBD was estimated, using the human epithelial carcinoma cell line Caco-2, a common intestinal in vitro model (Hidalgo et al., 1989). The polyphenolic compound curcumin, which is found in the rhizome of Curcuma longa, has been amongst others described to show strong antioxidant and anti-inflammatory effects. Therefore, it is currently tested for its potential therapeutic applicabilities in a variety of diseases (Aggarwal et al., 2003; Han et al., 2002; Joe and Lokesh, 1994; Subramanian et al., 1994). So far, the mechanisms that cause beneficial effects of curcumin are not fully understood, but in several studies it could be established that curcumin inhibits MAPK family signalling, activation of the transcription factor NF-κB and AP-1 as well as the release of downstream inflammatory mediators like TNF-α and Cox-2 (Binion et al., 2008; Jobin and Sartor, 2000; Sandur et al., 2007; Singh and Aggarwal, 1995). Furthermore, curcumin has been shown to block cytokine stimulated expression of the pro-inflammatory interleukins IL-6 and IL-8 (Chaudhary and Avioli, 1996; Rafiee et al., 2009). Presently, the cytotoxic potential of NC and curcumin was tested in Caco-2 cells. After long term treatment of the cells cytotoxicity was neither observed with NC nor with curcumin in a range of 5 to 20 µM. In the literature cytotoxicity of curcumin has been reported at concentrations exceeding than 20 µM (Woo et al., 2003). More importantly, in contrast to NC, curcumin was found to cause oxidative DNA damage in the Caco-2 cells as a short term effect. Present findings are in line with previous investigations of our group. Li *et al.* showed that curcumin is a strong inducer of oxidative DNA damage at non-cytotoxic and anti-inflammatory concentrations in the human lung epithelial cell line A549, as well as in the

rat lung epithelial cell line RLE cells and the rat macrophage cell line NR8383 (Li et al., 2008). Such pro-oxidative potential of curcumin has also been described by others. Curcumin has been demonstrated to trigger DNA damage in Jurkat T-lymphocytes as well as 8-oxo-dG induction and DNA strand breakage formation in human hepatoma G2 cells (Cao et al., 2006; Kelly et al., 2001). Consequently, curcumin possesses a contradictory role as an anti-oxidant and pro-oxidant. Such property is also described for other phenolic compounds such as quercetin. Quercetin is capable of scavenging reactive species, but during this process converts itself in an oxidant (Boots et al., 2007). Therefore, the presence of other antioxidants is necessary to provide protection from oxidative stress by quercetin. For curcumin, it has been discussed that ROS production may be due to conversion of the NADPH oxidase activity as a result of its binding on thioredoxin reductase (Fang et al., 2005). During oxidative stress, cells are known to activate antioxidant defence mechanisms. This includes the Nrf2 mediated synthesis of glutathione, one of the major cellular antioxidant enzymes, which acts as reducing agent and serves as electron donor for free radicals and oxidants (Rahman and MacNee, 1999; Shih et al., 2003). The limiting step in the synthesis of GSH is the activity of the enzyme γ-GCS (Richman and Meister, 1975). In concordance with this, besides oxidative DNA lesions in the current work, curcumin also caused a significant increase of γ-GCS mRNA expression. This effect further supports that curcumin triggers oxidative stress. Additionally, the intracellular total GSH amount tended to increase in a concentration-dependent manner after curcumin treatment, although this effect was not statistically significant. However, in contrat to curcumin, NC did not cause a significant change in γ-GCS mRNA profile, although GSH levels were slightly enhanced as well. This GSH increase was not as strong as with curcumin, but also in a concentration-dependent manner. Finally, the mRNA expression of another oxidative stress marker, heme oxygenase-1 (HO-1), was also significantly affected in the Caco-2 cells by curcumin exposure, but not in response to NC. The main function of HO-1 is associated with the degradation of heme to iron, carbon monoxide and biliverdin, which is converted by the biliverdin reductase to the anti-oxidative bilirubin (Stocker et al., 1987; Tenhunen et al., 1969). It has been established that bilirubin protects endothelial cells against hydrogen peroxide-mediated injury (Motterlini et al., 1996). Motterlini *et al.* has shown that curcumin is a potent inducer of HO-1 in vascular endothelial cells. It is suggested that this activation is promoted by activation of the Nrf2 signalling pathway (Balogun et al., 2003). Additionally it was established that the curcumin-mediated cytoprotection against oxidative stress was not present in HO-1 depleted cells (Motterlini et al., 2000). Interestingly, in the present study, the curcumin induced gene expression of both anti-oxidative markers, γ-GCS and HO-1, occurred in time-dependent manner with a peak at 8 hours and a resolution to control levels at 24 hours. Furthermore, neither after long-term incubation (24 hour) of curcumin nor after the long-term incubation

with NC, oxidative DNA damage was increased in Caco-2 cells. This permits the following conclusions: firstly, the pro-oxidative activity of curcumin only appears to be an early event and secondly, Caco-2 cells are able to repair these oxidative DNA lesions within 24 hours by cellular DNA repair mechanisms. In this context, the oxidative DNA damage repair kinetics in Caco-2 cells was also analysed after treatment with the ROS generating photosensitizer Ro19-8022. These studies demonstrated that the Caco-2 cells have indeed the capacity to repair 8-oxo-dG lesions in a half life of approximately 4 hours. Lorenzo *et al*. investigated the kinetics of DNA repair using the same photosensitizer in various cell lines and found similar DNA repair kinetics (Lorenzo et al., 2009). Even though the mechanism is not yet clearly understood, the hypothesis of the inconsistent pro-oxidative capacity of antioxidants like curcumin is that the produced free radicals induce endogenous stress responses (Sakihama et al., 2002; Sandur et al., 2007). In response to adaptive processes the cells might subsequently be protected against exogenous radicals. In our hands, NC treatment appeared not to cause pro-oxidative effects. Thus, it may be hypothesised that the observed protective effects of the NC might be mediated by pathways that differ from the non-particulate curcumin. It is undoubted that the GSH status in cells is essential for the cellular defence in response to oxidative stress. Therefore, the protective function of GSH was further investigated by depleting its levels via pre-incubation of the Caco-2 cells with BSO. This chemical interrupts the GSH production by inhibition of γ-GCS synthesis (Drew and Miners, 1984). Indeed, the GSH level was found to be significantly depleted in Caco-2 cells by BSO in a concentration-dependent manner. Consequently, DNA strand breakage as well as oxidative DNA damage induction by hydrogen peroxide (H_2O_2) treatment increased with increasing BSO concentration, i.e. decreasing GSH levels in Caco-2 cells. However, although both NC and curcumin could enhance the total GSH level, neither of these compounds prevented hydrogen peroxide induced cytotoxicity in Caco-2 cells. Interestingly however, similar to curcumin (Liu and Zheng, 2002), NC was found to offer significant protection against hydrogen peroxide induced DNA stand breakage in the Caco-2 cells in a concentration-dependent manner. The strongest protective effect of NC was received at a 20 µM dose. At 80 µM NC pre-treatment increasing DNA damage was observed, suggesting that high NC concentrations exhibit toxic capacity, similar to curcumin.The preventive effect of NC towards DNA damaging oxidants could also be confirmed in the more physiologically relevant *in vitro* co-culture model composed of Caco-2 cells and neutrophils. As immune cells in the first line of host defence, neutrophils are able to induce oxidative burst and thereby generate oxidative damage in different cellular components, amongst others in DNA (Babior, 2000b; Gungor et al., 2010; Knaapen et al., 2006). In the used co-culture model, the activated neutrophils generated a significant increase in oxidative DNA lesions. This effect could be blocked by pre-incubation of the Caco-2 cells with the NC. These findings suggest

that NC is a promising compound in the prevention of DNA damaging and mutagenic effects observed in chronic inflammatory diseases like IBD, especially in view of the observed associations between such diseases and carcinogenesis (Collins et al., 1987; Ekbom et al., 1990).

Although both curcumin and NC were shown to offer antioxidant capacity and to protect cells from oxygen induced DNA damage in vitro, different mechanisms of action may be proposed. Whereas curcumin induces oxidative stress as an early event after cell exposure, NC has no early pro-oxidative side effect. This might be a further reason for the preferential use of NC compared to the native curcumin in future. Indeed, curcumin has been forwarded as a promising anticarcinogenic agent, but its potential pro-carcinogenic effects have also been addressed (Lopez-Lazaro, 2008). The differences between curcumin and NC might be explained by the fact that from the PLGA the curcumin will be released in a sustained manner. Consequently, the dose rate for the exposed cells differs from the free curcumin treatment where the full dose is immediately available to the cell cultures. Moreover, the encapsulation of curcumin affects the uptake kinetics and possibly subcellular localisation of the drug. It may be hypothesised that free curcumin or one of its metabolites can reach the nucleus in contrast to the encapsulated curcumin and thus induce oxidative DNA damage effects as observed in present work. The nuclear envelope is a well-known barrier to particles (Feldherr and Akin, 1997). However, further research is necessary to verify such contrasting subcellular translocation and possibly associated cell compartment-specific effects. A further aspect could be that the curcumin in association with the PLGA is better protected from intracellular metabolism, e.g. reaction with other compounds in the cells like thioredoxin reductase, or elimination pathways. Also this hypothesis needs to be evaluated. The observed advantages of NC make the development of new drug release systems very interesting in the future. However, more investigations are necessary for a better understanding of the protective pathways of curcumin and NC as well as an improvement and optimisation of the development of suitable drug delivery systems in terms of material composition and preparation technique.

5.4 Effects of curcumin and NC in two murine models of colitis

The promising *in vitro* findings with respect to observed beneficial anti-oxidative properties of NC were expanded to two further in vivo studies. In these studies, the therapeutic potential of NC towards IBD was tested, also direct compared to curcumin. For this purpose, two independent murine colitis models were used, the commonly used DSS-induced colitis model (Chapter 4.3) and the *Winnie* model (Chapter 4.4), which is considered to exhibit a more

physiological element of colitis development compared to chemically induced colitis. The DSS model of colitis is based on a mechanism of chemical disruption of the mucosal barrier. DSS is directly toxic to intestinal epithelial cells and as such causes a massive infiltration of inflammatory cells into the lamina propria, resulting in severe inflammation (Wirtz and Neurath, 2007). In contrast, *Winnie* mice manifest a genetically induced colitis. Due to a single nucleotide polymorphism in the D3 domain of the Muc2 gene, leading to a replacement of cysteine with tyrosine, the mice develop colitis as a result from an aberrant Muc2 expression. The impaired Muc2 expression results in depletion of the secreted mucus layer and has been demonstrated to cause ER stress. The histological phenotype of the *Winnie* mice is characterised by a reduced goblet cell number and decreased mature Muc2 protein expression (Heazlewood et al., 2008). This specific phenotype could be verified in the present study by evaluation of Pas/Alcain blue stained Swiss role tissue sections: The sections clearly indicated a reduced amount of blue stained mucin in the goblet cell theca and the presence of Pas-positive but Alcain blue negative magenta stained accumulations of premature Muc2 in cytoplasm vacuoles of goblet cells. Moreover, the significantly reduced Muc2 gene expression in the *Winnie* mice could be confirmed by mRNA expression analysis of the intestine tissue homogenates. Finally, a diminishment of unspliced XBP1 (usXBP1) gene expression was found, indicative of the presence of ER stress: The usXBP1 mRNA encodes a transcription factor which represses unfolded protein response (UPR) target genes. In presence of ER stress, XBP1 is spliced and encodes then a transcription factor for UPR target genes including chaperons and ER-associated degradation (ERAD) components (Kaser et al., 2013). Consequently, the elevated ratio of spliced to unspliced XBP1 mRNA in *Winnie* mice represents the level of UPR activation associated with ER stress. As described in Heazlewood *et al.*, the consequences of this effect are spontaneous inflammation mediated via NF-κB pathway with an increase of inflammatory cytokines such as IL-1β, TNF-α and IFN-γ (Heazlewood et al., 2008). Present findings are in coincidence with many publications in which ER stress and UPR activation is reported within intestinal epithelial cells in human inflammatory bowel diseases (Kaser et al., 2008; Shkoda et al., 2007; Treton et al., 2011). Further, an altered O-glycosylation profile of Muc2 was demonstrated in UC (Boltin et al., 2013; Larsson et al., 2011).

In line with earlier findings (Heazlewood et al., 2008), in the present study, the *Winne* mice had increased protein expression of IL-1β. Surprisingly, however, IL-23, a stimulator of $CD4^+$T-cell differentiation and IL-17 production was expressed to a significantly lower extent in the *Winnie* mice than in the healthy mice. The IL-23/IL-17 axis has been increasingly discussed as a key regulator mechanism of colitis and hence as promising target for therapeutic interventions (Abraham and Cho, 2009; Hue et al., 2006). However, also some anti-inflammatory features of IL-23 have been postulated (Cox et al., 2012), and the

observed expression differences in present study might therefore reflect compensatory mechanisms in the used young age animals. Further research is needed to clarify the role of IL-23 in the *Winnie* model, in relation to the aging of the mice during which their colitis phenotype increases.

Interestingly, in the present work it was also found that the gene expression of the DNA repair enzyme OGG1 was significanty reduced in the intestinal tissues of the *Winnie* mice compared to the intestines of the wild type. A further DNA repair gene, APE/Ref1 was also slightly reduced on mRNA level, albeit not statistically significant. Together, these findings may implicate that the disturbed intestinal homeostasis in the *Winnie* mice affects oxidative DNA damage and/or its repair in this organ. Earlier it was already demonstrated that OGG1 deficient mice have an increased susceptibility of ulcerative colitis-induced carcinoma development (Hofseth et al., 2003; Liao et al., 2008; Westbrook et al., 2009). This finding is interesting as chronic inflammatory bowel diseases are associated with oxidative stress and the development of cancer (Seril et al., 2003). This suggests that the *Winnie* mice might be a relevant model in to address mutagenic and carcinogenic effects of chronic inflammation in the intestine.

In both animal models of colitis, a typical disease pattern was detectable based on macroscopic colitis scores, i.e. rate and extent of weight loss, colon length, colon weight and changes in stool scores. Furthermore, the histological colitis score manifested as well typically colitis pathology in both models. Notably however, the DSS and the *Winnie* colitis model exhibited several crucial differences. After 7 days DSS application, the mice had significant changes in body weight, colon length and colitis score with diarrhoea and rectal bleeding, as typically described in the literature (Wirtz et al., 2007). In contrast, the *Winnie* mice exhibited significant changes in colon weight and suffered only from diarrhoea. In addition, during the two experimental weeks, the *Winnie* mice did not lose weight. Apparently, the symptoms were not yet very severe in the young (6 to 8 week old) *Winnie* mice. Typically, the colitis symptoms increase with age and achieve a very high level in one year old *Winnie* mice (Heazlewood et al., 2008). However, differences between the DSS and the *Winnie* model were not solely observed on the macroscopical level but also immunologically identified on the basis of the diverse cytokine expression patterns in the colon tissue. Next to the coincident overexpression of the pro-inflammatory cytokines IL-1β and KC in both models, the mice fed with DSS exhibited a significant increase in the pro-inflammatory chemokine MIP-1α, whereas the *Winnie* mice showed an increase of the chemo-attractant RANTES, compared to their respective control group mice. MIP-1α is produced mainly by macrophages, causing local inflammatory responses. It recruits proinflammatory cells and induces the release of further macrophage- and fibroblast-

produced cytokines (Maurer and von Stebut, 2004). The cytokine RANTES is known to recruit T cells, eosinophils and basophils into inflammatory regions (Kuna et al., 1998). Consequently, this variable cytokine pattern suggests an involvement of different immune responses in the two colitis models. Furthermore, the dimension of the cytokine response in both models was found to differ in intensity, indicating a much stronger inflammation response in DSS mice. In this model, almost all cytokines were enhanced (at least 1.5 fold compared to the control), whereas in Winnie mice only three out of all measured cytokines were slightly higher than 1.5 fold above control group levels.

Remarkably, in the *Winnie* mouse model study a strong correlation of IL-1β mRNA expression and IL-1β cytokine levels could be detected, which indicates inflammasome activation. This correlation was not established in the DSS model since mRNA expression analysis was not performed in the tissues of these mice. Indeed, several studies point out that the inflammasome is a critical regulator of colonic microbial ecology (Elinav et al., 2013). Presently, still relatively little is understood about the mechanism of inflammasome-mediated orchestration and regulation of the intestinal immune responses and maintenance of intestinal homeostasis. It has been suggested that the Caspase-1 signalling is a central mediator of the pathogenesis of auto-inflammation (Elinav et al., 2013). Based on these individual features, it was interesting to observe that NC and curcumin display distinctive patterns of particular colitis symptoms and pathology in the different murine models. These findings are summarised in Table 5.1.

Table 5.1: Overview of the impact of nanocurcumin and curcumin application in the DSS induced colitis model and the Muc2-deficient colitis model Winnie

	Curcumin *			Nanocurcumin *		
	7 days	14 days		7 days	14 days	
	DSS	C57BL/6	Winnie	DSS	C57BL/6	Winnie
colitis features	-	-	-	-	-	col. score ↓ col. Weight ↓
Histological colitis score						
Caecum	40 mg/kg ↓	-	-	-	-	-
Proximal colon	-	-	-	-	-	-
Mid Colon	40 mg/kg ↓	-	-	-	-	-
Distal Colon/Rectum	40mg/kg & 80 mg/kg ↓	-	-	-	-	-
		-	-	80 mg/kg ↓	-	-
inflammatory markers	n.d.	IL-1β in DC ↓	-	n.d.	-	-
ER stress markers	n.d.	-	sXBP1 in DC & PC ↓	n.d.	ratio sXBP1/ usXBP1 ↓	sXBP1 in PC ↓
DNA repair markers	n.d.	-	-	n.d.	-	-
cytokine levels	IL-1β in DC ↓	-	-	-	-	-
chemokine levels	-	-	-	KC in DC ↑	-	-

* The errors indicate a significant change in parameter due to curcumin or nanocurcumin treatment, $p<0.05$ using test as indicated in the Figures in the result section. DC: distal colon; PC: proximal colon; n.d.:not determined

Recent studies have already demonstrated that curcumin can prevent the development of DSS-induced colitis in mice. The improvement of the histological colitis score was associated with the inhibition of NF-κB activation, the suppression of the STAT3 pathway as well as the blockade of infiltration of inflammatory cells (Arafa et al., 2009; Deguchi et al., 2007; Liu et al., 2013). Additionally, MPO activity, IL-1β and TNF-α expression was found to be reduced (Liu et al., 2013). Arafa *et al.* identified that the colonic total GSH level was enhanced after curcumin application whereas, in contrast, the total NO level was notably decreased (Arafa et al., 2009). The authors suggested that these findings reflect a protective role of curcumin via an anti-oxidative function in experimental ulcerative colitis. Also in other models of chemically induced colitis studies, in particular TNBS-induced colitis studies, beneficial effects of curcumin could be demonstrated, e.g. in the form of a reduction of neutrophil infiltration and lipid peroxidation (Salh et al., 2003; Sugimoto et al., 2002; Ukil et al., 2003). Sandur *et al*. have suggested that the anti-inflammatory activity of curcumin is mediated through its ability to modulate the redox status in the cell (Sandur et al., 2007). In the current work, curcumin also showed some beneficial effects in the mouse model of DSS-induced colitis. The histological colitis score, consisting of inflammatory severity, infiltration extent and epithelial damage (extent and rate), was significantly ameliorated in the cecum, the mid colon and the distal colon/rectum after the daily application of 40 mg/kg curcumin in DSS fed mice. Furthermore, 80 mg/kg curcumin improved the distal histological pathology as well. In the same colon region also the levels of the pro-inflammatory cytokine IL-1β were significantly decreased in the curcumin treated DSS animals compared to the DSS control group, demonstrating anti-inflammatory activity of curcumin. However, in contrast to the chemically induced colitis, curcumin did not affect colitis symptoms in the *Winnie* mice, neither the macroscopically evaluated colitis features nor the histological colitis score consisting of crypt architecture, crypt abscesses, crypt length, tissue damage, goblet cell loss, inflammatory cell infiltration and neutrophil number in lamina propria. However, in the wild type C57BL/6 mice, curcumin offered anti-inflammatory activity by diminishing IL-1β mRNA expression. Moreover, in the Winnie mice the mRNA expression of the ER stress marker sXBP1 was reduced. Thus suggests that even if the histological pathology was not yet improved in Winnie mice after 2 weeks treatment, curcumin might have an impact on ER stress and the inflammation status in the colon tissue.

Taken together, present results indicate several beneficial effects of curcumin in experimental colitis. However, despite an improvement of the histological pathology and diminishment of inflammatory markers in DSS-induced colitis, the mice still suffered from bloody diarrhoea and intestinal inflammation. Several of the published chemically induced colitis model studies illustrate a preventive function of curcumin caused by pre-treatment shortly before colitis induction (Arafa et al., 2009; Ukil et al., 2003). Even the exact

mechanism is not fully understood, the activation of cellular defence mechanisms are suggested to adapt and protect the colon tissue from intended injury. The effect of curcumin might differ markedly in an already inflamed colon, when compared to healthy tissue. However, Liu *et al.* (2013) detected a beneficial effect of curcumin in inflamed colon tissue after DSS treatment. It is generally known that after DSS detoxification the injured tissue is capable to recover, and curcumin might support this effect. Deguchi *et al*. (2007) showed that DSS-induced colitis was significantly attenuated on day 14 with simultaneous curcumin application. In the current study with only 7 treatment days, this clearly identified role of curcumin as beneficial therapeutic in ulcerative colitis could not be full confirmed. A longer treatment period with curcumin might be necessary.

The colitis symptoms in *Winnie* mice could not be improved by the curcumin administrations, but curcumin exhibited a potential impact on ER stress. This effect may offer protection against the development of more severe colitis symptoms, which will take place during the aging of the *Winnie* mice. It will therefore be interesting to investigate the therapeutic curcumin effect after a long-term treatment in older *Winnie* mice.

About the influence of PLGA encapsulated curcumin nanoparticles in experimental murine colitis is not much known to date. In the presented DSS colitis study, the application of NC ameliorated the histological pathology in the distal colon at a concentration of 80 mg/kg NC. In contrast to curcumin, 40 mg/kg NC did not change the histological colitis score, similar to the empty PLGA vehicle. This might be a consequence of the different dose rate of administration. Due to the PLGA encapsulation the release of curcumin will likely be sustained, but the plateau level reached may be lower than achieved by the native curcumin. Notably however, both groups NC and PLGA (80 mg/kg respectively) also showed increased tissue levels of the neutrophil activator KC. Moreover, the PLGA treatment group mice showed enhanced protein levels of MIP-1α, suggesting a pro-inflammatory effect of the nano sized material in DSS-induced colitis.

In contrast, the *Winnie* mice possessed a significant improvement in colitis features such as diarrhoea and colon weight after NC application. Even though the histological pathology was not affected, NC caused a decrease of ER stress marker sXBP1 in the proximal colon, similar to the effect of curcumin in the distal colon. However, also in the *Winnie* mouse model NC induced slight (albeit non-significant) pro-inflammatory responses, as observed with IL-1β, IL-6, KC and MCP-1. Taken together, NC might have a specific beneficial effect on ER stress regulation, but apparently the nano sized material also triggers mild pro-inflammatory effects in both colitis models. Thus, the question arises if NC, or even other PLGA encapsulated drugs, might trigger adverse side effects in inflamed tissues due to their particulate properties. During inflammation many inflammatory cells such as macrophages

are recruited which have a key role in the uptake and clearance of particulates as well as in the orchestration of inflammation (Hume, 2006; Wilhelmi et al., 2013). In the respective fields of nanomedicine and nanotoxicology the role of professional phagocytes (including intestinal macrophages, pulmonary macrophages, Kupffer cells, dendritic cells) is being considered as a critical component of the therapeutic potential of nanoencapsulated drugs on the one hand and the toxic hazard of nanoparticles on the other hand (as summarised in Figure 5.1).

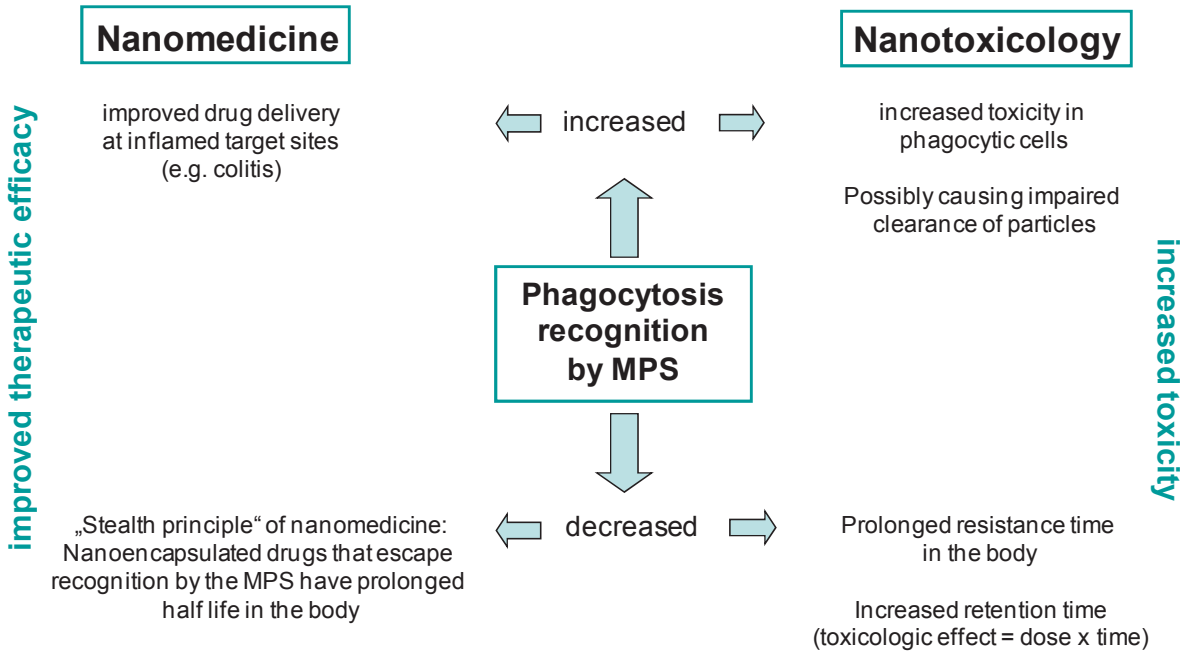

Figure 5.1: Nanoparticle uptake by the mononuclear phagocytic system (MPS): The recognition of NP by the MPS is widely discussed in the nanomedicine field (des Rieux et al., 2006). The successful elimination of toxic NP by uptake and clearance by professional phagocytes is also discussed as a critical component in nanotoxicology, a concept that has emerged from the classical field of particle inhalation toxicology (Geiser and Kreyling, 2010; Oberdörster et al., 2005).

Depending on properties such as size, shape, surface charge and modification, particles are taken up with an enhanced or decreased efficacy by phagocytes. As such, the therapeutic efficacy for (nano)particle-based drug delivery approaches is likely to be influenced. Increased uptake by the MPS leads to accumulation of the drug in this compartment and therapies targeting e.g. inflamed tissue should thus aim for development of particulate drugs that enhance recognition and uptake. If drugs need to be targeted elsewhere, the opposite should be aimed at, namely to develop 'stealth' particles, typically in the nanosize range that escape the uptake and clearance by the MPS. Such modification is aimed to lead to a prolonged residence time (e.g. increasing circulation time by avoiding uptake by Kupffer cells). A key challenge of the nanomedicine field is to continuously develop "smarter" types of

nanodrugs with specific surface modifications to target the desired cells, tissues or organs. Similarly, the preferential uptake of toxic nanoparticles by the MPS will determine the likely target for potential adverse health effects. For instance, inhaled nano-size particles are known to escape recognition and uptake by macrophages in the alveolar lumen and thereby may cause increased toxicity in the pulmonary interstitium and even become translocated into the systemic circulation. This may lead to toxicity in secondary organs after inhalation (Geiser and Kreyling, 2010; Geiser et al., 2013). On the other hand, toxic microsize particles like crystalline silica are well-known to be taken up by macrophages after inhalation. Because of their intrinsically higher toxicity, these mineral particles can impair the function of the macrophages and as such indirectly cause lung toxicity (Bermudez et al., 2002; Bermudez et al., 2004; Driscoll et al., 1991). Interestingly, also specific types of nanoparticles have been shown to impair macrophage function, and are thereby considered to cause toxicity (Renwick et al., 2001). Currently in the nanotechnology field, there is increasing interest in the development of safer-by-design nanoparticles, e.g. by applying controlled surface-modifications during their engineering.

To date the majority of studies in which PLGA based therapeutic strategies are tested, merely highlight the potential beneficial role of PLGA encapsulation for drug delivery. Only a few of them also have a critical view on potential negative side effects. For instance, Xiong *et al*. has demonstrated the potential of smaller PLGA nanoparticles (100 nm) to trigger the release of TNF-α (Xiong et al., 2013). One suggestion of the size-dependent adverse effect of PLGA is that smaller particles with a larger specific surface area can absorb more biomolecules such as proteins from the biological microenvironment. This particle corona might enhance the clearance of particles with an increased toxicity in phagocytic cells (Elsaesser and Howard, 2012; Mahon et al., 2012; Xiong et al., 2013). In contrast, Nicolete *et al*. showed that PLGA microparticles are more inflammatory than nanoparticles by inducing NF-κB activation and cytokine production (TNF-α and IL-1β) in J774 macrophages. Furthermore, they demonstrated that PLGA microparticles (5-7 μm) are not phagocytosed with the same avidity as nanoparticles (389 nm) by J774 macrophages, but were attached to the cell membrane (Nicolete et al., 2011). They also discussed that both nano-and microparticles are able to restore the IL-1β level after NF-κB inhibition. Their observations hint towards a role for NF-κB independent, inflammasome pathway dependent pro-inflammatory effects of PLGA particles. The observations in present studies on the increased presence of specific inflammatory mediators in the colon tissue of mice that received NC or the PLGA vehicle may be in line with these effects. Nevertheless, many published studies indicate that biodegradable nanoparticles are an effective drug delivery system in experimental colitis. For instance, Lamprecht *et al.* demonstrated prolonged anti-inflammatory activity and reduced adverse effects after PLGA rolipram nanoparticles

compared to rolipram in solution in the DSS colitis model (Lamprecht et al., 2001). This group established that nanoparticles adhere more to inflamed than to non-inflamed areas of intestinal mucosa, rendering them more relevant as a therapeutic approach serving as local drug depot. Such target site-specific accumulation of nanoparticles is explained by the enhanced uptake of nanoparticles by invading immune cells, as described before in Nicolete *et al*. (2011), and the facilitated penetration of nanoparticles into the intracellular junctions of an inflamed epithelium (Lamprecht et al., 2001). However, a study in human IBD patients demonstrated an opposite effect in terms of PLGA nano- and microparticle accumulation, indicating discrepancy between animal models of IBD and the human clinical situation (Schmidt et al., 2013). After rectal application of fluoresceinamine-labelled carriers without an active drug, Schmidt *et al*. found an obvious accumulation of microparticle (3 µm), whereas nanoparticles were only observed in traces in the mucosa of the IBD patients (Schmidt et al., 2013). It could be established in the study that the nanoparticles were translocated to the serosal compartment, which suggests a systemic absorption with possible induction of adverse side effects.

Altogether the available literature still contains some controversies with regard to the benefits of PLGA and other nanoparticle based treatments in IBD. More research is necessary to understand the whole role of nanoparticles in inflammation. A possible explanation for the pro-inflammatory effect of the PLGA particles that were prepared in the present study could be that the hydrophobic surface of the PLGA nanoparticles caused a rapid and preferential uptake by professional phagocytes in the intestine and their subsequent activation. Therefore, an interesting approach in the future would be to test curcumin-PLGA particles which are surface modified with hydrophilic polymers such as poly ethylene glycol (PEG). In the bloodstream, such PEGylated particles have been shown indeed to possess an increased circulation time (De Jong and Borm, 2008; Kumari et al., 2010a).

5.5 Nanoencapsulation of curcumin: benefits and disadvantages

In summary, curcumin and NC were capable to impair some colitis relevant symptoms in both murine colitis models. In the chemically induced colitis model oral application of curcumin improved significantly histological colitis properties like crypt abscess and inflammatory cell infiltration in nearly all colon parts and a reduced level of inflammatory cytokines (IL-1β and MIP-1α). Also oral delivery of NC affected the intestinal histological pathology in the most concerned distal colon part of the DSS treated mice, but at the same time, it exhibited some enhanced pro-inflammatory cytokine levels reflecting possible enhanced inflammation. In the genetically induced colitis model *Winnie*, curcumin and NC

might influence ER stress. Furthermore, NC decreased in control mice the UPR activation (ratio sXBP1 to usXBP1) which suggests a possible protection against IBD development. Apart from the impact on ER stress, *Winnie* mice also suffered significantly less from diarrhoea after 14 days NC application. However, in murine experimental colitis neither NC nor curcumin was able to fully abrogate the colitis symptoms, and neither of the treatments did cause a sustained effect. More importantly, no obvious advantage of NC over curcumin was observed in both mouse models of colitis. Quite contrary, the nano-delivery approach was associated with enhanced expression of various pro-inflammatory mediators, which may indicate that adverse effects may become enhanced during existing inflammation. A key finding from the current work is the inalienable need to evaluate not only the potential therapeutic impact of encapsulated drug delivery systems, but also to evaluate the effects of the carriers without their bioactive components. Hence, possible (positive or negative) side effects of the carrier itself can be discovered. Furthermore, the present work has manifested that in a therapeutic study, it is absolutely necessary to simultaneously compare the efficacy of the nano-sized drug with the efficacy of the bulk material. Only with this approach the real benefit, i.e. the level of improvement of the newly developed therapeutic, can be determined. If there is no obvious advantage in the use of nanoparticles over the use of the non-particulate based drug, the extra costs are unjustifiable.

Of further relevance is the choice of the test model. The results from this work show that *in vitro* NC was found to offer promising advantages over curcumin, via covering protection of intestinal epithelial cells to oxidative stress. However, for the *in vivo* colitis models it could not be confirmed that NC is a more eligible candidate than curcumin during intestinal inflammation. Here, the whole body metabolism and the complex interactions with biological structures including the immune system have to be considered. In vivo, the therapeutic efficacy is influenced by the ADME (absorption, distribution, metabolism and excretion) principle, which dictates the kinetics of the drug exposure concentrations at the desired site of action. A major strategy in the field of nanomedicine is to utilize changed ADME properties of NP compared to the native drug. It is established that the small size permits NP to cross biological barriers more easily and thus allow for an enhanced absorption and distribution within the body. As discussed before, also the surface modification may have essential influence on ADME. Such complex pharmacological properties of (nano)drugs can only be investigated using *in vivo* models under realistic exposure (drug delivery) conditions. In the current study two independent murine colitis models were used, a chemically induced colitis model and a genetically induced colitis model. The DSS-induced colitis model is well established and commonly used, but in pharmacological studies this chemical can interfere with the (nano)drugs if given at or near the same treatment periods. If given in a subsequent or alternating order, it is may be difficult to titrate the level of intestinal inflammation in a

reproducible manner. As such, it is of relevance to investigate the pharmacological efficacy also in non-chemically induced colitis models, like the genetically engineered *Winnie* model. Last, but not least, both types of colitis models also have a different underlying mechanistic (molecular) basis, driven by severe epithelium damage or impaired mucus layer formation, respectively. The impact of any potential drug on such different processes may be very heterogeneous.

It has to be acknowledged also, that murine models are able to give a valid first clue about drug potency but, at the end it has to be confirmed in human trials. To date many *in vitro* and *in vivo* studies suggest promising efficacy of curcumin in IBD due to the fact that curcumin modulates inflammatory pathways. However, so far only two encouraging early-phase human trials have been completed (Ali et al., 2012; Hanai et al., 2006; Holt et al., 2005; Irving et al., 2011). Indeed, this gap should be closed in the near future. Studies on curcumin and IBD are of high relevance, also in comparison to NC, next to further mechanistic *in vitro* and *in vivo* studies. However, a mono-therapy of curcumin (or NC) in IBD seems currently implausible. In fact, it might be of greater benefit to use curcumin (whether or not in nanocarrier-based applications) as co-therapeutic agent together with more specific immune-modulating drugs, such as 6-mercaptopurine or anti-TNF agents to maintain the remission in IBD patients. Ali et al. suggested that a side-effect in the current anti-TNF therapy occurs due to a shift in the inflammatory pathway in which TNF may not be a major cytokine but others, which could be controlled by curcumin (Ali et al., 2012).

5.6 Outlook

In conclusion, the highly promising in vitro observations with NC in the Caco-2 cell culture model, and also specifically its improved value compared to native curcumin, could not be established in two independent in vivo studies. Both *in vivo* models appeared to be very suitable to address colitis, featuring distinctive clinical symptoms. In contrast to the DSS-induced colitis, the *Winnie* mice have the advantage to offer a more physiological element of colitis development. In view of the observed DNA repair gene expression differences, the *Winnie* mouse model may also be relevant to study inflammation-associated mutagenesis and carcinogenesis processes. This might be of specific interest for further research on curcumin, since specific pro-oxidative features were observed for this compound in the in vitro experiments, while NC did not trigger such effects. The genetically induced colitis is likely also more adequate in pharmacological studies since no additional chemical compound has to be applied to induce colitis. Above all, the *Winnie* mice exhibited a promising reduction of colitis symptoms and of ER stress after NC application. Therefore it can be considered to

perform a longer term-study (i.e. > 3 months) in aging *Winnie* mice, to evaluate whether a stronger pharmacological effect can be obtained after long-term NC application. In an optimal way, PEGylated curcumin-loaded PLGA nanoparticles should be used in such studies in view of their prolonged half-life in the body. To further increase efficacy, applications should occur at least daily, or even twice a day. A particularly relevant strategy might be a combination therapy approach with NC and anti-TNF in the genetically induced colitis model. Finally, long term nanodrug delivery studies could also be considered in very young *Winnie* mice (i.e. not be older than 6 to 8 weeks). In these animals colitis symptoms are just developing and not yet very severe, thus offering an opportunity to investigate potential preventive effects instead of therapeutic effects.

6. Summary

Inflammatory bowel diseases like ulcerative colitis and Crohn's disease, characterised by chronic and relapsing gastrointestinal inflammation, are associated with significant morbidity and mortality. There is an urgent call for improved therapies for these prevalent diseases. In the current work, PLGA encapsulated curcumin nanoparticles (nanocurcumin, NC) were prepared by emulsification-solvent-evaporation technique and characterised for size and stability. The therapeutic efficacy of NC to reduce inflammation and oxidative stress responses was tested using *in vitro* and *in vivo* models, in comparison to native curcumin as well as the PLGA carriers. In Caco-2 human intestinal epithelial cells, NC offered significant protection against H_2O_2-induced DNA stand breakage. It also reduced oxidative DNA adduct formation in the epithelial cells as induced upon co-incubation with phorbol-ester activated neutrophils. Importantly, NC did not trigger several pro-oxidative side effects. In contrast, at non-cytotoxic concentrations, curcumin was found to cause oxidative DNA damage in the Caco-2 cells as well as an increased mRNA expression of the oxidative stress markers gamma-glutamylcysteine synthetase and heme oxygenase-1. The therapeutic potential of NC and the native curcumin was also assessed in mice in a chemically induced colitis using dextran sulphate sodium (DSS) as well as in the genetically induced colitis model *Winnie*. Although neither curcumin nor NC was able to fully abrogate colitis, both were found to affect specific symptoms. In the DSS model curcumin significantly ameliorated histological colitis scores in most colon regions, including crypt abscess and inflammatory cell infiltration. The anti-inflammatory properties of curcumin were supported by reduced levels of Interleukin-1β. Also NC reduced intestinal histopathology in the most concerned distal colon part of DSS treated mice. However, at the same time NC, and even the curcumin-free PLGA vehicle, exhibited specific pro-inflammatory characteristics in the DSS mice, respectively detected by increased levels of keratinocyte chemoattractant (KC) and macrophage inflammatory protein-1α (MIP-1α). The Winnie mice featured a depletion of the secreted mucus layer, visualised by Pas/Alcain blue staining and an impaired Muc2 mRNA expression. Beneficial effects of NC in this colitis model were indicated by a diminished diarrhoea severity. Moreover, a lowered mRNA expression ratio of spliced to unspliced X-box binding protein 1 was measured, indicating that NC may reduce endoplasmic reticulum stress. However, also in this model some pro-inflammatory properties of NC were observed, shown by increased trends in distal colon tissue cytokine expression levels. In conclusion, NC showed stronger antioxidant properties than free curcumin in an *in vitro* model of intestinal epithelium, but its improved efficacy could not be demonstrated in two distinct murine models of colitis. Present studies underscore the importance of the concomitant investigation of the effects of a nano-formulated drug with the bulky drug as well as the drug-free nanocarrier to determine its true pharmaceutical potency.

7. Zusammenfassung

Chronisch-entzündliche Darmerkrankungen, wie Morbus Crohn und Colitis ulcerosa, sind durch wiederkehrende gastrointestinale Entzündungen gekennzeichnet und mit einer hohen Morbidität und Mortalität verbunden. Für eine erfolgreiche, nachhaltige Behandlung ist die Entwicklung neuer, verbesserter Therapien unabdingbar. In dieser Arbeit wurden PLGA-verkapselte Curcumin-Nanopartikel (Nanocurcumin, NC) mittels Emulgierung und anschließender Lösungsmittelverdampfung hergestellt. Nach Bestimmung der Partikelgröße und Stabilität wurde die therapeutische Wirksamkeit von NC bei Entzündung und oxidativem Stress mittels *in vitro* und *in vivo* Modellen untersucht und mit der Wirksamkeit von nativem Curcumin sowie den PLGA-Trägerpartikeln verglichen. In humanen intestinalen Epithelzellen Caco-2 schützte NC signifikant vor H_2O_2-induzierten DNA-Strangbrüchen. Außerdem verringerte es im Kokultur-System mit Phorbolester-aktivierten neutrophilen Granulozyten die Bildung von oxidativen DNA-Addukten in den Epithelzellen. NC zeigte hierbei keine pro-oxidativen Eigenschaften, die im Gegensatz dazu bei nicht-zytotoxische Konzentrationen von Curcumin induziert wurden, wie oxidative DNA-Schäden und eine erhöhten mRNA-Expression der oxidativen Stress Marker Gamma-Glutamylcystein Synthetase und Hämoxygenase-1. Des Weiteren wurde das therapeutische Potenzial von NC sowie von freiem Curcumin in zwei Maus-Colitismodellen untersucht, dem DSS (Dextran Sulfate Sodium)-induzierten sowie dem genetisch-induzierten *Winnie*-Model. Obwohl weder Curcumin noch NC die Kolitis vollständig heilen konnten, hatten beide Einfluss auf spezifische Symptome. In dem DSS-Modell verringerte Curcumin in fast allen Kolonabschnitten signifikant die histopathologischen Veränderungen, einschließlich der Darmkrypten-Abszesse und der Einwanderung von Entzündungszellen. Bestätigt wurden diese anti-entzündlichen Eigenschaften von Curcumin ebenfalls durch die verringerte Interleukin-1β Expression. Auch NC verbesserte die Histopathologie in dem stark geschädigten distalen Kolon von DSS-behandelten Mäusen. Jedoch zeigten sowohl NC als auch Curcumin-freie-PLGA-Partikel in DSS-behandelten Mäusen pro-inflammatorische Eigenschaften, nachgewiesen durch eine erhöhte Expression an KC (keratinocyte chemoattractant) und MIP-1 α (macrophage inflammatory protein-1 α). In den *Winnie* Mäusen war die reduzierte Mukusschicht durch eine Pas/Alcain Blau-Färbung sowie eine veränderte Muc2 mRNA-Expression detektierbar. In diesem Kolitis-Modell verringerte NC die klinische Symptomatik. Außerdem reduzierte NC das mRNA-Expressionsverhältnis von gespleißtem und ungespleißtem XBP1 (x-Box binding protein 1), als Hinweis auf eine mögliche Verringerung des Endoplasmatischen Retikulum Stresses. Jedoch weisen auch in diesem Modell erhöhte Zytokinlevel im distalen Kolongewebe auf pro-inflammatorische Eigenschaften des NC hin. Zusammenfassend weist NC in dem *in vitro* Modell zwar im

Vergleich zu Curcumin größere anti-oxidative Eigenschaften auf, diese verbesserte Wirksamkeit wurde aber *in vivo* nicht bestätigt. Des Weiteren unterstreicht die Studie die Notwendigkeit, die Effekte der Nano-Medikamente hinsichtlich ihrer therapeutischen Wirksamkeit immer im Zusammenhang mit dem herkömmlichen nativen Medikament sowie dem nicht-beladenen Trägermaterial zu untersuchen.

8. References

Abraham, C., and Cho, J. (2009). Interleukin-23/Th17 pathways and inflammatory bowel disease. Inflammatory bowel diseases *15*, 1090-1100.

Abraham, C., and Medzhitov, R. (2011). Interactions between the host innate immune system and microbes in inflammatory bowel disease. Gastroenterology *140*, 1729-1737.

Adams, D.H., and Lloyd, A.R. (1997). Chemokines: leucocyte recruitment and activation cytokines. Lancet *349*, 490-495.

Afif, W., and Loftus, E.V., Jr. (2010). Safety profile of IBD therapeutics: infectious risks. The Medical clinics of North America *94*, 115-133.

Aggarwal, B.B., Kumar, A., and Bharti, A.C. (2003). Anticancer potential of curcumin: preclinical and clinical studies. Anticancer research *23*, 363-398.

Ali, T., Shakir, F., and Morton, J. (2012). Curcumin and inflammatory bowel disease: biological mechanisms and clinical implication. Digestion *85*, 249-255.

Anand, P., Kunnumakkara, A.B., Newman, R.A., and Aggarwal, B.B. (2007). Bioavailability of curcumin: problems and promises. Molecular pharmaceutics *4*, 807-818.

Anand, P., Nair, H.B., Sung, B., Kunnumakkara, A.B., Yadav, V.R., Tekmal, R.R., and Aggarwal, B.B. (2010). Design of curcumin-loaded PLGA nanoparticles formulation with enhanced cellular uptake, and increased bioactivity in vitro and superior bioavailability in vivo. Biochemical pharmacology *79*, 330-338.

Anand, P., Thomas, S.G., Kunnumakkara, A.B., Sundaram, C., Harikumar, K.B., Sung, B., Tharakan, S.T., Misra, K., Priyadarsini, I.K., Rajasekharan, K.N., *et al.* (2008). Biological activities of curcumin and its analogues (Congeners) made by man and Mother Nature. Biochemical pharmacology *76*, 1590-1611.

Arafa, H.M., Hemeida, R.A., El-Bahrawy, A.I., and Hamada, F.M. (2009). Prophylactic role of curcumin in dextran sulfate sodium (DSS)-induced ulcerative colitis murine model. Food Chem Toxicol *47*, 1311-1317.

Araki, K., and Nagata, K. (2012). Protein folding and quality control in the ER. Cold Spring Harbor perspectives in biology *4*, a015438.

Artis, D. (2008). Epithelial-cell recognition of commensal bacteria and maintenance of immune homeostasis in the gut. Nature reviews Immunology *8*, 411-420.

Artursson, P. (1990). Epithelial transport of drugs in cell culture. I: A model for studying the passive diffusion of drugs over intestinal absorptive (Caco-2) cells. Journal of pharmaceutical sciences *79*, 476-482.

Babior, B.M. (2000a). The NADPH oxidase of endothelial cells. IUBMB life *50*, 267-269.

Babior, B.M. (2000b). Phagocytes and oxidative stress. The American journal of medicine *109*, 33-44.

Backhed, F., Ley, R.E., Sonnenburg, J.L., Peterson, D.A., and Gordon, J.I. (2005). Host-bacterial mutualism in the human intestine. Science *307*, 1915-1920.

Bainton, D.F., and Farquhar, M.G. (1968). Differences in enzyme content of azurophil and specific granules of polymorphonuclear leukocytes. I. Histochemical staining of bone marrow smears. The Journal of cell biology *39*, 286-298.

Balogun, E., Hoque, M., Gong, P., Killeen, E., Green, C.J., Foresti, R., Alam, J., and Motterlini, R. (2003). Curcumin activates the haem oxygenase-1 gene via regulation of Nrf2 and the antioxidant-responsive element. The Biochemical journal *371*, 887-895.

Barthel, A., and Klotz, L.O. (2005). Phosphoinositide 3-kinase signaling in the cellular response to oxidative stress. Biological chemistry *386*, 207-216.

Bermudez, E., Mangum, J.B., Asgharian, B., Wong, B.A., Reverdy, E.E., Janszen, D.B., Hext, P.M., Warheit, D.B., and Everitt, J.I. (2002). Long-term pulmonary responses of three laboratory rodent species to subchronic inhalation of pigmentary titanium dioxide particles. Toxicological sciences : an official journal of the Society of Toxicology *70*, 86-97.

Bermudez, E., Mangum, J.B., Wong, B.A., Asgharian, B., Hext, P.M., Warheit, D.B., and Everitt, J.I. (2004). Pulmonary responses of mice, rats, and hamsters to subchronic inhalation of ultrafine titanium dioxide particles. Toxicological sciences : an official journal of the Society of Toxicology *77*, 347-357.

Bertolotti, A., Wang, X., Novoa, I., Jungreis, R., Schlessinger, K., Cho, J.H., West, A.B., and Ron, D. (2001). Increased sensitivity to dextran sodium sulfate colitis in IRE1beta-deficient mice. The Journal of clinical investigation *107*, 585-593.

Bhawana, Basniwal, R.K., Buttar, H.S., Jain, V.K., and Jain, N. (2011). Curcumin nanoparticles: preparation, characterization, and antimicrobial study. Journal of agricultural and food chemistry *59*, 2056-2061.

Billerey-Larmonier, C., Uno, J.K., Larmonier, N., Midura, A.J., Timmermann, B., Ghishan, F.K., and Kiela, P.R. (2008). Protective effects of dietary curcumin in mouse model of chemically induced colitis are strain dependent. Inflammatory bowel diseases *14*, 780-793.

Binion, D.G., Otterson, M.F., and Rafiee, P. (2008). Curcumin inhibits VEGF-mediated angiogenesis in human intestinal microvascular endothelial cells through COX-2 and MAPK inhibition. Gut *57*, 1509-1517.

Bisht, S., Feldmann, G., Soni, S., Ravi, R., Karikar, C., Maitra, A., and Maitra, A. (2007). Polymeric nanoparticle-encapsulated curcumin ("nanocurcumin"): a novel strategy for human cancer therapy. Journal of nanobiotechnology *5*, 3.

Biswas, S.K., McClure, D., Jimenez, L.A., Megson, I.L., and Rahman, I. (2005). Curcumin induces glutathione biosynthesis and inhibits NF-kappaB activation and interleukin-8 release in alveolar epithelial cells: mechanism of free radical scavenging activity. Antioxidants & redox signaling *7*, 32-41.

Bjoras, M., Luna, L., Johnsen, B., Hoff, E., Haug, T., Rognes, T., and Seeberg, E. (1997). Opposite base-dependent reactions of a human base excision repair enzyme on DNA containing 7,8-dihydro-8-oxoguanine and abasic sites. The EMBO journal *16*, 6314-6322.

Blumberg, R., Cho, J., Lewis, J., and Wu, G. (2011). Inflammatory bowel disease: an update on the fundamental biology and clinical management. Gastroenterology *140*, 1701-1703.

Boiteux, S., O'Connor, T.R., Lederer, F., Gouyette, A., and Laval, J. (1990). Homogeneous Escherichia coli FPG protein. A DNA glycosylase which excises imidazole ring-opened

purines and nicks DNA at apurinic/apyrimidinic sites. The Journal of biological chemistry *265*, 3916-3922.

Boltin, D., Perets, T.T., Vilkin, A., and Niv, Y. (2013). Mucin function in inflammatory bowel disease: an update. Journal of clinical gastroenterology *47*, 106-111.

Bongartz, T., Sutton, A.J., Sweeting, M.J., Buchan, I., Matteson, E.L., and Montori, V. (2006). Anti-TNF antibody therapy in rheumatoid arthritis and the risk of serious infections and malignancies: systematic review and meta-analysis of rare harmful effects in randomized controlled trials. JAMA : the journal of the American Medical Association *295*, 2275-2285.

Boots, A.W., Li, H., Schins, R.P., Duffin, R., Heemskerk, J.W., Bast, A., and Haenen, G.R. (2007). The quercetin paradox. Toxicology and applied pharmacology *222*, 89-96.

Borm, P.J. (2002). Particle toxicology: from coal mining to nanotechnology. Inhalation toxicology *14*, 311-324.

Borm, P.J., Schins, R.P., and Albrecht, C. (2004). Inhaled particles and lung cancer, part B: paradigms and risk assessment. International journal of cancer *110*, 3-14.

Borregaard, N., Lollike, K., Kjeldsen, L., Sengelov, H., Bastholm, L., Nielsen, M.H., and Bainton, D.F. (1993). Human neutrophil granules and secretory vesicles. European journal of haematology *51*, 187-198.

Bosani, M., Ardizzone, S., and Porro, G.B. (2009). Biologic targeting in the treatment of inflammatory bowel diseases. Biologics : targets & therapy *3*, 77-97.

Brown, D.M., Wilson, M.R., MacNee, W., Stone, V., and Donaldson, K. (2001). Size-dependent proinflammatory effects of ultrafine polystyrene particles: a role for surface area and oxidative stress in the enhanced activity of ultrafines. Toxicology and applied pharmacology *175*, 191-199.

Buanne, P., Di Carlo, E., Caputi, L., Brandolini, L., Mosca, M., Cattani, F., Pellegrini, L., Biordi, L., Coletti, G., Sorrentino, C.*, et al.* (2007). Crucial pathophysiological role of CXCR2 in experimental ulcerative colitis in mice. Journal of leukocyte biology *82*, 1239-1246.

Buffinton, G.D., and Doe, W.F. (1995). Depleted mucosal antioxidant defences in inflammatory bowel disease. Free radical biology & medicine *19*, 911-918.

Bundy, R., Walker, A.F., Middleton, R.W., and Booth, J. (2004). Turmeric extract may improve irritable bowel syndrome symptomology in otherwise healthy adults: a pilot study. Journal of alternative and complementary medicine *10*, 1015-1018.

Camacho-Barquero, L., Villegas, I., Sanchez-Calvo, J.M., Talero, E., Sanchez-Fidalgo, S., Motilva, V., and Alarcon de la Lastra, C. (2007). Curcumin, a Curcuma longa constituent, acts on MAPK p38 pathway modulating COX-2 and iNOS expression in chronic experimental colitis. International immunopharmacology *7*, 333-342.

Cao, J., Jia, L., Zhou, H.M., Liu, Y., and Zhong, L.F. (2006). Mitochondrial and nuclear DNA damage induced by curcumin in human hepatoma G2 cells. Toxicological sciences : an official journal of the Society of Toxicology *91*, 476-483.

Chaudhary, L.R., and Avioli, L.V. (1996). Regulation of interleukin-8 gene expression by interleukin-1beta, osteotropic hormones, and protein kinase inhibitors in normal human bone marrow stromal cells. The Journal of biological chemistry *271*, 16591-16596.

Chaudhry, Q., Scotter, M., Blackburn, J., Ross, B., Boxall, A., Castle, L., Aitken, R., and Watkins, R. (2008). Applications and implications of nanotechnologies for the food sector. Food additives & contaminants *25*, 241-258.

Cheng, F.Y., Wang, S.P., Su, C.H., Tsai, T.L., Wu, P.C., Shieh, D.B., Chen, J.H., Hsieh, P.C., and Yeh, C.S. (2008). Stabilizer-free poly(lactide-co-glycolide) nanoparticles for multimodal biomedical probes. Biomaterials *29*, 2104-2112.

Chichlowski, M., and Hale, L.P. (2008). Bacterial-mucosal interactions in inflammatory bowel disease: an alliance gone bad. American journal of physiology Gastrointestinal and liver physiology *295*, G1139-1149.

Chomczynski, P., and Sacchi, N. (1987). Single-step method of RNA isolation by acid guanidinium thiocyanate-phenol-chloroform extraction. Analytical biochemistry *162*, 156-159.

Clift, M.J., and Rothen-Rutishauser, B. (2013). Studying the oxidative stress paradigm in vitro: a theoretical and practical perspective. Methods in molecular biology *1028*, 115-133.

Coburn, L.A., Gong, X., Singh, K., Asim, M., Scull, B.P., Allaman, M.M., Williams, C.S., Rosen, M.J., Washington, M.K., Barry, D.P.*, et al.* (2012). L-arginine supplementation improves responses to injury and inflammation in dextran sulfate sodium colitis. PloS one *7*, e33546.

Collins, R.H., Jr., Feldman, M., and Fordtran, J.S. (1987). Colon cancer, dysplasia, and surveillance in patients with ulcerative colitis. A critical review. The New England journal of medicine *316*, 1654-1658.

Coombes, J.L., and Powrie, F. (2008). Dendritic cells in intestinal immune regulation. Nature reviews Immunology *8*, 435-446.

Corazziari, E.S. (2009). Intestinal mucus barrier in normal and inflamed colon. Journal of pediatric gastroenterology and nutrition *48 Suppl 2*, S54-55.

Costantini, C., Micheletti, A., Calzetti, F., Perbellini, O., Pizzolo, G., and Cassatella, M.A. (2010). Neutrophil activation and survival are modulated by interaction with NK cells. International immunology *22*, 827-838.

Couvreur, P. (2013). Nanoparticles in drug delivery: past, present and future. Advanced drug delivery reviews *65*, 21-23.

Cox, J.H., Kljavin, N.M., Ota, N., Leonard, J., Roose-Girma, M., Diehl, L., Ouyang, W., and Ghilardi, N. (2012). Opposing consequences of IL-23 signaling mediated by innate and adaptive cells in chemically induced colitis in mice. Mucosal immunology *5*, 99-109.

Crosnier, C., Stamataki, D., and Lewis, J. (2006). Organizing cell renewal in the intestine: stem cells, signals and combinatorial control. Nature reviews Genetics *7*, 349-359.

D'Inca, R., Cardin, R., Benazzato, L., Angriman, I., Martines, D., and Sturniolo, G.C. (2004). Oxidative DNA damage in the mucosa of ulcerative colitis increases with disease duration and dysplasia. Inflammatory bowel diseases *10*, 23-27.

Danhier, F., Ansorena, E., Silva, J.M., Coco, R., Le Breton, A., and Preat, V. (2012). PLGA-based nanoparticles: an overview of biomedical applications. J Control Release *161*, 505-522.

De Jong, W.H., and Borm, P.J. (2008). Drug delivery and nanoparticles:applications and hazards. International journal of nanomedicine *3*, 133-149.

Deguchi, Y., Andoh, A., Inatomi, O., Yagi, Y., Bamba, S., Araki, Y., Hata, K., Tsujikawa, T., and Fujiyama, Y. (2007). Curcumin prevents the development of dextran sulfate Sodium (DSS)-induced experimental colitis. Digestive diseases and sciences *52*, 2993-2998.

Denning, T.L., Wang, Y.C., Patel, S.R., Williams, I.R., and Pulendran, B. (2007). Lamina propria macrophages and dendritic cells differentially induce regulatory and interleukin 17-producing T cell responses. Nature immunology *8*, 1086-1094.

Deodhar, S.D., Sethi, R., and Srimal, R.C. (1980). Preliminary study on antirheumatic activity of curcumin (diferuloyl methane). The Indian journal of medical research *71*, 632-634.

des Rieux, A., Fievez, V., Garinot, M., Schneider, Y.J., and Preat, V. (2006). Nanoparticles as potential oral delivery systems of proteins and vaccines: a mechanistic approach. J Control Release *116*, 1-27.

DeSesso, J.M., and Jacobson, C.F. (2001). Anatomical and physiological parameters affecting gastrointestinal absorption in humans and rats. Food Chem Toxicol *39*, 209-228.

Donaldson, K., Tran, L., Jimenez, L.A., Duffin, R., Newby, D.E., Mills, N., MacNee, W., and Stone, V. (2005). Combustion-derived nanoparticles: a review of their toxicology following inhalation exposure. Particle and fibre toxicology *2*, 10.

Drew, R., and Miners, J.O. (1984). The effects of buthionine sulphoximine (BSO) on glutathione depletion and xenobiotic biotransformation. Biochemical pharmacology *33*, 2989-2994.

Driscoll, K.E., Lindenschmidt, R.C., Maurer, J.K., Perkins, L., Perkins, M., and Higgins, J. (1991). Pulmonary response to inhaled silica or titanium dioxide. Toxicology and applied pharmacology *111*, 201-210.

Drost, E.M., and MacNee, W. (2002). Potential role of IL-8, platelet-activating factor and TNF-alpha in the sequestration of neutrophils in the lung: effects on neutrophil deformability, adhesion receptor expression, and chemotaxis. European journal of immunology *32*, 393-403.

Durgaprasad, S., Pai, C.G., Vasanthkumar, Alvres, J.F., and Namitha, S. (2005). A pilot study of the antioxidant effect of curcumin in tropical pancreatitis. The Indian journal of medical research *122*, 315-318.

Ekbom, A., Helmick, C., Zack, M., and Adami, H.O. (1990). Ulcerative colitis and colorectal cancer. A population-based study. The New England journal of medicine *323*, 1228-1233.

Elinav, E., Henao-Mejia, J., and Flavell, R.A. (2013). Integrative inflammasome activity in the regulation of intestinal mucosal immune responses. Mucosal immunology *6*, 4-13.

Elsaesser, A., and Howard, C.V. (2012). Toxicology of nanoparticles. Advanced drug delivery reviews *64*, 129-137.

Epstein, J., Docena, G., MacDonald, T.T., and Sanderson, I.R. (2010a). Curcumin suppresses p38 mitogen-activated protein kinase activation, reduces IL-1beta and matrix metalloproteinase-3 and enhances IL-10 in the mucosa of children and adults with inflammatory bowel disease. The British journal of nutrition *103*, 824-832.

Epstein, J., Sanderson, I.R., and Macdonald, T.T. (2010b). Curcumin as a therapeutic agent: the evidence from in vitro, animal and human studies. The British journal of nutrition *103*, 1545-1557.

Eri, R.D., Adams, R.J., Tran, T.V., Tong, H., Das, I., Roche, D.K., Oancea, I., Png, C.W., Jeffery, P.L., Radford-Smith, G.L., *et al.* (2010). An intestinal epithelial defect conferring ER stress results in inflammation involving both innate and adaptive immunity. Mucosal immunology *4*, 354-364.

Evangelista, V., Manarini, S., Rotondo, S., Martelli, N., Polischuk, R., McGregor, J.L., de Gaetano, G., and Cerletti, C. (1996). Platelet/polymorphonuclear leukocyte interaction in dynamic conditions: evidence of adhesion cascade and cross talk between P-selectin and the beta 2 integrin CD11b/CD18. Blood *88*, 4183-4194.

Fang, J., Lu, J., and Holmgren, A. (2005). Thioredoxin reductase is irreversibly modified by curcumin: a novel molecular mechanism for its anticancer activity. The Journal of biological chemistry *280*, 25284-25290.

Fatahzadeh, M. (2009). Inflammatory bowel disease. Oral surgery, oral medicine, oral pathology, oral radiology, and endodontics *108*, e1-10.

Feldherr, C.M., and Akin, D. (1997). The location of the transport gate in the nuclear pore complex. Journal of cell science *110 (Pt 24)*, 3065-3070.

Fels, D.R., and Koumenis, C. (2006). The PERK/eIF2alpha/ATF4 module of the UPR in hypoxia resistance and tumor growth. Cancer biology & therapy *5*, 723-728.

Ferin, J., and Oberdorster, G. (1992). Polymer degradation and ultrafine particles: potential inhalation hazards for astronauts. Acta astronautica *27*, 257-259.

Fonte, P., Soares, S., Costa, A., Andrade, J.C., Seabra, V., Reis, S., and Sarmento, B. (2012). Effect of cryoprotectants on the porosity and stability of insulin-loaded PLGA nanoparticles after freeze-drying. Biomatter *2*, 329-339.

Freitas, M., Lima, J.L., and Fernandes, E. (2009). Optical probes for detection and quantification of neutrophils' oxidative burst. A review. Analytica chimica acta *649*, 8-23.

Fritz, G. (2000). Human APE/Ref-1 protein. The international journal of biochemistry & cell biology *32*, 925-929.

Fuss, I.J., Heller, F., Boirivant, M., Leon, F., Yoshida, M., Fichtner-Feigl, S., Yang, Z., Exley, M., Kitani, A., Blumberg, R.S., *et al.* (2004). Nonclassical CD1d-restricted NK T cells that produce IL-13 characterize an atypical Th2 response in ulcerative colitis. The Journal of clinical investigation *113*, 1490-1497.

Geiser, M., and Kreyling, W.G. (2010). Deposition and biokinetics of inhaled nanoparticles. Particle and fibre toxicology *7*, 2.

Geiser, M., Quaile, O., Wenk, A., Wigge, C., Eigeldinger-Berthou, S., Hirn, S., Schaffler, M., Schleh, C., Moller, W., Mall, M.A., *et al.* (2013). Cellular uptake and localization of inhaled gold nanoparticles in lungs of mice with chronic obstructive pulmonary disease. Particle and fibre toxicology *10*, 19.

Gerloff, K., Albrecht, C., Boots, A.W., Förster, I., and Schins, R.P.F. (2009). Cytotoxicity and oxidative DNA damage by nanoparticles in human intestinal Caco-2. Nanotoxicology.

Gerloff, K., Fenoglio, I., Carella, E., Kolling, J., Albrecht, C., Boots, A.W., Forster, I., and Schins, R.P. (2012a). Distinctive toxicity of TiO2 rutile/anatase mixed phase nanoparticles on Caco-2 cells. Chemical research in toxicology *25*, 646-655.

Gerloff, K., Pereira, D.I., Faria, N., Boots, A.W., Kolling, J., Forster, I., Albrecht, C., Powell, J.J., and Schins, R.P. (2012b). Influence of simulated gastrointestinal conditions on particle-induced cytotoxicity and interleukin-8 regulation in differentiated and undifferentiated Caco-2 cells. Nanotoxicology.

Goel, A., Kunnumakkara, A.B., and Aggarwal, B.B. (2008). Curcumin as "Curecumin": from kitchen to clinic. Biochemical pharmacology *75*, 787-809.

Gomez, C.R., Nomellini, V., Faunce, D.E., and Kovacs, E.J. (2008). Innate immunity and aging. Experimental gerontology *43*, 718-728.

Gradishar, W.J., Tjulandin, S., Davidson, N., Shaw, H., Desai, N., Bhar, P., Hawkins, M., and O'Shaughnessy, J. (2005). Phase III trial of nanoparticle albumin-bound paclitaxel compared with polyethylated castor oil-based paclitaxel in women with breast cancer. J Clin Oncol *23*, 7794-7803.

Griffith, O.W. (1999). Biologic and pharmacologic regulation of mammalian glutathione synthesis. Free radical biology & medicine *27*, 922-935.

Grisham, M.B. (1994). Oxidants and free radicals in inflammatory bowel disease. Lancet *344*, 859-861.

Gungor, N., Knaapen, A.M., Munnia, A., Peluso, M., Haenen, G.R., Chiu, R.K., Godschalk, R.W., and van Schooten, F.J. (2010). Genotoxic effects of neutrophils and hypochlorous acid. Mutagenesis *25*, 149-154.

Hamilton, M.J., Snapper, S.B., and Blumberg, R.S. (2012). Update on biologic pathways in inflammatory bowel disease and their therapeutic relevance. Journal of gastroenterology *47*, 1-8.

Hampton, M.B., Kettle, A.J., and Winterbourn, C.C. (1998). Inside the neutrophil phagosome: oxidants, myeloperoxidase, and bacterial killing. Blood *92*, 3007-3017.

Han, S.S., Keum, Y.S., Seo, H.J., and Surh, Y.J. (2002). Curcumin suppresses activation of NF-kappaB and AP-1 induced by phorbol ester in cultured human promyelocytic leukemia cells. Journal of biochemistry and molecular biology *35*, 337-342.

Hanai, H., Iida, T., Takeuchi, K., Watanabe, F., Maruyama, Y., Andoh, A., Tsujikawa, T., Fujiyama, Y., Mitsuyama, K., Sata, M.*, et al.* (2006). Curcumin maintenance therapy for ulcerative colitis: randomized, multicenter, double-blind, placebo-controlled trial. Clinical gastroenterology and hepatology : the official clinical practice journal of the American Gastroenterological Association *4*, 1502-1506.

Hansson, G.C. (2012). Role of mucus layers in gut infection and inflammation. Current opinion in microbiology *15*, 57-62.

Harding, H.P., Novoa, I., Zhang, Y., Zeng, H., Wek, R., Schapira, M., and Ron, D. (2000). Regulated translation initiation controls stress-induced gene expression in mammalian cells. Molecular cell *6*, 1099-1108.

Heazlewood, C.K., Cook, M.C., Eri, R., Price, G.R., Tauro, S.B., Taupin, D., Thornton, D.J., Png, C.W., Crockford, T.L., Cornall, R.J.*, et al.* (2008). Aberrant mucin assembly in mice

causes endoplasmic reticulum stress and spontaneous inflammation resembling ulcerative colitis. PLoS medicine *5*, e54.

Hendrickson, B.A., Gokhale, R., and Cho, J.H. (2002). Clinical aspects and pathophysiology of inflammatory bowel disease. Clinical microbiology reviews *15*, 79-94.

Hermiston, M.L., and Gordon, J.I. (1995). Inflammatory bowel disease and adenomas in mice expressing a dominant negative N-cadherin. Science *270*, 1203-1207.

Hidalgo, I.J., Raub, T.J., and Borchardt, R.T. (1989). Characterization of the human colon carcinoma cell line (Caco-2) as a model system for intestinal epithelial permeability. Gastroenterology *96*, 736-749.

Hill, D.A., and Artis, D. (2010). Intestinal bacteria and the regulation of immune cell homeostasis. Annual review of immunology *28*, 623-667.

Hilsden, R.J., Verhoef, M.J., Rasmussen, H., Porcino, A., and DeBruyn, J.C. (2011). Use of complementary and alternative medicine by patients with inflammatory bowel disease. Inflammatory bowel diseases *17*, 655-662.

Hirsch, C., Gauss, R., Horn, S.C., Neuber, O., and Sommer, T. (2009). The ubiquitylation machinery of the endoplasmic reticulum. Nature *458*, 453-460.

Hofseth, L.J., Khan, M.A., Ambrose, M., Nikolayeva, O., Xu-Welliver, M., Kartalou, M., Hussain, S.P., Roth, R.B., Zhou, X., Mechanic, L.E.*, et al.* (2003). The adaptive imbalance in base excision-repair enzymes generates microsatellite instability in chronic inflammation. The Journal of clinical investigation *112*, 1887-1894.

Holland, S.M. (2010). Chronic granulomatous disease. Clinical reviews in allergy & immunology *38*, 3-10.

Holt, P.R., Katz, S., and Kirshoff, R. (2005). Curcumin therapy in inflammatory bowel disease: a pilot study. Digestive diseases and sciences *50*, 2191-2193.

Hotamisligil, G.S. (2010). Endoplasmic reticulum stress and the inflammatory basis of metabolic disease. Cell *140*, 900-917.

Hue, S., Ahern, P., Buonocore, S., Kullberg, M.C., Cua, D.J., McKenzie, B.S., Powrie, F., and Maloy, K.J. (2006). Interleukin-23 drives innate and T cell-mediated intestinal inflammation. The Journal of experimental medicine *203*, 2473-2483.

Hume, D.A. (2006). The mononuclear phagocyte system. Current opinion in immunology *18*, 49-53.

Hur, S.J., Kang, S.H., Jung, H.S., Kim, S.C., Jeon, H.S., Kim, I.H., and Lee, J.D. (2012). Review of natural products actions on cytokines in inflammatory bowel disease. Nutrition research *32*, 801-816.

Ichiseki, T., Ueda, Y., Katsuda, S., Kitamura, K., Kaneuji, A., and Matsumoto, T. (2006). Oxidative stress by glutathione depletion induces osteonecrosis in rats. Rheumatology *45*, 287-290.

Irving, G.R., Karmokar, A., Berry, D.P., Brown, K., and Steward, W.P. (2011). Curcumin: the potential for efficacy in gastrointestinal diseases. Best practice & research Clinical gastroenterology *25*, 519-534.

Izcue, A., Hue, S., Buonocore, S., Arancibia-Carcamo, C.V., Ahern, P.P., Iwakura, Y., Maloy, K.J., and Powrie, F. (2008). Interleukin-23 restrains regulatory T cell activity to drive T cell-dependent colitis. Immunity *28*, 559-570.

Jagetia, G.C., and Aggarwal, B.B. (2007). "Spicing up" of the immune system by curcumin. Journal of clinical immunology *27*, 19-35.

Jaillon, S., Galdiero, M.R., Del Prete, D., Cassatella, M.A., Garlanda, C., and Mantovani, A. (2013). Neutrophils in innate and adaptive immunity. Seminars in immunopathology *35*, 377-394.

Jain, K.K. (2010). Advances in the field of nanooncology. BMC medicine *8*, 83.

Jain, R.A. (2000). The manufacturing techniques of various drug loaded biodegradable poly(lactide-co-glycolide) (PLGA) devices. Biomaterials *21*, 2475-2490.

Jeney, V., Balla, J., Yachie, A., Varga, Z., Vercellotti, G.M., Eaton, J.W., and Balla, G. (2002). Pro-oxidant and cytotoxic effects of circulating heme. Blood *100*, 879-887.

Jess, T., Loftus, E.V., Jr., Velayos, F.S., Harmsen, W.S., Zinsmeister, A.R., Smyrk, T.C., Schleck, C.D., Tremaine, W.J., Melton, L.J., 3rd, Munkholm, P.*, et al.* (2006). Risk of intestinal cancer in inflammatory bowel disease: a population-based study from olmsted county, Minnesota. Gastroenterology *130*, 1039-1046.

Jobin, C., and Sartor, R.B. (2000). NF-kappaB signaling proteins as therapeutic targets for inflammatory bowel diseases. Inflammatory bowel diseases *6*, 206-213.

Joe, B., and Lokesh, B.R. (1994). Role of capsaicin, curcumin and dietary n-3 fatty acids in lowering the generation of reactive oxygen species in rat peritoneal macrophages. Biochimica et biophysica acta *1224*, 255-263.

Kang, K.W., Lee, S.J., and Kim, S.G. (2005). Molecular mechanism of nrf2 activation by oxidative stress. Antioxidants & redox signaling *7*, 1664-1673.

Kasai, H. (1997). Analysis of a form of oxidative DNA damage, 8-hydroxy-2'-deoxyguanosine, as a marker of cellular oxidative stress during carcinogenesis. Mutation research *387*, 147-163.

Kaser, A., Adolph, T.E., and Blumberg, R.S. (2013). The unfolded protein response and gastrointestinal disease. Seminars in immunopathology *35*, 307-319.

Kaser, A., Lee, A.H., Franke, A., Glickman, J.N., Zeissig, S., Tilg, H., Nieuwenhuis, E.E., Higgins, D.E., Schreiber, S., Glimcher, L.H.*, et al.* (2008). XBP1 links ER stress to intestinal inflammation and confers genetic risk for human inflammatory bowel disease. Cell *134*, 743-756.

Kastelein, R.A., Hunter, C.A., and Cua, D.J. (2007). Discovery and biology of IL-23 and IL-27: related but functionally distinct regulators of inflammation. Annual review of immunology *25*, 221-242.

Kelly, M.R., Xu, J., Alexander, K.E., and Loo, G. (2001). Disparate effects of similar phenolic phytochemicals as inhibitors of oxidative damage to cellular DNA. Mutation research *485*, 309-318.

Kim, Y.S., and Ho, S.B. (2010). Intestinal goblet cells and mucins in health and disease: recent insights and progress. Current gastroenterology reports *12*, 319-330.

Klotz, L.O. (2002). Oxidant-induced signaling: effects of peroxynitrite and singlet oxygen. Biological chemistry *383*, 443-456.

Knaapen, A.M., Gungor, N., Schins, R.P., Borm, P.J., and Van Schooten, F.J. (2006). Neutrophils and respiratory tract DNA damage and mutagenesis: a review. Mutagenesis *21*, 225-236.

Kobelt, G. (2006). Health economic issues in rheumatoid arthritis. Scandinavian journal of rheumatology *35*, 415-425.

Krause, W.J., Yamada, J., and Cutts, J.H. (1985). Quantitative distribution of enteroendocrine cells in the gastrointestinal tract of the adult opossum, Didelphis virginiana. Journal of anatomy *140 (Pt 4)*, 591-605.

Krokan, H.E., Nilsen, H., Skorpen, F., Otterlei, M., and Slupphaug, G. (2000). Base excision repair of DNA in mammalian cells. FEBS letters *476*, 73-77.

Kuhn, R., Lohler, J., Rennick, D., Rajewsky, K., and Muller, W. (1993). Interleukin-10-deficient mice develop chronic enterocolitis. Cell *75*, 263-274.

Kumar, V., and Sharma, A. (2010). Neutrophils: Cinderella of innate immune system. International immunopharmacology *10*, 1325-1334.

Kumari, A., Yadav, S.K., Pakade, Y.B., Singh, B., and Yadav, S.C. (2010a). Development of biodegradable nanoparticles for delivery of quercetin. Colloids and surfaces *80*, 184-192.

Kumari, A., Yadav, S.K., and Yadav, S.C. (2010b). Biodegradable polymeric nanoparticles based drug delivery systems. Colloids and surfaces *75*, 1-18.

Kuna, P., Alam, R., Ruta, U., and Gorski, P. (1998). RANTES induces nasal mucosal inflammation rich in eosinophils, basophils, and lymphocytes in vivo. American journal of respiratory and critical care medicine *157*, 873-879.

Lamprecht, A., Ubrich, N., Yamamoto, H., Schafer, U., Takeuchi, H., Maincent, P., Kawashima, Y., and Lehr, C.M. (2001). Biodegradable nanoparticles for targeted drug delivery in treatment of inflammatory bowel disease. The Journal of pharmacology and experimental therapeutics *299*, 775-781.

Lao, C.D., Ruffin, M.T.t., Normolle, D., Heath, D.D., Murray, S.I., Bailey, J.M., Boggs, M.E., Crowell, J., Rock, C.L., and Brenner, D.E. (2006). Dose escalation of a curcuminoid formulation. BMC complementary and alternative medicine *6*, 10.

Larmonier, C.B., Midura-Kiela, M.T., Ramalingam, R., Laubitz, D., Janikashvili, N., Larmonier, N., Ghishan, F.K., and Kiela, P.R. (2011). Modulation of neutrophil motility by curcumin: implications for inflammatory bowel disease. Inflammatory bowel diseases *17*, 503-515.

Larsson, J.M., Karlsson, H., Crespo, J.G., Johansson, M.E., Eklund, L., Sjovall, H., and Hansson, G.C. (2011). Altered O-glycosylation profile of MUC2 mucin occurs in active ulcerative colitis and is associated with increased inflammation. Inflammatory bowel diseases *17*, 2299-2307.

Lee, E.G., Boone, D.L., Chai, S., Libby, S.L., Chien, M., Lodolce, J.P., and Ma, A. (2000). Failure to regulate TNF-induced NF-kappaB and cell death responses in A20-deficient mice. Science *289*, 2350-2354.

Lee, K., Tirasophon, W., Shen, X., Michalak, M., Prywes, R., Okada, T., Yoshida, H., Mori, K., and Kaufman, R.J. (2002). IRE1-mediated unconventional mRNA splicing and S2P-mediated ATF6 cleavage merge to regulate XBP1 in signaling the unfolded protein response. Genes & development *16*, 452-466.

Ley, R.E., Peterson, D.A., and Gordon, J.I. (2006). Ecological and evolutionary forces shaping microbial diversity in the human intestine. Cell *124*, 837-848.

Li, H., van Berlo, D., Shi, T., Speit, G., Knaapen, A.M., Borm, P.J., Albrecht, C., and Schins, R.P. (2008). Curcumin protects against cytotoxic and inflammatory effects of quartz particles but causes oxidative DNA damage in a rat lung epithelial cell line. Toxicology and applied pharmacology *227*, 115-124.

Liao, J., Seril, D.N., Lu, G.G., Zhang, M., Toyokuni, S., Yang, A.L., and Yang, G.Y. (2008). Increased susceptibility of chronic ulcerative colitis-induced carcinoma development in DNA repair enzyme Ogg1 deficient mice. Molecular carcinogenesis *47*, 638-646.

Lih-Brody, L., Powell, S.R., Collier, K.P., Reddy, G.M., Cerchia, R., Kahn, E., Weissman, G.S., Katz, S., Floyd, R.A., McKinley, M.J.*, et al.* (1996). Increased oxidative stress and decreased antioxidant defenses in mucosa of inflammatory bowel disease. Digestive diseases and sciences *41*, 2078-2086.

Linden, S.K., Sutton, P., Karlsson, N.G., Korolik, V., and McGuckin, M.A. (2008). Mucins in the mucosal barrier to infection. Mucosal immunology *1*, 183-197.

Liu, G.A., and Zheng, R.L. (2002). Protection against damaged DNA in the single cell by polyphenols. Die Pharmazie *57*, 852-854.

Liu, L., Liu, Y.L., Liu, G.X., Chen, X., Yang, K., Yang, Y.X., Xie, Q., Gan, H.K., Huang, X.L., and Gan, H.T. (2013). Curcumin ameliorates dextran sulfate sodium-induced experimental colitis by blocking STAT3 signaling pathway. International immunopharmacology *17*, 314-320.

Livak, K.J., and Schmittgen, T.D. (2001). Analysis of relative gene expression data using real-time quantitative PCR and the 2(-Delta Delta C(T)) Method. Methods *25*, 402-408.

Loftus, E.V., Jr. (2004). Clinical epidemiology of inflammatory bowel disease: Incidence, prevalence, and environmental influences. Gastroenterology *126*, 1504-1517.

Lomer, M.C., Harvey, R.S., Evans, S.M., Thompson, R.P., and Powell, J.J. (2001). Efficacy and tolerability of a low microparticle diet in a double blind, randomized, pilot study in Crohn's disease. European journal of gastroenterology & hepatology *13*, 101-106.

Lomer, M.C., Hutchinson, C., Volkert, S., Greenfield, S.M., Catterall, A., Thompson, R.P., and Powell, J.J. (2004). Dietary sources of inorganic microparticles and their intake in healthy subjects and patients with Crohn's disease. The British journal of nutrition *92*, 947-955.

Lopez-Lazaro, M. (2008). Anticancer and carcinogenic properties of curcumin: considerations for its clinical development as a cancer chemopreventive and chemotherapeutic agent. Molecular nutrition & food research *52 Suppl 1*, S103-127.

Lorenzo, Y., Azqueta, A., Luna, L., Bonilla, F., Dominguez, G., and Collins, A.R. (2009). The carotenoid beta-cryptoxanthin stimulates the repair of DNA oxidation damage in addition to acting as an antioxidant in human cells. Carcinogenesis *30*, 308-314.

Mabbott, N.A., Donaldson, D.S., Ohno, H., Williams, I.R., and Mahajan, A. (2013). Microfold (M) cells: important immunosurveillance posts in the intestinal epithelium. Mucosal immunology *6*, 666-677.

Mahon, E., Salvati, A., Baldelli Bombelli, F., Lynch, I., and Dawson, K.A. (2012). Designing the nanoparticle-biomolecule interface for "targeting and therapeutic delivery". J Control Release *161*, 164-174.

Maiti, K., Mukherjee, K., Gantait, A., Saha, B.P., and Mukherjee, P.K. (2007). Curcumin-phospholipid complex: Preparation, therapeutic evaluation and pharmacokinetic study in rats. International journal of pharmaceutics *330*, 155-163.

Mantovani, A., Cassatella, M.A., Costantini, C., and Jaillon, S. (2011). Neutrophils in the activation and regulation of innate and adaptive immunity. Nature reviews Immunology *11*, 519-531.

Maturana, A., Krause, K.H., and Demaurex, N. (2002). NOX family NADPH oxidases: do they have built-in proton channels? The Journal of general physiology *120*, 781-786.

Maurer, M., and von Stebut, E. (2004). Macrophage inflammatory protein-1. The international journal of biochemistry & cell biology *36*, 1882-1886.

McAuley, J.L., Linden, S.K., Png, C.W., King, R.M., Pennington, H.L., Gendler, S.J., Florin, T.H., Hill, G.R., Korolik, V., and McGuckin, M.A. (2007). MUC1 cell surface mucin is a critical element of the mucosal barrier to infection. The Journal of clinical investigation *117*, 2313-2324.

McGuckin, M.A., Eri, R., Simms, L.A., Florin, T.H., and Radford-Smith, G. (2009). Intestinal barrier dysfunction in inflammatory bowel diseases. Inflammatory bowel diseases *15*, 100-113.

McGuckin, M.A., Linden, S.K., Sutton, P., and Florin, T.H. (2011). Mucin dynamics and enteric pathogens. Nature reviews Microbiology *9*, 265-278.

Medzhitov, R. (2007). Recognition of microorganisms and activation of the immune response. Nature *449*, 819-826.

Mitsuyama, K., Toyonaga, A., Sasaki, E., Watanabe, K., Tateishi, H., Nishiyama, T., Saiki, T., Ikeda, H., Tsuruta, O., and Tanikawa, K. (1994). IL-8 as an important chemoattractant for neutrophils in ulcerative colitis and Crohn's disease. Clinical and experimental immunology *96*, 432-436.

Moghimi, S.M., Hunter, A.C., and Murray, J.C. (2005). Nanomedicine: current status and future prospects. FASEB journal : official publication of the Federation of American Societies for Experimental Biology *19*, 311-330.

Molodecky, N.A., and Kaplan, G.G. (2010). Environmental risk factors for inflammatory bowel disease. Gastroenterology & hepatology *6*, 339-346.

Morris, G.P., Beck, P.L., Herridge, M.S., Depew, W.T., Szewczuk, M.R., and Wallace, J.L. (1989). Hapten-induced model of chronic inflammation and ulceration in the rat colon. Gastroenterology *96*, 795-803.

Motterlini, R., Foresti, R., Bassi, R., and Green, C.J. (2000). Curcumin, an antioxidant and anti-inflammatory agent, induces heme oxygenase-1 and protects endothelial cells against oxidative stress. Free radical biology & medicine *28*, 1303-1312.

Motterlini, R., Foresti, R., Intaglietta, M., and Winslow, R.M. (1996). NO-mediated activation of heme oxygenase: endogenous cytoprotection against oxidative stress to endothelium. The American journal of physiology *270*, H107-114.

Murai, M., Turovskaya, O., Kim, G., Madan, R., Karp, C.L., Cheroutre, H., and Kronenberg, M. (2009). Interleukin 10 acts on regulatory T cells to maintain expression of the transcription factor Foxp3 and suppressive function in mice with colitis. Nature immunology *10*, 1178-1184.

Nagler-Anderson, C. (2001). Man the barrier! Strategic defences in the intestinal mucosa. Nature reviews Immunology *1*, 59-67.

Naito, Y., Takagi, T., and Yoshikawa, T. (2007). Neutrophil-dependent oxidative stress in ulcerative colitis. Journal of clinical biochemistry and nutrition *41*, 18-26.

Nathan, C. (2006). Neutrophils and immunity: challenges and opportunities. Nature reviews Immunology *6*, 173-182.

Nauseef, W.M. (2007). How human neutrophils kill and degrade microbes: an integrated view. Immunological reviews *219*, 88-102.

Nel, A., Xia, T., Madler, L., and Li, N. (2006). Toxic potential of materials at the nanolevel. Science *311*, 622-627.

Nenci, A., Becker, C., Wullaert, A., Gareus, R., van Loo, G., Danese, S., Huth, M., Nikolaev, A., Neufert, C., Madison, B.*, et al.* (2007). Epithelial NEMO links innate immunity to chronic intestinal inflammation. Nature *446*, 557-561.

Neutra, M.R. (1999). M cells in antigen sampling in mucosal tissues. Current topics in microbiology and immunology *236*, 17-32.

Nicolete, R., dos Santos, D.F., and Faccioli, L.H. (2011). The uptake of PLGA micro or nanoparticles by macrophages provokes distinct in vitro inflammatory response. International immunopharmacology *11*, 1557-1563.

Niederreiter, L., and Kaser, A. (2011). Endoplasmic reticulum stress and inflammatory bowel disease. Acta gastro-enterologica Belgica *74*, 330-333.

Oberdörster, G., Oberdörster, E., and Oberdörster, J. (2005). Nanotoxicology: an emerging discipline evolving from studies of ultrafine particles. Environmental health perspectives *113*, 823-839.

Obtulowicz, T., Swoboda, M., Speina, E., Gackowski, D., Rozalski, R., Siomek, A., Janik, J., Janowska, B., Ciesla, J.M., Jawien, A.*, et al.* (2010). Oxidative stress and 8-oxoguanine repair are enhanced in colon adenoma and carcinoma patients. Mutagenesis *25*, 463-471.

Okayasu, I., Hatakeyama, S., Yamada, M., Ohkusa, T., Inagaki, Y., and Nakaya, R. (1990). A novel method in the induction of reliable experimental acute and chronic ulcerative colitis in mice. Gastroenterology *98*, 694-702.

Pan, M.H., Huang, T.M., and Lin, J.K. (1999). Biotransformation of curcumin through reduction and glucuronidation in mice. Drug metabolism and disposition: the biological fate of chemicals *27*, 486-494.

Panda, A., Arjona, A., Sapey, E., Bai, F., Fikrig, E., Montgomery, R.R., Lord, J.M., and Shaw, A.C. (2009). Human innate immunosenescence: causes and consequences for immunity in old age. Trends in immunology *30*, 325-333.

Panwala, C.M., Jones, J.C., and Viney, J.L. (1998). A novel model of inflammatory bowel disease: mice deficient for the multiple drug resistance gene, mdr1a, spontaneously develop colitis. Journal of immunology *161*, 5733-5744.

Panyam, J., and Labhasetwar, V. (2003). Biodegradable nanoparticles for drug and gene delivery to cells and tissue. Advanced drug delivery reviews *55*, 329-347.

Parveen, S., Misra, R., and Sahoo, S.K. (2012). Nanoparticles: a boon to drug delivery, therapeutics, diagnostics and imaging. Nanomedicine *8*, 147-166.

Pastore, A., Mozzi, A.F., Tozzi, G., Gaeta, L.M., Federici, G., Bertini, E., Lo Russo, A., Mannucci, L., and Piemonte, F. (2003). Determination of glutathionyl-hemoglobin in human erythrocytes by cation-exchange high-performance liquid chromatography. Analytical biochemistry *312*, 85-90.

Pfeffer, S.R., and Rothman, J.E. (1987). Biosynthetic protein transport and sorting by the endoplasmic reticulum and Golgi. Annual review of biochemistry *56*, 829-852.

Pinto Reis, C., Neufeld, R.J., Ribeiro, A.J., and Veiga, F. (2006). Nanoencapsulation I. Methods for preparation of drug-loaded polymeric nanoparticles. Nanomedicine *2*, 8-21.

Pompella, A., Visvikis, A., Paolicchi, A., De Tata, V., and Casini, A.F. (2003). The changing faces of glutathione, a cellular protagonist. Biochemical pharmacology *66*, 1499-1503.

Prucksunand, C., Indrasukhsri, B., Leethochawalit, M., and Hungspreugs, K. (2001). Phase II clinical trial on effect of the long turmeric (Curcuma longa Linn) on healing of peptic ulcer. The Southeast Asian journal of tropical medicine and public health *32*, 208-215.

Rachmawati, H. (2013). Curcumin nanoforms promise better therapeutic values. International Journal of Research in Pharmaceutical Sciences *4*, 211-220.

Rafiee, P., Nelson, V.M., Manley, S., Wellner, M., Floer, M., Binion, D.G., and Shaker, R. (2009). Effect of curcumin on acidic pH-induced expression of IL-6 and IL-8 in human esophageal epithelial cells (HET-1A): role of PKC, MAPKs, and NF-kappaB. American journal of physiology Gastrointestinal and liver physiology *296*, G388-398.

Rahman, I., and MacNee, W. (1999). Lung glutathione and oxidative stress: implications in cigarette smoke-induced airway disease. The American journal of physiology *277*, L1067-1088.

Ramachandran, A., Madesh, M., and Balasubramanian, K.A. (2000). Apoptosis in the intestinal epithelium: its relevance in normal and pathophysiological conditions. Journal of gastroenterology and hepatology *15*, 109-120.

Ramassamy, C. (2006). Emerging role of polyphenolic compounds in the treatment of neurodegenerative diseases: a review of their intracellular targets. European journal of pharmacology *545*, 51-64.

Ramsewak, R.S., DeWitt, D.L., and Nair, M.G. (2000). Cytotoxicity, antioxidant and anti-inflammatory activities of curcumins I-III from Curcuma longa. Phytomedicine : international journal of phytotherapy and phytopharmacology *7*, 303-308.

Rao, R.V., and Bredesen, D.E. (2004). Misfolded proteins, endoplasmic reticulum stress and neurodegeneration. Current opinion in cell biology *16*, 653-662.

Remijsen, Q., Kuijpers, T.W., Wirawan, E., Lippens, S., Vandenabeele, P., and Vanden Berghe, T. (2011). Dying for a cause: NETosis, mechanisms behind an antimicrobial cell death modality. Cell death and differentiation *18*, 581-588.

Renwick, L.C., Donaldson, K., and Clouter, A. (2001). Impairment of alveolar macrophage phagocytosis by ultrafine particles. Toxicology and applied pharmacology *172*, 119-127.

Richaud-Patin, Y., Soto-Vega, E., and Llorente, L. (2005). The gut: beyond immunology. Reumatologia clinica *1*, 121-128.

Richman, P.G., and Meister, A. (1975). Regulation of gamma-glutamyl-cysteine synthetase by nonallosteric feedback inhibition by glutathione. The Journal of biological chemistry *250*, 1422-1426.

Roessner, A., Kuester, D., Malfertheiner, P., and Schneider-Stock, R. (2008). Oxidative stress in ulcerative colitis-associated carcinogenesis. Pathology, research and practice *204*, 511-524.

Rosenzweig, S.D. (2008). Inflammatory manifestations in chronic granulomatous disease (CGD). Journal of clinical immunology *28 Suppl 1*, S67-72.

Ruby, A.J., Kuttan, G., Babu, K.D., Rajasekharan, K.N., and Kuttan, R. (1995). Anti-tumour and antioxidant activity of natural curcuminoids. Cancer letters *94*, 79-83.

Rutgeerts, P., Vermeire, S., and Van Assche, G. (2007). Mucosal healing in inflammatory bowel disease: impossible ideal or therapeutic target? Gut *56*, 453-455.

Sadlack, B., Merz, H., Schorle, H., Schimpl, A., Feller, A.C., and Horak, I. (1993). Ulcerative colitis-like disease in mice with a disrupted interleukin-2 gene. Cell *75*, 253-261.

Sahoo, S.K., and Labhasetwar, V. (2003). Nanotech approaches to drug delivery and imaging. Drug discovery today *8*, 1112-1120.

Sakihama, Y., Cohen, M.F., Grace, S.C., and Yamasaki, H. (2002). Plant phenolic antioxidant and prooxidant activities: phenolics-induced oxidative damage mediated by metals in plants. Toxicology *177*, 67-80.

Salh, B., Assi, K., Templeman, V., Parhar, K., Owen, D., Gomez-Munoz, A., and Jacobson, K. (2003). Curcumin attenuates DNB-induced murine colitis. American journal of physiology Gastrointestinal and liver physiology *285*, G235-243.

Sambuy, Y., De Angelis, I., Ranaldi, G., Scarino, M.L., Stammati, A., and Zucco, F. (2005). The Caco-2 cell line as a model of the intestinal barrier: influence of cell and culture-related factors on Caco-2 cell functional characteristics. Cell biology and toxicology *21*, 1-26.

Sandur, S.K., Ichikawa, H., Pandey, M.K., Kunnumakkara, A.B., Sung, B., Sethi, G., and Aggarwal, B.B. (2007). Role of pro-oxidants and antioxidants in the anti-inflammatory and apoptotic effects of curcumin (diferuloylmethane). Free radical biology & medicine *43*, 568-580.

Sansonetti, P.J. (2004). War and peace at mucosal surfaces. Nature reviews Immunology *4*, 953-964.

Sarra, M., Pallone, F., Macdonald, T.T., and Monteleone, G. (2010). IL-23/IL-17 axis in IBD. Inflammatory bowel diseases *16*, 1808-1813.

Sartor, R.B. (2006). Mechanisms of disease: pathogenesis of Crohn's disease and ulcerative colitis. Nature clinical practice Gastroenterology & hepatology *3*, 390-407.

Saveyn, H., De Baets, B., Thas, O., Hole, P., Smith, J., and Van der Meeren, P. (2010). Accurate particle size distribution determination by nanoparticle tracking analysis based on 2-D Brownian dynamics simulation. Journal of colloid and interface science *352*, 593-600.

Schins, R.P., and Knaapen, A.M. (2007). Genotoxicity of poorly soluble particles. Inhalation toxicology *19 Suppl 1*, 189-198.

Schmid, K., and Riediker, M. (2008). Use of nanoparticles in Swiss Industry: a targeted survey. Environmental science & technology *42*, 2253-2260.

Schmidt, C., Lautenschlaeger, C., Collnot, E.M., Schumann, M., Bojarski, C., Schulzke, J.D., Lehr, C.M., and Stallmach, A. (2013). Nano- and microscaled particles for drug targeting to inflamed intestinal mucosa: a first in vivo study in human patients. J Control Release *165*, 139-145.

Schroder, A.K., and Rink, L. (2003). Neutrophil immunity of the elderly. Mechanisms of ageing and development *124*, 419-425.

Schroder, M., and Kaufman, R.J. (2005). ER stress and the unfolded protein response. Mutation research *569*, 29-63.

Schulz, O., and Pabst, O. (2013). Antigen sampling in the small intestine. Trends in immunology *34*, 155-161.

Schwab, M., Schaeffeler, E., Marx, C., Fromm, M.F., Kaskas, B., Metzler, J., Stange, E., Herfarth, H., Schoelmerich, J., Gregor, M.*, et al.* (2003). Association between the C3435T MDR1 gene polymorphism and susceptibility for ulcerative colitis. Gastroenterology *124*, 26-33.

Seril, D.N., Liao, J., Yang, G.Y., and Yang, C.S. (2003). Oxidative stress and ulcerative colitis-associated carcinogenesis: studies in humans and animal models. Carcinogenesis *24*, 353-362.

Shaikh, J., Ankola, D.D., Beniwal, V., Singh, D., and Kumar, M.N. (2009). Nanoparticle encapsulation improves oral bioavailability of curcumin by at least 9-fold when compared to curcumin administered with piperine as absorption enhancer. Eur J Pharm Sci *37*, 223-230.

Sheng, Y.H., Hasnain, S.Z., Florin, T.H., and McGuckin, M.A. (2012). Mucins in inflammatory bowel diseases and colorectal cancer. Journal of gastroenterology and hepatology *27*, 28-38.

Shibutani, S., Takeshita, M., and Grollman, A.P. (1991). Insertion of specific bases during DNA synthesis past the oxidation-damaged base 8-oxodG. Nature *349*, 431-434.

Shih, A.Y., Johnson, D.A., Wong, G., Kraft, A.D., Jiang, L., Erb, H., Johnson, J.A., and Murphy, T.H. (2003). Coordinate regulation of glutathione biosynthesis and release by Nrf2-expressing glia potently protects neurons from oxidative stress. The Journal of neuroscience : the official journal of the Society for Neuroscience *23*, 3394-3406.

Shishodia, S., Amin, H.M., Lai, R., and Aggarwal, B.B. (2005a). Curcumin (diferuloylmethane) inhibits constitutive NF-kappaB activation, induces G1/S arrest,

suppresses proliferation, and induces apoptosis in mantle cell lymphoma. Biochemical pharmacology *70*, 700-713.

Shishodia, S., Sethi, G., and Aggarwal, B.B. (2005b). Curcumin: getting back to the roots. Annals of the New York Academy of Sciences *1056*, 206-217.

Shkoda, A., Ruiz, P.A., Daniel, H., Kim, S.C., Rogler, G., Sartor, R.B., and Haller, D. (2007). Interleukin-10 blocked endoplasmic reticulum stress in intestinal epithelial cells: impact on chronic inflammation. Gastroenterology *132*, 190-207.

Sies, H. (1997). Oxidative stress: oxidants and antioxidants. Experimental physiology *82*, 291-295.

Sies, H. (1999). Glutathione and its role in cellular functions. Free radical biology & medicine *27*, 916-921.

Simon, S.I., and Kim, M.H. (2010). A day (or 5) in a neutrophil's life. Blood *116*, 511-512.

Singh, S., and Aggarwal, B.B. (1995). Activation of transcription factor NF-kappa B is suppressed by curcumin (diferuloylmethane) [corrected]. The Journal of biological chemistry *270*, 24995-25000.

Snoeck, V., Goddeeris, B., and Cox, E. (2005). The role of enterocytes in the intestinal barrier function and antigen uptake. Microbes and infection / Institut Pasteur *7*, 997-1004.

Speit, G., Dennog, C., Eichhorn, U., Rothfuss, A., and Kaina, B. (2000). Induction of heme oxygenase-1 and adaptive protection against the induction of DNA damage after hyperbaric oxygen treatment. Carcinogenesis *21*, 1795-1799.

Stocker, R., Yamamoto, Y., McDonagh, A.F., Glazer, A.N., and Ames, B.N. (1987). Bilirubin is an antioxidant of possible physiological importance. Science *235*, 1043-1046.

Stone, V., Johnston, H., and Schins, R.P. (2009). Development of in vitro systems for nanotoxicology: methodological considerations. Critical reviews in toxicology *39*, 613-626.

Strober, W., and Fuss, I.J. (2011). Proinflammatory cytokines in the pathogenesis of inflammatory bowel diseases. Gastroenterology *140*, 1756-1767.

Subramanian, M., Sreejayan, Rao, M.N., Devasagayam, T.P., and Singh, B.B. (1994). Diminution of singlet oxygen-induced DNA damage by curcumin and related antioxidants. Mutation research *311*, 249-255.

Sugimoto, K., Hanai, H., Tozawa, K., Aoshi, T., Uchijima, M., Nagata, T., and Koide, Y. (2002). Curcumin prevents and ameliorates trinitrobenzene sulfonic acid-induced colitis in mice. Gastroenterology *123*, 1912-1922.

Suzuki, Y., and Lehrer, R.I. (1980). NAD(P)H oxidase activity in human neutrophils stimulated by phorbol myristate acetate. The Journal of clinical investigation *66*, 1409-1418.

Takeda, K., Clausen, B.E., Kaisho, T., Tsujimura, T., Terada, N., Forster, I., and Akira, S. (1999). Enhanced Th1 activity and development of chronic enterocolitis in mice devoid of Stat3 in macrophages and neutrophils. Immunity *10*, 39-49.

Tenhunen, R., Marver, H.S., and Schmid, R. (1969). Microsomal heme oxygenase. Characterization of the enzyme. The Journal of biological chemistry *244*, 6388-6394.

Thornton, D.J., Rousseau, K., and McGuckin, M.A. (2008). Structure and function of the polymeric mucins in airways mucus. Annual review of physiology *70*, 459-486.
Tiede, K., Boxall, A.B., Tear, S.P., Lewis, J., David, H., and Hassellov, M. (2008). Detection and characterization of engineered nanoparticles in food and the environment. Food additives & contaminants *25*, 795-821.

Tietze, F. (1969). Enzymic method for quantitative determination of nanogram amounts of total and oxidized glutathione: applications to mammalian blood and other tissues. Analytical biochemistry *27*, 502-522.

Tirasophon, W., Lee, K., Callaghan, B., Welihinda, A., and Kaufman, R.J. (2000). The endoribonuclease activity of mammalian IRE1 autoregulates its mRNA and is required for the unfolded protein response. Genes & development *14*, 2725-2736.

Toruner, M., Loftus, E.V., Jr., Harmsen, W.S., Zinsmeister, A.R., Orenstein, R., Sandborn, W.J., Colombel, J.F., and Egan, L.J. (2008). Risk factors for opportunistic infections in patients with inflammatory bowel disease. Gastroenterology *134*, 929-936.

Treton, X., Pedruzzi, E., Cazals-Hatem, D., Grodet, A., Panis, Y., Groyer, A., Moreau, R., Bouhnik, Y., Daniel, F., and Ogier-Denis, E. (2011). Altered endoplasmic reticulum stress affects translation in inactive colon tissue from patients with ulcerative colitis. Gastroenterology *141*, 1024-1035.

Ukil, A., Maity, S., Karmakar, S., Datta, N., Vedasiromoni, J.R., and Das, P.K. (2003). Curcumin, the major component of food flavour turmeric, reduces mucosal injury in trinitrobenzene sulphonic acid-induced colitis. British journal of pharmacology *139*, 209-218.

Ullman, T.A., and Itzkowitz, S.H. (2011). Intestinal inflammation and cancer. Gastroenterology *140*, 1807-1816.

Unfried, K., Albrecht, C., Klotz, L.O., Von Mikecz, A., Grether-Beck, S., and Schins, R.P.F. (2007). Cellular responses to nanoparticles: target structures and mechanisms. Nanotoxicology *Vol. 1*, 52-71.

Valko, M., Leibfritz, D., Moncol, J., Cronin, M.T., Mazur, M., and Telser, J. (2007). Free radicals and antioxidants in normal physiological functions and human disease. The international journal of biochemistry & cell biology *39*, 44-84.

van Berlo, D., Wessels, A., Boots, A.W., Wilhelmi, V., Scherbart, A.M., Gerloff, K., van Schooten, F.J., Albrecht, C., and Schins, R.P. (2010). Neutrophil-derived ROS contribute to oxidative DNA damage induction by quartz particles. Free radical biology & medicine *49*, 1685-1693.

Van Klinken, B.J., Dekker, J., Buller, H.A., and Einerhand, A.W. (1995). Mucin gene structure and expression: protection vs. adhesion. The American journal of physiology *269*, G613-627.

Van Klinken, B.J., Van der Wal, J.W., Einerhand, A.W., Buller, H.A., and Dekker, J. (1999). Sulphation and secretion of the predominant secretory human colonic mucin MUC2 in ulcerative colitis. Gut *44*, 387-393.

Waetzig, G.H., Seegert, D., Rosenstiel, P., Nikolaus, S., and Schreiber, S. (2002). p38 mitogen-activated protein kinase is activated and linked to TNF-alpha signaling in inflammatory bowel disease. Journal of immunology *168*, 5342-5351.

Wang, S., and Kaufman, R.J. (2012). The impact of the unfolded protein response on human disease. The Journal of cell biology *197*, 857-867.

Weaver, C.T., Hatton, R.D., Mangan, P.R., and Harrington, L.E. (2007). IL-17 family cytokines and the expanding diversity of effector T cell lineages. Annual review of immunology *25*, 821-852.

Weinberg, J.B., Misukonis, M.A., Shami, P.J., Mason, S.N., Sauls, D.L., Dittman, W.A., Wood, E.R., Smith, G.K., McDonald, B., Bachus, K.E.*, et al.* (1995). Human mononuclear phagocyte inducible nitric oxide synthase (iNOS): analysis of iNOS mRNA, iNOS protein, biopterin, and nitric oxide production by blood monocytes and peritoneal macrophages. Blood *86*, 1184-1195.

Wells, C.L., Jechorek, R.P., and Erlandsen, S.L. (1995). Inhibitory effect of bile on bacterial invasion of enterocytes: possible mechanism for increased translocation associated with obstructive jaundice. Critical care medicine *23*, 301-307.

Wells, J.M., Loonen, L.M., and Karczewski, J.M. (2010). The role of innate signaling in the homeostasis of tolerance and immunity in the intestine. International journal of medical microbiology : IJMM *300*, 41-48.

Wessels, I., Jansen, J., Rink, L., and Uciechowski, P. (2010). Immunosenescence of polymorphonuclear neutrophils. TheScientificWorldJournal *10*, 145-160.

Westbrook, A.M., Szakmary, A., and Schiestl, R.H. (2010). Mechanisms of intestinal inflammation and development of associated cancers: lessons learned from mouse models. Mutation research *705*, 40-59.

Westbrook, A.M., Wei, B., Braun, J., and Schiestl, R.H. (2009). Intestinal mucosal inflammation leads to systemic genotoxicity in mice. Cancer research *69*, 4827-4834.

Wilhelmi, V., Fischer, U., Weighardt, H., Schulze-Osthoff, K., Nickel, C., Stahlmecke, B., Kuhlbusch, T.A., Scherbart, A.M., Esser, C., Schins, R.P.*, et al.* (2013). Zinc oxide nanoparticles induce necrosis and apoptosis in macrophages in a p47phox- and Nrf2-independent manner. PloS one *8*, e65704.

Will, O., Gocke, E., Eckert, I., Schulz, I., Pflaum, M., Mahler, H.C., and Epe, B. (1999). Oxidative DNA damage and mutations induced by a polar photosensitizer, Ro19-8022. Mutation research *435*, 89-101.

Wirtz, S., Neufert, C., Weigmann, B., and Neurath, M.F. (2007). Chemically induced mouse models of intestinal inflammation. Nature protocols *2*, 541-546.

Wirtz, S., and Neurath, M.F. (2007). Mouse models of inflammatory bowel disease. Advanced drug delivery reviews *59*, 1073-1083.

Woo, J.H., Kim, Y.H., Choi, Y.J., Kim, D.G., Lee, K.S., Bae, J.H., Min, D.S., Chang, J.S., Jeong, Y.J., Lee, Y.H.*, et al.* (2003). Molecular mechanisms of curcumin-induced cytotoxicity: induction of apoptosis through generation of reactive oxygen species, down-regulation of Bcl-XL and IAP, the release of cytochrome c and inhibition of Akt. Carcinogenesis *24*, 1199-1208.

Wu, H.J., and Wu, E. (2012). The role of gut microbiota in immune homeostasis and autoimmunity. Gut microbes *3*, 4-14.

Wullaert, A. (2010). Role of NF-kappaB activation in intestinal immune homeostasis. International journal of medical microbiology : IJMM *300*, 49-56.

Xavier, R.J., and Podolsky, D.K. (2007). Unravelling the pathogenesis of inflammatory bowel disease. Nature *448*, 427-434.

Xia, T., Kovochich, M., Brant, J., Hotze, M., Sempf, J., Oberley, T., Sioutas, C., Yeh, J.I., Wiesner, M.R., and Nel, A.E. (2006). Comparison of the abilities of ambient and manufactured nanoparticles to induce cellular toxicity according to an oxidative stress paradigm. Nano letters *6*, 1794-1807.

Xiong, S., George, S., Yu, H., Damoiseaux, R., France, B., Ng, K.W., and Loo, J.S. (2013). Size influences the cytotoxicity of poly (lactic-co-glycolic acid) (PLGA) and titanium dioxide (TiO(2)) nanoparticles. Archives of toxicology *87*, 1075-1086.

Yallapu, M.M., Gupta, B.K., Jaggi, M., and Chauhan, S.C. (2010a). Fabrication of curcumin encapsulated PLGA nanoparticles for improved therapeutic effects in metastatic cancer cells. Journal of colloid and interface science *351*, 19-29.

Yallapu, M.M., Jaggi, M., and Chauhan, S.C. (2010b). Poly(beta-cyclodextrin)/curcumin self-assembly: a novel approach to improve curcumin delivery and its therapeutic efficacy in prostate cancer cells. Macromolecular bioscience *10*, 1141-1151.

Yanaka, A., Zhang, S., Tauchi, M., Suzuki, H., Shibahara, T., Matsui, H., Nakahara, A., Tanaka, N., and Yamamoto, M. (2005). Role of the nrf-2 gene in protection and repair of gastric mucosa against oxidative stress. Inflammopharmacology *13*, 83-90.

Yang, H., Li, K., Liu, Y., Liu, Z., and Miyoshi, H. (2009). Poly(D,L-lactide-co-glycolide) nanoparticles encapsulated fluorescent isothiocyanate and paclitaxol: preparation, release kinetics and anticancer effect. Journal of nanoscience and nanotechnology *9*, 282-287.

Yih, T.C., and Al-Fandi, M. (2006). Engineered nanoparticles as precise drug delivery systems. Journal of cellular biochemistry *97*, 1184-1190.

Zhao, F., Edwards, R., Dizon, D., Afrasiabi, K., Mastroianni, J.R., Geyfman, M., Ouellette, A.J., Andersen, B., and Lipkin, S.M. (2010). Disruption of Paneth and goblet cell homeostasis and increased endoplasmic reticulum stress in Agr2-/- mice. Developmental biology *338*, 270-279.

Zheng, W., Rosenstiel, P., Huse, K., Sina, C., Valentonyte, R., Mah, N., Zeitlmann, L., Grosse, J., Ruf, N., Nurnberg, P.*, et al.* (2006). Evaluation of AGR2 and AGR3 as candidate genes for inflammatory bowel disease. Genes and immunity *7*, 11-18.

Danke an…

…PD Dr. Klaus Unfried für die sofortige Bereitschaft und unkomplizierte Übernahme meiner Betreuung an der Mathematisch-Naturwissenschaftlichen Fakultät und die wohlwollende Unterstützung.

…Prof. Dr. Johannes Hegemann für die bereitwillige Übernahme des Zweitgutachtens.

…Dr. Roel Schins für die freundliche, offene Aufnahme in die Partikelgruppe und die Möglichkeit an diesem spannenden Thema zu arbeiten. Besonders danke ich ihm für seine wissenschaftliche Anleitung und Unterstützung, die stete Diskussionsbereitschaft und das Gewähren der Freiheit zur Entwicklung und Einbringung eigener Ideen. Mit seiner motivierenden und mitreisenden Begeisterung für die Forschung, hat er maßgeblich zum Gelingen dieser Arbeit beigetragen und meine Forschungsphilosophie nachhaltig beeinflusst.

…Dr. Catrin Albrecht für die uneingeschränkte Unterstützung in wissenschaftlichen sowie in nicht-wissenschaftlichen Fragen. Vielen Dank für die vielen zielführenden Diskussionen, Beratungen und Anleitungen, die meine Arbeit sehr bereichert haben.

…alle Kollegen und Mit-Doktoranden, die mich in den vergangenen Jahren mit bereichernden Tipps und Diskussionsbeiträgen fachlich und emotional begleitet haben: Dr. Damien van Berlo, Dr. Agnes Boots, Dr. Kirsten Gerloff, Dr. Bryan Hellack, Dr. Maja Hullmann, Dr. Andrea Neumeyer, Dr. Agnes Scherbart, Daniela Schwotzer, Waluree Thongkam und Dr. Verena Wilhelmi.

… Frau Christel Weishaupt und Frau Gabriele Wick für die Unterstützung im Laboralltag.

Vielen Dank an euch alle für das tolle Arbeitsklima und die gute Zusammenarbeit. Dank euch hatte ich eine sehr schöne und unvergessliche Doktorandenzeit!

…Prof. Dr. Claus-Michael Lehr für die freundliche und hilfsbereite Aufnahme als Gastwissenschaftler an dem Institut für Biopharmazie und Pharmazeutische Technologie an der Universität des Saarlandes. Als Saarländerin war es mir eine besondere Freude zurück an „meine alte Uni“ im „schönsten Bundesland der Welt“ zu kommen. Vielen Dank auch an Dr. Eva-Maria Collnot für die Anleitung zur Herstellung der Nanocurcuminpartikel.

…Prof. Dr. Michael McGuckin und der gesamten Mucin Gruppe des Mater Medical Research Institutes in Brisbane für die nette Aufnahme und Unterstützung während meines Gastaufenthaltes. Vielen Dank für die bereitwillige Zurverfügungstellung des speziellen genetisch modifizierten Kolitis-Maus-Modells *Winnie*, sowie für die fachliche Anleitung in den beiden *in vivo* Studien. Vielen Dank für eine sehr spannende und lehrreiche Zeit in Down Under!

…das Graduiertenkolleg 1427 unter der Leitung von Prof. Dr. Wim Wätjen für die Aufnahme und die Möglichkeit am Postgraduiertenstudium „Fachtoxikologie DGPT“ teilzunehmen.

…Dr. Kirsten Gerloff für die Einarbeitungszeit in der Partikelgruppe. Unvergessen bleibt auch die gemeinsame Forschungsarbeit in Brisbane.

...Dr. Agnes Boots für die stets hilfsbereite Unterstützung während ihrer Zeit in der Partikelgruppe am IUF, aber auch darüber hinaus, als sie an der Universität Maastricht die Messung der Zytokinlevel in den Darmgewebeproben mittels Luminex Assay übernommen hat.

..Dr. Henrike Peuschel und Dr. Marcus Koch vom INM-Leibniz Institut für Neue Materialien in Saarbrücken, für die elektronenmikroskopischen Aufnahmen der Nanocurcuminpartikel.

...Way (Waluree Thongkam) u.a. für die Einführung in die originale Thai Küche. Nicht nur an das Essen bringt sie stets die von uns geliebte thailändische Würze, sondern auch in unsere Arbeitsgruppe und insbesondere in unsere persönliche Freundschaft.

...Dr. Eva Weber, z.Z. an der Universität von Haifa, für die spontane Bereitschaft meine Arbeit Korrektur zu lesen und die jahrelange Freundschaft, die uns schon viel länger verbindet als die gemeinsame Leidenschaft zur Forschung.

…meine Familie, meine Eltern Bernd und Birgitte und meine Zwillingsschwester Miriam, die mich immer unterstützt und ermutigt haben auf meinem Weg und mir stets beratend zur Seite standen. Vielen Dank, dass ihr immer für mich da ward!

Eidesstattliche Erklärung

Hiermit versichere ich, dass ich die vorliegende Arbeit selbstständig verfasst und keine anderen als die angegebenen Quellen und Hilfsmittel verwendet habe.

Ferner versichere ich, dass ich weder an der Heinrich-Heine-Universität Düsseldorf noch an einer anderen Universität versucht habe, diese Doktorarbeit einzureichen.

Ebenso habe ich bisher keine erfolglosen Promotionsversuche unternommen.

Düsseldorf, den 15.01.2014

_____

Julia Kolling